Aus dem Pharmakologischen Institut

Direktor: Prof. Dr. med. Thomas Worzfeld

des Fachbereichs Medizin der Philipps-Universität Marburg

Identification and characterization of critical determinants in plexin signaling

Inaugural-Dissertation

zur Erlangung des Doktorgrades der Naturwissenschaften

(Dr. rer. nat.)

dem Fachbereich Medizin der Philipps-Universität Marburg

vorgelegt von

Carsten William Höß

aus Gießen

Marburg, 2020

Angenommen vom Fachbereich Medizin der Philipps-Universität Marburg am:

29.10.2020

Gedruckt mit Genehmigung des Fachbereichs Medizin.

Dekan i.V. der Prodekan: Herr Prof. Dr. R. Müller

Referent: Herr Prof. Dr. T. Worzfeld

1. Korreferent: Herr Prof. Dr. O. Hantschel

Alle großen Dinge sind einfach, aber zu den einfachsten Erkenntnissen braucht man die längste Zeit.

Justus von Liebig

Content

1 Abbreviations

%	Percentage
(E)GFP	(enhanced) Green fluorescent protein
°C	Degree Celsius
µ	Micro
Ab	Antibody
AKT	Protein kinase B
AP	Alkaline phosphatase
APS	Ammonium persulfate
ATP	Adenosine triphosphate
BAPTA-AM	1,2-Bis(2-aminophenoxy)ethane-N,N,N′,N′-tetraacetic acid tetrakis
BBS	BES-buffered saline
BES	N,N-Bis(2-hydroxyethyl)-2-aminoethanesulfonic acid
BSA	Bovine serum albumin
BTK	Bruton tyrosine kinase
CA	Constitutively active
CAKUT	Congenital anomalies of the kidney and urinary tract
CCK_2	Cholecystokinin B receptor
cDNA	Complementary DNA
CHO	Chinese hamster ovary
CO-IP	Co-Immunoprecipitation
DAPI	4′,6-Diamidin-2-phenylindol (DAPI)
dC	Lack of two C2 domains
DMSO	Dimethyl sulfoxide
DN	Dominant negative
DNA	Deoxyribonucleic acid
dNTP	Deoxyribose nucleoside triphosphate
dPH	Lack of PH domain
DTT	Dithiothreitol
ECL	Enterochromaffin-like
ECL	Enhanced chemiluminescence
EDTA	Ethylenediaminetetraacetic acid

EGF	Epidermal growth factor
EGTA	Ethylene glycol-bis(β-aminoethyl ether)-*N*,*N*,*N*′,*N*′-tetraacetic acid
ENS	Enteric nervous system
ErbB-2	Human epidermal growth factor receptor 2
ERK	Extracellular signal-regulated kinase
FBS	Fetal bovine serum
FCS	Fetal calf serum
FI	Fluorescence intensity
g	Gravitation
GAP	GTPase activating protein
GAPDH	Glyceraldehyde 3-phophate dehydrogenase
GARNL4	Rap1GAP2
gDNA	Genomic DNA
GDP	Guanosine diphosphate
GEF	Guanine nucleotide exchange factor
GMEM	Glashow's minimum essential medium
GPI	Glycosylphosphatidylinositol
GRP	Gastrin releasing peptide
GST	glutathione S-transferase
GTP	Guanosine triphosphate
GTPase	Small guanosine triphosphatase
h	Hour
HA	Human influenza hemagglutinin
HB-EGF	Heparin-binding EGF
HBSS	Hank's balanced salt solution
HRP	Horseradish peroxidase
IAA	Roti-Phenol/Chloroform/Isoamyl alcohol (IAA)
IF	Immunofluorescence
IPTG	isopropyl β-D-1-thiogalactopyranoside
kb	Kilo bases
kDA	Kilo Dalton
l	Liter

LARG	Leukemia-associated Rho guanine nucleotide exchange factor
LB	Lysogeny broth
LBG	Lysis buffer for preparation of GST-RBD
LPA	Lysophosphatidic acid
M	Molar
mAb	Monoclonal Ab
MAPK	Mitogen-activated protein kinase
min	Minutes
mutGAP	Mutated GAP domain
NF1	Neurofibromin
ng	Nanogram
NSAID	Nonsteroidal anti-inflammatory drug
OD	Optical density
PACAP	acetylcholine and pituitary adenylate cyclase-activating peptide
PBS	Phosphate-buffered saline
PCR	Polymerase chain reaction
PFA	Para-formaldehyde
PH	Pleckstrinhomology
PI3K	Phosphatidylinositol 3-kinase
PITX1	Paired-like homeodomain 1
PLB	Pulldown lysis buffer
PLCγ	Phospholipase C gamma
pNPP	4-nitrophenyl phosphate disodium salt hexahydrate
PO_4	Phosphate group
PSI	Plexin-semaphorin-integrin
PTEN	Phosphatase and tensin homolog
PTM	Post-translational modifications
PVDF	Polyvinylidene fluoride
RA	Triple arginine mutation
Rap	Ras-related protein
RBD	RHO-GTPase binding domain
RBD	Ras-binding domain

RHO	Ras homolog family member
RIPA	Radioimmunoprecipitation buffer
RNA	Ribonucleic acid
ROI	Region of interest
R-Ras	Related to Ras
RT	Room temperature
RT	Reverse transcription
RTK	Receptor tyrosine kinase
RT-qPCR	Quantitative real-time RT-PCR
s	Seconds
SDS-PAGE	SDS-polyacrylamide-gel electrophoresis
Sema	Semaphorin
SH2	Src homology 2
shRNA	Small hairpin RNA
T_A	Annealing temperature
TBS-T	Tris-buffered saline with 0,1% Tween20
T_m	Melting temperature
TMTC1-4	Tetra-trico-peptide repeat-containing proteins 1-4
v	Volume
VSV	Vesicular stomatitis virus
w	Weight
WB	Western blot
WT	Wildtype

2 List of figures

3 List of tables

4 Introduction

4.1 Semaphorins and plexins

Plexins are a family of transmembrane receptors and their ligands are semaphorins (He and Tessier-Lavigne 1997; Kolodkin et al. 1997).

Semaphorins were named after the maritime telegraphy system flag semaphore (Kolodkin et al. 1993) and have been discovered as repulsive guidance cues that can steer neuronal growth cones in the chick brain (Luo et al. 1993). The semaphorin protein family consists of 5 classes (3-7) with 20 members (Unified nomenclature for the semaphorins/collapsins. Semaphorin Nomenclature Committee 1999; Worzfeld and Offermanns 2014). They can be either secreted (class 3), transmembrane (classes 4-6) or glycosylphosphatidylinositol (GPI)-anchored (class 7) proteins (Worzfeld and Offermanns 2014). The extracellular domain of class 4 semaphorins can be proteolytically cleaved and act as a soluble ligand as well (Wang et al. 2001). All semaphorins have an N-terminal sema domain and a plexin-semaphorin-integrin (PSI) domain that form a propeller-like homodimer (Klostermann et al. 1998; Love et al. 2003) to mediate semaphorin interaction with plexins (Nogi et al. 2010; Janssen et al. 2010).

Plexins were historically discovered as proteins expressed in retinal plexiform layers of xenopus (Ohta et al. 1992) and represented a novel adhesion molecule that plays a role in neuronal cell-cell interactions (Ohta et al. 1995). Nowadays, the plexin protein family has been divided into four subfamilies (A-D) consisting of 9 members (Tamagnone et al. 1999; Worzfeld and Offermanns 2014). The binding of a semaphorin homodimer to two plexin monomers takes place at an extracellular sema-PSI domain. This indirect formation of plexin homodimers is necessary to induce intracellular plexin signaling (Nogi et al. 2010; Janssen et al. 2010). The diversity and specificity of semaphorin-plexin interaction is determined by characteristic insertions in the binding interface of semaphorins and plexins (Worzfeld and Offermanns 2014). In addition to that, some plexins need neuropilins as co-receptors to mediate semaphorin binding (Takahashi et al. 1999; Tamagnone et al. 1999).

From their initial description as axonal guidance molecules (Rohm et al. 2000), the semaphorin-plexin system has been further shown to play a diverse role in different cellular processes like angiogenesis (Gu and Giraudo 2013), neuronal development (Gu and Giraudo 2013; Pasterkamp 2012), immune response

(Kumanogoh and Kikutani 2013), osteogenesis (Tamagnone and Giordano 2006) or mitotic spindle orientation (Xia et al. 2015).

Furthermore, the semaphorin-plexin system has a high pathophysiological relevance since it has been connected to regulatory signaling in cancer (Tamagnone 2012), neuronal diseases (Pasterkamp and Giger 2009), the immune system (Takamatsu and Kumanogoh 2012) and aberrant angiogenesis contributing to cancer (Sakurai et al. 2012).

First therapeutic progress has been made by blocking plexin-semaphorin signaling in a preclinical set-up by RNA interference or small molecule inhibitors (Worzfeld and Offermanns 2014). In addition to that, an antibody against Semaphorin 4D is currently being tested in clinical studies for different types of cancer (Fisher et al. 2016).

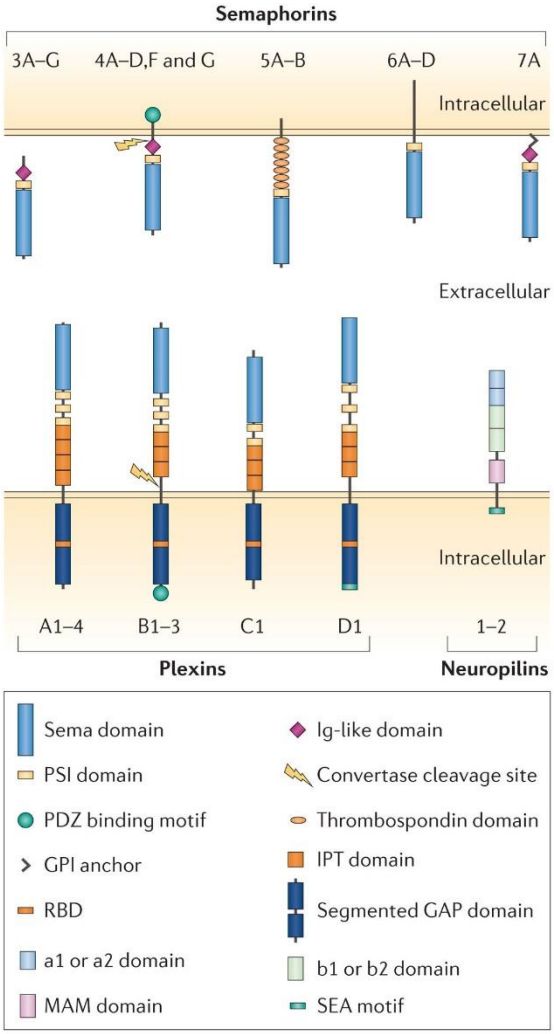

Figure 1. Domain structure of semaphorin and plexin subfamilies. Semaphorins are divided into 5 classes with 20 members and plexins into 4 subfamilies with 9 members. Neuropilins 1 and 2 are mostly associated as co-receptors with A plexins. All semaphorins have a sema domain that mediates binding to the sema domain of plexins. Semaphorins of class 3 are soluble ligands, while the classes

4-7 are membrane-bound. Members of semaphorin class 4 can be cleaved and act as a soluble ligand. Plexins are transmembrane receptors for semaphorins and have a segmented small guanosine triphosphatase (GTPase) activating protein (GAP) domain that mediates GTPase deactivation. Plexins of the B subfamily also have a PDZ binding motif that binds Rho guanine nucleotide exchange factors (RhoGEFs) and mediates Rho activation. Furthermore, B plexins have a cleavage site in their extracellular domain that is being processed to enhance signaling (Figure adapted from Worzfeld and Offermanns 2014).

4.1.1 Glycosylation of plexins

Glycosylation describes a diverse, regulated and abundant process of adding glycans to proteins or lipids. The responsible enzymes catalyzing these covalent reactions are glycosyltransferases and glycosidases (Ohtsubo and Marth 2006). In the last decade, several glycan-participating biological processes have been identified like cell adhesion, molecular trafficking/clearance, endocytosis and signal transduction (Ohtsubo and Marth 2006). In addition to that, disorders of glycosylation were found to play a role in auto-immune, infectious and chronic diseases, as well as in cancer (Reily et al. 2019). Glycosylation is taking place both in pro- and eukaryotes (Joshi et al. 2018), whereby in mammals, glycosylation generally depends on nine diet-derived monosaccharides that are linked to proteins via asparagine (N-glycosylation) or serine/threonine (O-glycosylation, proteoglycans) (Ohtsubo and Marth 2006; Schachter 2000). One of these monosaccharides is mannose, that is linked to serines/threonines through O-glycosylation by a conserved family of O-mannosyltransferases (POMT1/POMT2). While O-mannosylation is the only and abundant type of O-glycosylation in yeast, only a few O-mannosylated proteins are known in metazoans, among them α-dystroglycan, (proto)-cadherin and members of the IPT/TIG domain-carrying protein family (including plexins) (Larsen et al. 2017a; Larsen et al. 2017b), but the functional role of plexin glycosylation is not known. Furthermore, Larsen et al. identified a new class of O-mannosyltransferases, the tetra-trico-peptide repeat-containing proteins 1-4 (TMTC1-4) that selectively O-mannosylate the cadherin superfamily independently of POMT1/POMT2.
Additionally, mutations in TMTC3 can cause cobblestone lissencephaly, indicating an important function of O-mannosylation in a pathophysiological manner (Larsen et al. 2017a).

4.1.2 Function of the plexin intracellular domain

The intracellular domain of plexins contains a conserved GTPase activating protein (GAP) domain separated by a Ras homolog family member (RHO)-GTPase-binding domain (RBD) (Hota and Buck 2012; Siebold and Jones 2013). The GAP domain has been reported as a GAP for the small guanosine triphosphatases (GTPases) R-Ras, M-Ras and Ras-related protein (Rap) of which R-Ras and M-Ras need an additional binding of GTPases of the RND family (Oinuma et al. 2004a; Saito et al. 2009; Wang et al. 2012). The intrinsic GAP activity of plexins is controversial and the detailed mechanism remains unclear (Tong et al. 2009; Sakurai et al. 2010; Pascoe et al. 2015). Moreover, B plexins have in addition a C-terminal PDZ domain, that serves as a binding motive for the RHO guanine nucleotide exchange factors (GEFs) PDZ-RHOGEF and leukemia-associated Rho guanine nucleotide exchange factor (LARG) that activate the GTPases RHOA and RHOC upon semaphorin stimulation (Swiercz et al. 2002; Aurandt et al. 2002).

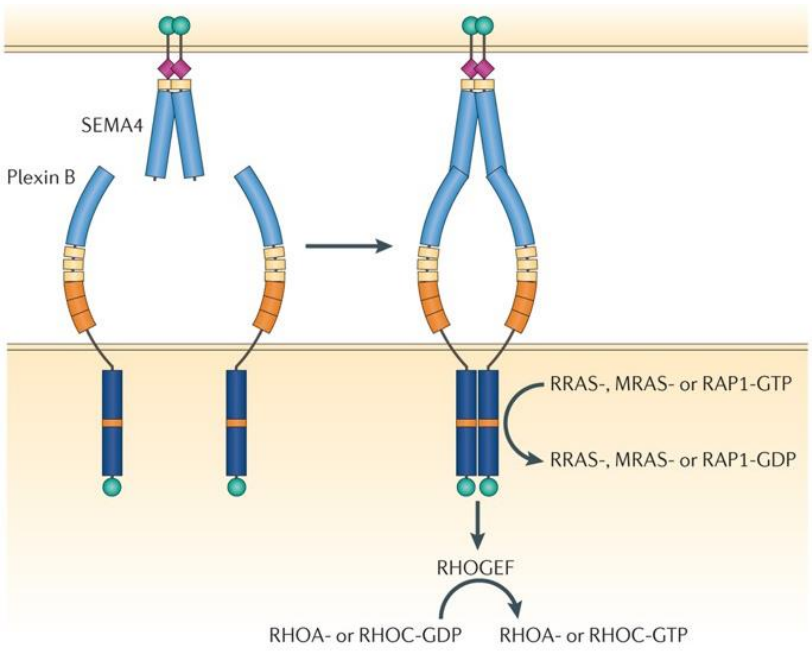

Figure 2. B Plexin signaling. The binding of a Semaphorin 4 (SEMA4) homodimer to a B plexin monomer via the sema domain (light blue) induces plexin dimerization of the intracellular domain (dark blue and green) and mediates the deactivation of R-Ras, M-Ras or Rap1 via the GAP-domain (dark blue) and the activation of RhoGEF-mediated RhoA/RhoC via the PDZ domain (green) (modified from Worzfeld and Offermanns 2014).

4.2 Ras GTPases

4.2.1 The Ras small GTPase superfamily

The Ras small GTPase superfamily consists of five major families: Ran, Ras, Rab, Rho, and Arf (Wennerberg et al. 2005). Small GTPases are monomeric molecules that act as binary switches: They cycle between an inactive guanosine diphosphate (GDP)- and an active guanosine triphosphate (GTP)-bound state (Vetter and Wittinghofer 2001). The GTP-binding domain of Ras proteins is highly conserved across all superfamily members and has a low intrinsic GTPase activity (Wennerberg et al. 2005). Due to this low intrinsic activity, another protein family, the so called GAPs act as catalysators for GTP hydrolysis (Bernards and Settleman 2004). The Ras re-activating exchange of GDP with GTP is performed by a molecule class called GEFs (Schmidt and Hall 2002).

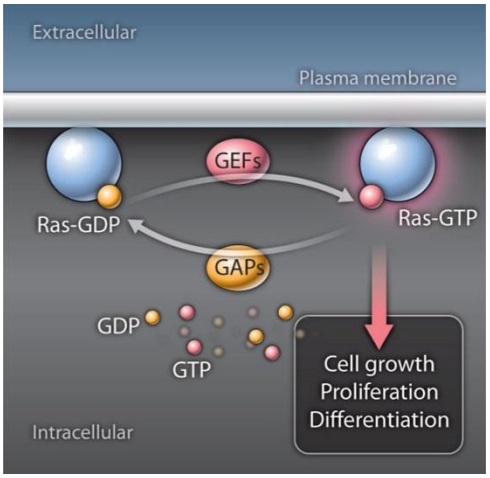

Figure 3. RasGTPases cycle between an active and an inactive state. GDP-bound Ras is being loaded with GTP by guanine nucleotide exchange factors (GEFs) resulting in the activation of Ras downstream effectors that mediate cell growth, proliferation and differentiation. Due to low intrinsic GTPase activity, Ras GTPase activating proteins (RasGAPs) catalyze the GTP hydrolysis, cycling Ras back into its GDP-bound inactive state (adapted from King et al. 2013).

4.2.2 The Ras family and R-Ras

The Ras small GTPase family plays an important role in human oncogenesis, as Ras signaling leads to downstream effects like cytoplasmic signaling and regulation of cell proliferation, differentiation and survival upon activation by different extracellular stimuli (Wennerberg et al. 2005). The main downstream signaling pathways of Ras are the Ras-Raf-MEK-ERK, the phosphatidylinositol 3-

kinase (PI3K)/PTEN/Akt and the RalGEF/Ral pathway (Repasky et al. 2004; Drosten et al. 2010). Ras subfamilies are K-Ras, N-Ras, H-Ras and R-Ras (Related to Ras). The R-Ras subfamily consists of R-Ras1, R-Ras2 and R-Ras3 (also named M-Ras). R-Ras promotes integrin adhesion and hence controls mitogenesis and cytoskeleton organization. R-Ras overexpression and active R-Ras mutants have been found in some tumors (Colicelli 2004).

4.3 Ras GTPase activating proteins

4.3.1 The RasGAP superfamily

Since Ras proteins have a very low intrinsic GTPase activity under physiological conditions, RasGAPs can interact and accelerate GTP hydrolysis by several orders of magnitude (Bernards and Settleman 2004). After GAP binding, a critical arginine finger is moved into the enzyme's catalytic site, resulting in reorientation of Ras glutamine residues, stabilizing the GTPase transition state and exerting catalysis (Ahmadian et al. 1997; Kötting et al. 2008; Mittal et al. 1996; Nagy et al. 2016). Mutations in critical residues of Ras can lead to a hydrolysis defect, resulting in a constitutive active enzyme that can be found in 30% of all human cancers (Prior et al. 2012).

RasGAPs can be divided into four groups according to their structural properties: RASA1, NF1, GAP1^{m} family (Rasa2, Rasa3, Rasa4, Rasal1) and SynGAP family (SynGAP, DAB2ip, Rasal2, Rasal3). Their expression pattern is diverse and represents a complex level of Ras activity regulation in vascular, hematopoietic, immune and neuronal systems (King et al. 2013).

All RasGAPs have a GAP domain that mediates GAP activity on Ras. Furthermore, binding of RasGAPs to cell membranes and hence bringing them in proximity to Ras is mediated in RASA1 by a Src homology 2 (SH2) domain binding to phosphorylated receptor tyrosine kinases (RTKs), in NF1 and Rasa2/3 via a pleckstrin homology (PH) domain that binds to (glycerol-)phospholipids and in the case of Rasa4/Rasal1 by a calcium-sensitive protein kinase C2 homology domain binding phospholipids (King et al. 2013).

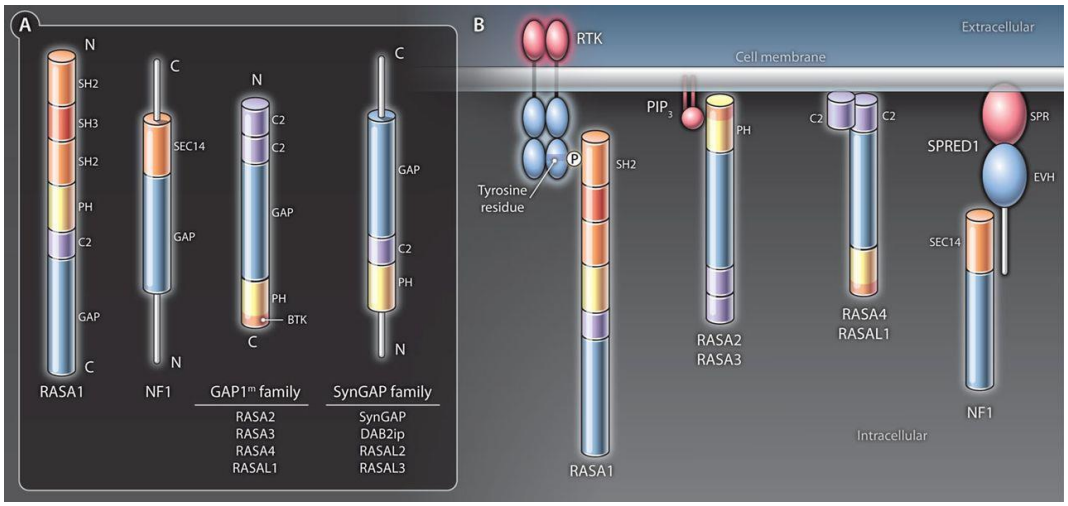

Figure 4. RasGAP family domain organization and their domain-directed membrane localization. (A) All RasGAPs have a GAP domain that is mostly flanked by C2 and/or pleckstrin homology (PH) domains that are responsible for membrane localization. (B) A constant membrane localization can be moderated by protein-protein interactions or by PH domains. In the case of Rasal1 and Rasa4, the temporary interaction with the membrane is achieved by C2 domains in a calcium-dependent manner (adapted from King et al. 2013).

4.3.2 The GAP1^m family and Rasal1

Members of the GAP1^m family have two N-terminal C2 domains, a GAP domain and a pleckstrin homology (PH) domain with a Bruton tyrosine kinase (BTK) motif (King et al. 2013).

Rasa3, Rasa4 and Rasal1 have been shown to possess bifunctional activity towards Ras and Rap (Kupzig et al. 2006; Sot et al. 2010) and their localization to membranes is important for their enzymatic activity (Sot et al. 2013). While Rasa3 is constitutively at membranes, Rasa4 and Rasal1 are translocated via the C2 domain with increasing intracellular calcium levels (King et al. 2013). Interestingly, Rasa4 remains attached to the membrane via its PH domain while Rasal1 oscillates with calcium concentration spikes and is believed to have a non-functional PH domain (Liu et al. 2005; Walker et al. 2004; Lockyer et al. 2001).

Rasal1 has been identified as a target gene of the tumor-suppressive transcription factor Paired-like homeodomain 1 (PITX1) and mediating thereby tumorigenic potential to Ras-dependent cell transformation (Kolfschoten et al. 2005). In cancer cells, Rasal1 expression is downregulated by CpG methylation in the promotor region, confirming a tumor suppressing role (Jin et al. 2007). Furthermore, Rasal1 deficiency has been identified in different cancer types like liver (Calvisi et al. 2011), colorectal (Ohta et al. 2009), thyroid (Liu et al. 2013), gastric (Seto et al.

2011) and bladder cancer (Zhu et al. 2011), as well as in kidney fibrosis (Bechtel et al. 2010).

4.4 B plexins

4.4.1 Plexin-B1/B2 signaling pathways

For this study, the focus was set on Plexin-B1 and Plexin-B2 as well as their ligands Semaphorin 4D and Semaphorin 4C, respectively. These two ligand-receptor systems are being extensively studied in the laboratory and are expressed in a lot of different organ systems and cell lines (Worzfeld et al. 2014).

R-Ras/M-Ras mediated Semaphorin 4D-Plexin-B1 signaling has been shown to be relevant in remodeling of hippocampal neurons (Oinuma et al. 2004b) via R-Ras-Phosphatase and tensin homolog (PTEN) signaling (Oinuma et al. 2010), in angiogenesis by Met recruitment (Conrotto et al. 2005), in endothelial cell migration via the phosphatidylinositol 3-kinase (PI3K)-Akt pathway (Basile et al. 2005; Ito et al. 2006) and by inhibiting cell migration via regulation of β-integrin activity (Oinuma et al. 2006).

PDZ-RHOGEF-RHO mediated Semaphorin 4D-Plexin-B1 signaling can also regulate integrin-dependent cell motility via activation of protein kinase B (AKT) and mitogen-activated protein kinase (MAPK)/extracellular signal-regulated kinase (ERK) (Basile et al. 2007; Aurandt et al. 2006) and suppress bone formation by osteoclast-osteoblast contact repulsion (Negishi-Koga et al. 2011; Deb Roy et al. 2017). In addition to that, RHOA activation/deactivation needs the recruitment of Receptor tyrosine-protein kinase erbB-2 (ErbB-2), Met and phospholipase C gamma (PLCγ) into the Plexin-B1 receptor complex (Swiercz et al. 2008, 2009). Recently, reverse signaling pathways through Plexin-B1-Semaphorin 4A and Plexin-B2-Semaphorin 4C have been described, indicating a bidirectional signaling ability of this ligand-receptor system (Battistini and Tamagnone 2016; Sun et al. 2017; Gurrapu et al. 2019). Interestingly, also Sema3C is a ligand for Plexin-B1, and has been implicated in driving cancer cell growth (Peacock et al. 2018).

R-/M-Ras-dependent Semaphorin 4C-Plexin-B2 signaling plays its key role during embryonal development in diverse tissues (Worzfeld et al. 2014). In contrast, RHO-dependent Plexin-B2 signaling controls breast cancer cell growth and tumorigenic potential (Gurrapu et al. 2018), regulates synaptic morphology in inflammatory pain

and fear memory (Paldy et al. 2017; Simonetti et al. 2019) and coordinates epithelial morphogenesis and repair via the CDC42 RHO GTPase (Xia et al. 2015).

4.4.2 Important residues for B plexin signal transduction

The signaling capability of plexins depends on functional domains that can induce dimerization after semaphorin stimulation, as well as the binding of GEFs and GTPases at their intracellular domain. Binding of Rho Family GTPase 1 (Rnd1), which interacts with the RBD domain of plexins and is important for R-Ras deactivation, can be prevented in human Plexin-B1 by the mutations L1849G, V1850G and P1851A (Oinuma et al. 2004b; Oinuma et al. 2004a). Furthermore, triple arginine mutations R1677A, R1678A, R1984A abolish the binding of R-Ras to human Plexin-B1 and R1484G, R1485A and R1770A to murine Plexin-B2 while not changing the interaction with Rnd1 (Oinuma et al. 2004a; Oinuma et al. 2004b; Worzfeld et al. 2014). Moreover, the deletion of the amino acids VTDL at the C-terminal end of murine Plexin-B2 successfully prevents the binding of RhoGEFs to the PDZ domain (Worzfeld et al. 2014). Recently, our laboratory cloned a murine Plexin-B2 mutant (E369G), that is unable to bind semaphorins.

4.4.3 Phosphorylation of B plexins

The phosphorylation and dephosphorylation of proteins are reversible posttranslational modifications that are catalyzed by protein kinases and protein phosphatases. Protein phosphorylation is a biochemical reaction, in which a phosphate group (PO_4) is being added to the polar group of amino acids from a donor ATP, mostly at serine, threonine and tyrosine residues (Ardito et al. 2017). Phosphorylation is influencing the function of proteins by increasing or decreasing activity, stability, localization and protein-protein interactions (Cohen 2002).
In plexin signaling, human epidermal growth factor receptor 2 (ErbB-2) can phosphorylate Plexin-B1 at a tyrosine residue and consequently activates it. At the same time, this leads to activation of PDZ-RHOGEF, LARG and hence RhoA/RhoC (Worzfeld et al. 2012). In addition to that, activation of RhoGEFs by Plexin-B1 phosphorylation is dependent on binding of phospholipase C gamma (PLCγ) into the receptor complex (Swiercz et al. 2009). Interestingly, the binding of Met to Plexin-B1 leads to phosphorylation of both receptors and mediates Rho inhibition. This mechanism is still controversial and might differ from cellular to

cellular context (Swiercz et al. 2008; Franco and Tamagnone 2008; Giordano et al. 2002).

4.5 Role of semaphorin/plexin signaling in physiology

The semaphorin/plexin system has been shown to play a versatile role in mammalian physiology, ranging from embryonic development (Worzfeld et al. 2014) to different organ- and tissue-specific functions in the adult organism (Alto and Terman 2017).

During development, semaphorin/plexin signaling is inter alia involved in neural tube closure, axonal guidance, vascular formation and skeletal morphogenesis (Worzfeld et al. 2014). Besides that, the development of the kidney and the lungs as well as other organs is regulated by semaphorins and plexins (Alto and Terman 2017), in particular, by epithelial branching morphogenesis (Michos 2009).

Moreover, endothelial tip cells that guide extending blood vessels during angiogenesis, are directed by semaphorin cues (Tamagnone and Mazzone 2011).

In the immune system, migration and maturation of thymocytes in the thymus are influenced by semaphorin-plexin interactions (Kumanogoh and Kikutani 2013; Takamatsu and Kumanogoh 2012). In addition to that, the cell-cell communication between different immune cell types during immune response requires the participation of semaphorins and plexins (Suzuki et al. 2008).

Furthermore, the formation and absorption of bone tissue, that are orchestrated by osteoblasts and osteoclasts, respectively, are influenced by semaphorin/plexin signaling (Kang and Kumanogoh 2013). Precisely, bone homeostasis is balanced by semaphorins, since they control differentiation and migration of osteoblasts and osteoclasts (Alto and Terman 2017).

In epithelial tissues, semaphorins and plexins regulate epithelial barrier formation through cellular junctions, and determine its architecture by influencing cell adhesion, polarity and division (Treps et al. 2013; Xia et al. 2015).

In this context, our laboratory focusses on the murine stomach epithelium and elaborates the impact of semaphorin/plexin signaling in physiology and disease.

4.6 Physiology of the gastric epithelium

4.6.1 Gastric acid secretion in the gastric epithelium

The human stomach is divided along the anterior/posterior axis into different anatomical regions: cardia, fundus/corpus and antrum/pylorus (Hoffmann 2015). The gastric mucosa of each of these regions contains gastric glands that are in funnel-shaped pits, its upper-layer towards the gastric lumen consists of different epithelial cell types (Hoffmann 2015). Their cell-type specific organization, composition and function varies between the different gastric regions.

Among these epithelial cells are parietal cells in the corpus region, that release gastric acid (Yao and Forte 2003). The production and release of gastric acid is controlled by the neuroendocrine system of the stomach, connecting nerves with hormone-producing epithelial cells (Engevik et al. 2020). Another cell type of the gastric epithelium, the G cells, are located in the antrum region and secrete the peptide hormone Gastrin (Schubert 2016). Subsequently, Gastrin mainly stimulates the release of histamine by enterochromaffin-like (ECL) cells via the cholecystokinin B receptor (CCK_2) and histamine again induces gastric acid secretion in parietal cells (Engevik et al. 2020).

Gastric acid renders diverse physiological functions like facilitation of food digestion, inactivation of bacteria and the support of mineral absorption (Schubert 2016). In a pathophysiological context, gastric acid is responsible for erosions and ulcers that can result in a barrier damage of the gastric mucosa, a possible life-threatening condition called peptic ulcer disease (Engevik et al. 2020; Lanas and Chan 2017).

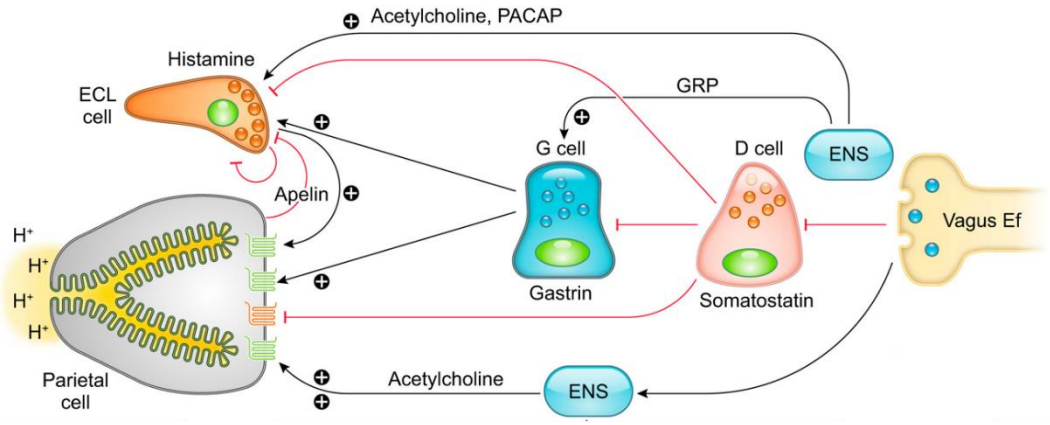

Figure 5. Cellular key-players in the regulation of gastric acid secretion. ECL cells secrete histamine and stimulate parietal cells to produce gastric acid. The release of histamine is regulated

by gastrin originating from G cells that have been stimulated by the enteric nervous system (ENS) through the gastrin releasing peptide (GRP). Additionally, the ENS can directly stimulate histamine release in ECL cells and gastric acid production in parietal cells via acetylcholine and pituitary adenylate cyclase-activating peptide (PACAP). Somatostatin, produced by D cells, is a negative regulator that acts on G cells, ECL cells and parietal cells (figure modified from Engevik et al. 2020).

4.6.2 Regulation of gastrin expression

The release of gastrin by G cells is stimulated by nutrients in the gastric lumen. Receptors on G cells can sense amino acids, calcium ions and an increase in pH and consequently secrete gastrin to respond to food intake, stimulate digestion and regulate nutrient absorption (Taylor et al. 1982; Feng et al. 2010; Rettenberger et al. 2015).

Considering gastrin expression on a molecular level, it has been shown that oncogenic K-Ras can induce Gastrin expression via the Ras-Raf-MEK-ERK signaling pathway in different human cancer cell lines (Nakata et al. 1998; Hori et al. 2003). Upstream of this pathway, the epidermal growth factor (EGF) and heparin-binding EGF-like growth factor (HB-EGF) can upregulate Gastrin expression through the EGF receptor (Ford et al. 1997; Gunawardhana et al. 2017). Sp1, a two zinc finger transcription factor, has been identified as a transcription factor for gastrin expression (Merchant 2000; Sergey Chupreta et al.). Since semaphorin-plexin signaling can regulate Ras activity (Oinuma et al. 2004a), Ras proteins are expressed in the gastrointestinal system and contribute to gastric cancer (Zhao et al. 2006; Pan et al. 2009), an involvement in the regulation of gastrin expression seems possible but is yet unknown.

4.7 Role of semaphorin/plexin signaling in pathophysiology

Beyond their involvement in the developing organism and in adult physiology, semaphorins and plexins play a crucial role in the pathogenesis of different diseases, that have mostly been investigated in murine disease models.

In this context, semaphorin/plexin signaling has been described to be involved in tumor growth and metastasis (Worzfeld and Offermanns 2014), regulating intercellular communication between different cell types in the tumor microenvironment and thereby contributing to angiogenesis, cell proliferation and invasiveness (Sakurai et al. 2012; Tamagnone 2012).

In addition to that, the semaphorin/plexin system seems to be involved in the regeneration of the central nervous system after injury, the emergence of epilepsy and in neurodegenerative diseases such as Alzheimer's disease and amyotrophic lateral sclerosis (Pasterkamp and Giger 2009).
Moreover, semaphorins and plexins are contributing to the progression of atherosclerosis by neovascularization of atherosclerotic plaques (Yukawa et al. 2010a) and in osteoporosis by inhibiting osteoblast-dependent bone formation (Negishi-Koga et al. 2011).
In the pathogenesis of autoimmune diseases, the semaphorin/plexin system has been shown to play a role in the emergence of multiple sclerosis due to impaired lymphocyte priming and in autoimmune glomerulonephritis (Takamatsu and Kumanogoh 2012).

4.8 Semaphorin/plexin mutations in human diseases

In humans, several publications could show a correlation between congenital mutations in semaphorins and plexins and the emergence of different diseases (Masuda and Taniguchi 2015).
For example, germline mutations in semaphorins have been described in patients suffering from retinitis pigmentosa and cone rod dystrophy (Abid et al. 2006; Bryant et al. 2018). Furthermore, semaphorin mutations have been associated with CHARGE syndrome, a disease with a variety of different symptoms such as cranial nerve dysfunction, ear abnormalities, cardiac defects, growth retardation and more (Lalani et al. 2004), as well as with Hirschsprung disease (Luzón-Toro et al. 2013) or Kallmann syndrome (Hanchate et al. 2012). In addition to that, semaphorin germline mutations have been found in familial colorectal cancer type X, increasing the disease prevalence in affected families (Schulz et al. 2014).
Pathophysiological plexin mutations have mainly been reported in the tumor context: mutations of plexins add tumorigenic potential to prostate cancer and breast cancer (Wong et al. 2007; Tong et al. 2008), as well as to pancreatic cancer and melanoma (Balakrishnan et al. 2009).
Moreover, congenital mutations of plexins have been identified in patients with truncus arteriosus (Ta-Shma et al. 2013) and Moebius syndrome (Nazaryan-Petersen et al. 2019).

5 Aim of the study

The aim of the study was a better understanding of the molecular mechanisms that underly plexin signaling. In particular, this thesis characterizes the functional relevance of extracellular posttranslational modifications of plexins, elucidates the mechanism how plexins control the activity of Ras GTPases via the RasGAP Rasal1, and analyzes the impact of human plexin mutations on plexin signaling.

6 Materials

Table 1. Antibodies

Antibody	Supplier	Dilution
Alexa Fluor Secondary Antibodies	ThermoFisher	1:200 (IF)
AP AffiniPure F(ab')$_2$ Fragment Goat α-Mouse IgG + IgM	Jackson IR	1:5000 (AP-assay)
Armenian Hamster α-human Plexin-B2 Monoclonal Ab	eBioscience	1:200 (IF)
Donkey α-Goat IgG, HRP	Jackson IR	1:3000 (WB)
Donkey α-Sheep IgG, HRP	BioRad	1:3000 (WB)
Goat Cy3 AffiniPure α-Armenian Hamster IgG (H+L)	Jackson IR	1:200 (IF)
Goat α-Rabbit IgG, HRP	BioRad	1:3000 (WB)
Goat α-VSV-G Tag Polyclonal Ab	Invitrogen	1:200 (IF), 1:3000 (WB)
Mouse Monoclonal α-FLAG M2	Sigma	1:200 (IF), 1:3000 (WB)
Mouse Monoclonal α-FLAG M2, HRP	Sigma	1:3000 (WB)
Mouse α-β-Actin mAb	Sigma	1:3000 (WB)
Rabbit α-c-Myc Ab	Sigma	1:200 (IF), 1:300 (WB)
Rabbit α-c-Myc, HRP	Sigma	1:3000 (WB)
Rabbit α-Ha Ab	Sigma	1:200 (IF), 1:3000 (WB)
Rabbit α-Ha Ab, HRP	Sigma	1:3000 (WB)
Rabbit α-R-Ras Ab	CST	1:1000 (WB)
Rabbit α-Tubulin (11H10) mAb	CST	1:3000 (WB)
Rabbit α-VSV-G Polyclonal Ab, HRP	Invitrogen	1:3000 (WB)

Sheep α-Human Plexin B2 Ab	R&D	1:3000 (WB)
Sheep α-Mouse IgG, HRP	GE Healthcare	1:3000 (WB)
Sheep α-Mouse Plexin B2 Ab	R&D	1:3000 (WB)

Table 2. Chemicals

Name	**Supplier**
1,2-Bis(2-aminophenoxy)ethane-N,N,N′,N′-tetraacetic acid tetrakis (acetoxymethyl ester) (BAPTA-AM)	Sigma
2-Mercaptoethanol	Sigma
4′,6-Diamidin-2-phenylindol (DAPI)	Sigma
4-nitrophenyl phosphate disodium salt hexahydrate (pNPP)	Sigma
5x Reaction buffer for reverse transcription	ThermoFisher
Acetic Acid	Roth
Adenosine triphosphate (ATP)	NEB
Agarose NEEO Ultra	Roth
Ammonium persulfate (APS)	Merck
Ampicillin	Roth
ANTI-FLAG M2 Affinity Agarose Gel	Sigma
Biotin-NHS	Sigma
Bovine serum albumin (BSA)	Roth
Bromophenol blue	Roth
Calcium chloride ($CaCl_2$)	Roth
Chloroform	Roth
Coomassie brilliant blue G250	Roth
Deoxyribose nucleoside triphosphate (dNTP)	Promega
Dimethyl sulfoxide (DMSO)	Roth
Disodium phosphate (Na_2HPO_4)	Roth
Dithiothreitol (DTT)	Roth
DMEM (HPSTA)	Capricorn Scientific
Ethanol	Roth
Ethidium bromide	Roth
Ethylene glycol-bis(β-aminoethyl ether)-*N*,*N*,*N*′,*N*′-tetraacetic acid (EGTA)	Sigma

Ethylenediaminetetraacetic acid (EDTA)	Sigma
Fetal bovine serum (FBS)	Gibco
Fetal calf serum (FCS)	ThermoFisher
Fluorescent mounting medium	DAKO
Fugene HD transfection reagent	Promega
GeneRuler DNA ladder 100bp plus	ThermoFisher
GeneRuler DNA ladder 1kb plus	ThermoFisher
Glasgow's MEM (GMEM)	Gibco
Glucose	Roth
Glycerol	Roth
Glycine	Sigma
GS supplement 50X	Sigma
Histamine dihydrochloride	Roth
Hydrogen peroxide (H_2O_2)	Sigma
iQ SYBR-Green Supermix	BioRad
Isopropanol	Sigma
Kanamycin	Roth
Lipofectamine 2000 Transfection Reagent	ThermoFisher
Lipofectamine RNAiMax Transfection Reagent	ThermoFisher
Magnesium chloride ($MgCl_2$)	Roth
Magnesium sulfate ($MgSO_4$)	Sigma
Methanol	Roth
Milk powder (fat-free)	Roth
Monopotassium phosphate (KH_2PO_4)	Roth
Monosodium phosphate (NaH_2PO_4)	Roth
N,N-Bis(2-hydroxyethyl)-2-aminoethanesulfonic acid (BES)	Sigma
NP-40	Sigma
OptiMEM	ThermoFisher
PageRuler Plus Prestained Protein Ladder	ThermoFisher
PageRuler Prestained Protein Ladder	ThermoFisher
Paraformaldehyde	Sigma
Penicillin/Streptomycin (100x)	PAA
peqGOLD TriFast	Peqlab
Phalloidin fluorophore-conjugated	ThermoFisher

Phosphatase inhibitor cocktail 3	Sigma
Phosphate-buffered saline (PBS)	Capricorn Scientific
Phusion Hot Start II High-Fidelity DNA Polymerase	ThermoFisher
Pierce™ Streptavidin Agarose	ThermoFisher
Polybren (Hexadimethrine bromide)	Sigma
Ponceau S solution	Sigma
Potassium chloride (KCl)	Roth
Protease inhibitor cocktail COMPLETE	Roche
Protein-A/G-Agarose	Santa Cruz
Puromycin	Capricorn
Random hexamers	ThermoFisher
Restriction enzymes	ThermoFisher
RevertAid Reverse Transcriptase	ThermoFisher
RiboLock RNase inhibitor	ThermoFisher
Roti-Phenol/Chloroform/Isoamyl alcohol (IAA)	Roth
RotiPhorese Gel 30 (Acrylamide-bisacrylamide solution)	Roth
Sodium acetate (NaOAc)	Roth
Sodium chloride (NaCl)	Roth
Sodium deoxycholate (NaDOC)	Sigma
Sodium dodecyl sulphate (SDS)	Roth
Sodium hydroxide (NaOH)	Sigma
T4 DNA Ligase	ThermoFisher
Taq DNA polymerase buffer	ThermoFisher
Taq DNA Polymerase, recombinant	ThermoFisher
Tetramethylethylenediamine (TEMED)	Roth
TRIS-HCl	Roth
Triton X-100	Sigma
Trypsin-EDTA 0,05%	Capricorn Scientific
Tryptone	Roth
Tween-20	Roth
Yeast extract	Roth
Zinc chloride ($ZnCl_2$)	Roth

Table 3. Solutions and buffers

Solution	Components	Concentration
BES-buffered saline (BBS) 2x	BES NaCl Na_2HPO_4	50 mM 280 mM 1,5 mM pH 6,94 – 7,00
Coomassie destaining solution	Acetic acid Methanol	10% (v/v) 20% (v/v)
Coomassie staining solution	Coomassie G250 Acetic acid Methanol	0,1% (w/v) 10% (v/v) 30% (v/v)
ECL solution 2	Tris-HCl H_2O_2	0,1 M 1,8% (v/v) pH 8,5
Enhanced chemiluminescence (ECL) solution 1	Tris-HCl Luminol p-Coumaric acid	0,1 M 2,5 mM 0,4 mM pH 8,5
Hank's balanced salt solution (HBSS)	NaCl KCl $CaCl_2$ $MgSO_4$ $MgCl_2$ Na_2HPO_4 KH_2PO4 Glucose $NaHCO_3$	150 mM 5 mM 1,5 mM 400 µM 1 mM 350 µM 450 µM 5 mM 4 mM
Laemmli buffer 4x	Tris-HCl EDTA Glycerol SDS Bromophenol blue 2-Mercaptoethanol	280 mM 10 mM 30% (v/v) 6% (w/v) 5 mM 60 mM
Lysis buffer for preparation of GST-RBD (LBG)	Tris-HCl NaCl EDTA	50 mM 150 mM 5 mM

	DTT	1 mM
Lysogeny broth (LB) agar	NaCl Yeast extract Tryptone Agarose	1% (w/v) 0,5% (w/v) 1% (w/v) 1,5% (w/v)
Lysogeny broth (LB) medium	NaCl Yeast extract Tryptone	1% (w/v) 0,5% (w/v) 1% (w/v)
NP-40 buffer	NP-40 NaCl EDTA Tris-HCl	1% (v/v) 100 mM 2 mM 50 mM pH = 7,4
Phosphate-buffered saline (PBS)	Na_2HPO_4 KH_2PO_4 NaCl KCl	8 mM 1,5 mM 135 mM 2,7 mM pH = 7,4
Phosphate-buffered saline (PBS-T)	PBS Triton X-100	1x 0,2% (v/v)
pNPP buffer	Glycine $MgCl_2$ $ZnCl_2$	0,1 M 1 mM 1 mM pH = 10,4
Ponceau S staining solution	Ponceau S Acetic acid	0,5% (w/v) 1% (v/v)
Pulldown lysis buffer (PLB)	NaCl Tris-HCl $MgCl_2$ SDS Triton X-100 NaDOC	500 mM 50 mM 100 mM 0,1% SDS 1% (v/v) 0,5% (v/v)
Radioimmunoprecipitation assay (RIPA) buffer	Tris-HCl NaCl EDTA Triton X-100	20-50 mM 150-500 mM 1-2 mM 1% (v/v)

	NaDOC SDS $MgCl_2$	0,25% (v/v) 0,1% (w/v) 5 mM pH 7,4
SDS-PAGE running buffer 1x	Tris-HCl Glycine SDS	25 mM 200 mM 0,1% (w/v) pH 8,3
SDS-PAGE separating gel	APS RotiPhorese Gel 30 SDS TEMED Tris-HCl	0,1% (w/v) 6-15% (v/v) 0,1% (w/v) 9,5 µM 0,36 M pH 8,8
SDS-PAGE stacking gel	APS RotiPhorese Gel 30 SDS TEMED Tris-HCl	0,15% (w/v) 19% (v/v) 0,1% (w/v) 14,5 µM 0,12 M pH 6,8
Transfer buffer	Tris-HCl Glycine Methanol SDS	25 mM 200 mM 10% (v/v) 0,2 % (w/v)
Tris-Acetate-EDTA (TAE) buffer	Tris-HCl EDTA Acetic acid	40 mM 2 mM 20 mM pH 8,0
Tris-buffered saline (TBS)-T buffer	NaCl Tris-HCl Tween-20	500 mM 20 mM 1% (v/v) pH 7,5
Tris-EDTA (TE) buffer	Tris-HCl EDTA	10 mM 1 mM pH = 7,4
Western blot blocking buffer	Milk powder	5% (w/v)

		In TBS-T

Table 4. Kits

Name	Supplier
Direct-zol RNA MicroPrep	Zymo Research
First Strand cDNA Synthesis kit	ThermoFisher
NucleoBond Xtra Midi	Macherey-Nagel
NucleoSpin gel and PCR clean-up	Macherey-Nagel
NucleoSpin Plasmid	Macherey-Nagel
QuickChange XL Site-Directed Mutagenesis Kit	Agilent Technologies
Ras Pull-Down Activation Assay Biochem Kit	Cytoskeleton, Inc.
SuperSignal West Femto Maximum Sensitivity ECL Western Blotting Substrate	ThermoFisher

Table 5. Devices and equipment

Name	Supplier
µ-Slide 8 well	Ibidi
Biofuge pico	Heraeus
Cell culture equipment	Sarstedt
Centrifuge 5415R	Eppendorf
Cover slips	Menzel-Gläser
FlexCycler^2	analytikjena
iMark Microplate Reader	BioRad
Incubator	Heraeus
INFINITY gel documentation	Peqlab
LSM 700 confocal microscope	Zeiss
Mini Rocker-shaker PMR-30	Gran-bio
Mini-Trans-Blot System	BioRad
NanoDrop 2000 Photospectrometer	ThermoFisher
Nikon Eclipse Ti microscope	Nikon
Pipetboy	Hirschmann Laborgeräte

Pipettes (10, 20, 200 µl; 1ml)	Gilson
PowerPack 300	BioRad
Protran Nitrocellulose Membrane 0,45 µM	Whatman
PVDF filter 0,22 µM/ 0,45 µM	Merck Millipore
Thermomixer compact	Eppendorf
Vortex shaker	ThermoFisher
X-Ray film	Kodak
X-Ray film processor MI-5	Medical Index GmbH

Table 6. Software

Name	Supplier
ApE	Open source
Illustrator CS6	Adobe
Image J	Open source
Microsoft Office 2016	Microsoft
Photoshop CC 2015	Adobe
Prism 5	Graph Pad Software
R/RStudio	Open source
SnapGene Viewer	GSL Biotech
Zen 2012	Zeiss

Table 7. Cell lines

Name	Species	Type	Medium
CHO	C. griseus	Epithelial-like ovary cells	GMEM (20% FBS, GS supplement)
COS-7	C. aethiops	Kidney fibroblast	DMEM (10% FCS, P/S)
HEK293T	H. sapiens	Kidney epithelium	DMEM (10% FCS, P/S)
HeLa	H. sapiens	Cervix epithelium	DMEM (10% FCS, P/S)
STC-1	M. musculus	Intestinal neuroendocrine tumor	DMEM (10% FCS, P/S)

Table 8. siRNA

Name	Sequence (5‘ – 3‘)	Supplier
Hs_TMEM260 s29747	GGATCCAGTATGTCTGAAATT	Ambion

Hs_TMEM260 s29746	GACTTACGAGTGGTATTTATT	Ambion
Hs_Rasal1 s16009	GGCTATCTGCTGAAGCGCATT	Ambion
Hs_Rasal1 s16011	CCAAGTCGATGGAACAGTTTT	Ambion
Mm_Rasal1 1397207	CTGGTGAAAGTGGATGACCAA	Qiagen
Mm_Rasal1 1397228	CACGCGCTTTGCCTTCAAGAA	Qiagen
Mm_Rasal1 1397214	AACGTGAATGACCTCAACCAA	Qiagen
Mm_Rasal1 1397221	TGGGAAGATCTCATTGACAA	Qiagen
Negative Control siRNA	AATTCTCCGAACGTGTCACGT	Qiagen

Table 9. Expression vectors and cDNA plasmids

Name	Application	Origin
FLAG-Rnd1	Overexpression, pcDNA3	cloned
GFP-K-Ras CA (G12V)	pEGFP-C1	D. Brandt, Marburg
GFP-Rasal1	pEGFP-C1	cloned
GFP-R-Ras CA (G38V)	pEGFP-C1	D. Brandt, Marburg
GST-Raf1	Bacterial expression	(Brtva et al. 1995)
HA-Rnd1	Overexpression, pcDNA3	cloned
HA-R-Ras	Overexpression, pcDNA3	J. Swiercz, Bad Nauheim
HA-R-Ras CA (G38V)	Overexpression, pcDNA3	cloned
HA-R-Ras DN (S43N)	Overexpression, pcDNA3	cDNA Resource Center
LARG-FLAG	Overexpression, pcDNA3	J. Swiercz, Bad Nauheim
mRasal1-FLAG dC2	Overexpression, pcDNA3	cloned
mRasal1-FLAG dPH	Overexpression, pcDNA3	cloned
mRasal1-FLAG mutGAP	Overexpression, pcDNA3	cloned
mRasal1-FLAG WT	Overexpression, pcDNA3	cloned
mRasal2-FLAG	Overexpression, pcDNA3	cloned
MYC-hPlexin-B2	Overexpression, pcDNA3	J. Swiercz, Bad Nauheim
MYC-mPlexin-B2 dIC	Overexpression, pcDNA3	cloned
MYC-mPlexin-B2 E369G	Overexpression, pcDNA3	cloned
MYC-mPlexin-B2 RA	Overexpression, pcDNA3	cloned
MYC-mPlexin-B2 T1359M	Overexpression, pcDNA3	Rufeng Dai, Boston, USA

MYC-mPlexin-B2 T1730M	Overexpression, pcDNA3	cloned
MYC-mPlexin-B2 T79M	Overexpression, pcDNA3	cloned
pEGFP-C1	Mammalian expression, GFP Tag	(Britton et al. 2014)
pMD2.G	Mammalian expression, lentiviral plasmid for virus production	Addgene
pSecTag2 empty vector	pSecTag2	Addgene
pSecTag2 Semaphorin 4B	Overexpression, pSecTag2	cloned
psPAX2	Mammalian expression, lentiviral plasmid for virus production	Addgene
Rasa4-FLAG	Overexpression	Origene
Rasa4-FLAG mutGAP	Overexpression	cloned
shRasal1_1	shRNA knockout	Sigma
shRasal1_2	shRNA knockout	Sigma
shRasal1_3	shRNA knockout	Sigma
shRasal1_4	shRNA knockout	Sigma
shRasal1_5	shRNA knockout	Sigma
VSV-mPlexin-B1	Overexpression, derived from pUC19	L. Tamagnone, Turin, Italy
VSV-mPlexin-B1 IC	Overexpression, derived from pUC19	cloned

Table 10. Primer for DNA cloning

Primer name	**Sequence (5' – 3')**
For_BamHI_Rasa4 mutGAP	ATATAGGATCCGCCACCATGGCCAAG
For_NotI_FLAG_PB1IC	TATATAGCGGCCGCATGGATTACAAGGATGACGACGATAAGAGGAGGAAGAGCAAGCAGGC
For_NotI_VSV_PB1IC	GCGGCCGCATGTATACAGACATAGAGATGAACCGACTTGGAAAGAGGAGGAAGAGCAAGCAGGC

For_NotI_VSV_PB1IC_2	TATATAGCGGCCGCATGTATACAGACATAGAGATGAACCGACTTGGAAAGAGGAGGAAGAGCAAGCAGGC
For_Rasa4mutGAP_AF	TATATACCAACACCCTGTTCGCGAGCAACTCTCTGG
For1_EcoRI_Rasal1wt	TATATAGAATTCTGCAGATATCATGGCCAAGAG
For1_NdeI_VSV-PB1GAP	TATATACATATGCCAAGTACGCCCCCTAT
For2_VSVPB1GAP_OVERLAP	AGGAGGAAGAGCAAGCAGGCCCTGAG
For-BAMHI-Rnd1_pEF-FLAG	TATATAGGATCCATGAAGGAGAGACGGG
For-EcoRI-L-Rasal1_pEGFP-C1	TATATAGAATTCGGGCGGCGGCAGCGGCGGCGGCGGCAGCGGCGGCGGCAGCATGGCCAAGAGCGGCTCGC
For-EcoRI-L-Rsl1_pEGFP-C1_2	TATATAGAATTCGGGCGGCGGCAGCGGCGGCGGCGGCAGCGGCGGCGGCAGCATGAAGGTGCGCCTCACTGA
HINDIII_Rnd1_FOR	ATATATAAGCTTATGAAGGAGAGACGGGCCCC
Rev_Rasa4mutGAP_AF	ATATATAGGCCAGAGAGTTGCTCGCGAACAGGGTGTTGG
Rev_Rasa4mutGAP_BclI	TATATATGATCAGCGGGTTTATCACTTATC
Rev_Rasal1wt_NotI	ATATATGCGGCCGCCTACTTGTCGTCATCGTCTTTGTAGTCTCCCCG
Rev1_VSVPB1GAP_OVERLAP	CTCAGGGCCTGCTTGCTCTTCCTCCTCTTACCCAGGCGGTTCATTTCGA
Rev2_VSVPB1GAP_NheI	TATATACTAGCTGGTCGACGCGTTAACTA
Rev3_VSVPB1GAP_NheI/BspOI	ATATATGCTAGCTGGTCGACGCGTTAACTA
Rev-Sal1-TAA-Rasal1_pEGFP-C1	TATATAGTCGACTTATCCCCGTTTCTGGAACTCCTCG
Rev-Sal1-TAA-Rsl1_pEGFP-C1_2	TATATAGTCGACTTACTCGTCCACATCCACCAGCT
REV-SpeI-Rnd1-pEF-FLAG	ATATATACTAGTTTACCATAATGGCATAATGGAACAG

Rnd1_Linker_FLAG _XBaI_REV	ATATATTCTAGATTACTTATCGTCGTCATCCTTGTAATCCC ATAATGGCATAATGGAACAGCTTTTGG

Table 11. Primer for qPCR

Primer name	Sequence (5‘ – 3‘)
csGAPDH_for1	GAAGGTGAAGGTCGGAGTCA
csGAPDH_rev1	TGACAAGCTTCCCGTTCTCA
csRasal1_for1	GAACGAGCTCAACCAGTGGC
csRasal1_rev1	TCCTCCAGTAATTTCAGCCTGAGC
For1_CS_TMEM260	GGTGAAAGCCAATGCGTGG
For1_MM_PB1_NIS	GTACAGCCACCACTTCGTGA
For2_Gastrin_NIS	AGATGCAGCGACTATGTGTGT
hGAPDH_for1	TGAAGACGGGCGGAGAGAAA
hGAPDH_rev1	TTCCCGTTCTCAGCCTTGAC
hRASAL1_for1	CGAGCACCAGGATGTGAAGT
hRASAL1_rev1	CATCCCCATCCACATCCACC
hsGastrin_for1	GCCTCTCATCATCGAAGGCA
hsGastrin_rev1	GCTTCTTGGACGGGTCTGC
mmGastrin_for1_NIS	AACAGCGCCAGTTCAACAAG
mmGastrin_rev1_NIS	TGAAGTGTTGAGGACCCTGG
mmRasal1_for1	TGGACCTGAACCGCTCTC
mmRasal1_for1_NIS	AGCATGCCAATTCAGAGCCT
mmRasal1_for2_NIS	CTGGACACAGCCCTTCCAAT
mmRasal1_for2_NIS	CCCCAGTCCGTTCTTCTGAG
mmRasal1_rev1	AGGCTGGTCTCCCGTACC
mmRasal1_rev1_NIS	GCATGCTCACGCATCACTTT
mmR-Ras_for1_NIS	CTGTGTCCTGCTGTAGCCAA
mmR-Ras_rev1_NIS	GTAAGTGTGAGGCAGCTGGT
Rev1_CS_TMEM260	GAGCGCAGGGAGGAGAAAAT
Rev1_MM_PB1_NIS	TGAAGGCACACTCGAGACAC
Rev2_Gastrin_NIS	CCCTGTACCTAAGGGTGCAT

7 Methods

7.1 Cell culture

All epithelial cell lines of different species (Table 7) were cultured at 37 °C and 5% CO_2. All media contained 10-20% fetal calf serum (FCS)/fetal bovine serum (FBS), 100 U/ml penicillin and 100 µg/ml streptomycin. For culture, the cells were split every other day by removing the medium, washing once with PBS and adding trypsin/ethylenediaminetetraacetic acid (EDTA) at 37 °C for detachment. Then, trypsin/EDTA was deactivated by dilution with medium; one part of the solution remained in the cell culture flask being filled up with an appropriate amount of medium, the other part was discarded or used for further analysis. For this purpose, cells were seeded in different concentrations into different sized well-plates and incubated for several hours to attach to the surface before further treatment was performed.

7.2 In-vitro cell manipulation

7.2.1 Transient Transfection

To introduce and transcribe complementary DNA (cDNA) plasmids transiently, COS-7 and STC-1 cells were transfected with Lipofectamine 2000 Transfection reagent (ThermoFisher) and HeLa cells with FuGENE HD Transfection Reagent (Promega) according to manufacturer's instructions. For a 12-well plate, 3 µl of Lipofectamine 2000 and 1 µg of cDNA plasmids were diluted in 100 µl OptiMEM, incubated for 30 min at room temperature (RT) and added dropwise to the cells. For FuGENE transfection in a 6-well plate, 6 µl of FuGENE and 2 µg of cDNA plasmid was diluted in 200 µl of OptiMEM and incubated for 10 min at RT before being added dropwise to the cells. In addition to that, HEK293T cells were transfected with calcium phosphate (Graham and van der Eb 1973; Worzfeld and Swiercz 2017) by mixing ddH_2O with cDNA plasmids and calcium chloride ($CaCl_2$). Afterwards, 2x BBS was shaken vigorously, added and incubated for 30 min at RT. Then, the mix was dropwise pipetted onto the seeded cells, incubated at 37 °C for 3 h followed by a medium change. After 24-48 h post transfection, the cells were used for further experiments.

For knocking-down a protein transiently, all seeded cells were transfected with Lipofectamine RNAiMAX Transfection Reagent according to manufacturer's instructions and analyzed 72 h post-transfection. Shortly, for a 6-well plate, 5 µl of RNAiMAX and 3 µl of 10 µM siRNA (Table 8) were diluted in 200 µl of OptiMEM and incubated for 20 min at RT before being added dropwise to the cells.

7.2.2 Stable cell lines

For stable reduction of protein expression, small hairpin RNAs (shRNAs) were used. Binding of complementary shRNAs to mRNA leads to degradation of the mRNA which results in no target protein production. The advantage of this method is the virus-mediated incorporation of foreign genetic material into the host's cell genome, allowing a stable knockdown of proteins in comparison to siRNA transfection. In addition to that, it allows to pick effectively transduced cells via an antibiotic selection. For this purpose, HEK293T cells were seeded and transfected with calcium phosphate to introduce lentiviral plasmids that encode for packaging proteins (psPAX), envelope proteins (pMDG.2) and a lentiviral vector that contained the DNA of choice. This system allows a constitutive expression of all necessary proteins to produce lentiviral particles that are capable of infecting mammalian cells and deliver the target DNA into the host cell without having the ability to produce infectious particles. 48 h post transfection, the supernatant was harvested and polybren (hexadimethrine bromide) was added to a final concentration of 8 µg/ml to enhance transduction efficiency (Davis et al. 2002). Afterwards, the supernatant was sterile filtered through a 0,45 µm polyvinylidene fluoride (PVDF, Merck) filter and added to previously seeded COS-7 or HEK293T cells. 24-48 h later, the supernatant was aspirated and the antibiotic selection and splitting of freshly transduced cells started.

As a preparation for antibiotic selection, a killing curve was performed for each cell line to determine the required concentration of puromycin to sufficiently kill wildtype cells (2 µg/ml for HEK293T and COS-7). This concentration was then used to select and afterwards cultivate the newly created cell line containing the shRNA sequence.

7.3 Biochemical methods

7.3.1 SDS-polyacrylamide-gel electrophoresis (SDS-PAGE)

For specific, antibody-mediated, detection of proteins from cell lysates, an SDS-polyacrylamide-gel electrophoresis (SDS-PAGE) was performed. This method allows a voltage dependent separation of proteins according to their molecular weight. The SDS-PAGE is a discontinuous electrophoresis, in which gels are made of a separation and a stacking gel allowing a better resolution of protein separation (Laemmli 1970).

Pre-treated or transfected cells were lysed either in Laemmli buffer and directly boiled at 99 °C for 5 min or in radioimmunoprecipitation (RIPA)/NP-40 buffer. Samples lysed in RIPA or NP-40 buffer were used for further biochemical methods, and afterwards Laemmli buffer was added and samples were boiled at 99 °C for 5 min for protein denaturation. Independently of the pre-treatment, all samples were centrifugated at 10.000 g for 3 min and loaded onto an SDS-polyacrylamide gel with different percentages depending on the expected molecular weight (Table 12). After loading, the proteins were weight-separated between 80-160 V for 90 min using the Mini-PROTEAN III cell gel system (BioRad). Afterwards, the separated proteins were stained with Coomassie brilliant blue or transferred to a nitrocellulose membrane via Western blot for immunodetection.

Table 12. Composition of stacking and separation gel for SDS-PAGE.

Components	Stacking gel	Separation gel
APS (w/v)	0,15%	0,1%
RotiPhorese Gel 30 (v/v)	19%	6-15%
SDS (w/v)	0,1%	0,1%
TEMED	14,5 µM	9,5 µM
Tris-HCl	0,12 M	0,36 M
pH	6,8	8,8

7.3.2 Coomassie brilliant blue staining

Proteins in an SDS-polyacrylamide gel were unspecifically stained with Coomassie brilliant blue, a dye that can electrostatically bind to amino and carboxyl groups of proteins (Bradford 1976) by incubating the gel in the staining solution for 30 min at

RT. Afterwards, the gel was de-stained with de-staining solution overnight (ON) and documented with a photo camera.

7.3.3 Western blot

The blotting of proteins from an SDS-polyacrylamide gel to a membrane is called Western blot (Burnette 1981) and allows unspecific staining or specific antibody-mediated detection of proteins.
The SDS-polyacrylamide gels from SDS-PAGE were transferred to a nitrocellulose membrane (pore size 0,45 µm, Whatman) with the Mini Trans-Blot Electrophoretic Transfer Cell system (BioRad). Usually, the transfer was performed at 350 mA for 75 min at RT. To check a successful transfer, a membrane staining with Ponceau S was performed to stain proteins unspecifically. To reverse this staining, the membrane was washed for several minutes in ddH_2O before being blocked in 5% milk powder in Tris-buffered saline with 0,1% Tween20 (TBS-T) for 30 min at RT. This step was followed by a first antibody incubation for 1 h at RT for directly conjugated antibodies to horseradish peroxidase (HRP). Alternatively, first antibodies were incubated at 4 °C ON, followed by three washing steps in TBS-T and an incubation with HRP-conjugated secondary antibody for 1 h at RT. Later, all membranes were washed for three times in TBS-T and were detected with ECL reagent by exposing the membrane to X-Ray films and development with an X-Ray film processor (Medical Index GmbH).

7.3.4 Pulldown assay

The glutathione S-transferase (GST)-Raf-1 pulldown is a biochemical method, that allows an enrichment of active, GTP-loaded Ras isoforms by binding to the Ras-binding domain (RBD) of the Raf-1 effector protein fused to GST. This recombinant protein can bind with strong affinity to glutathione agarose allowing the pulldown of active Ras (Worzfeld and Swiercz 2017).

7.3.4.1 Production of GST-Raf-1 agarose

This protocol has been reported previously by Worzfeld and Swiercz. Chemically competent Rosetta DE3 *E. coli* were transformed with the pGEX GST-Raf-1 plasmid as described in 7.2.1. For pre-culture, bacteria were transferred into

prepared Erlenmeyer flasks containing 250 ml LB medium with chloramphenicol (12,5 mg/ml, 1:1000) and ampicillin (100 mg/ml, 1:1000) and incubated ON at 37 °C. The next day, the overnight culture was diluted 1/10 with LB medium and antibiotics and further cultivated at 37 °C until the absorbance reached an optical density of 0,8 at 600 nm (OD_{600}). Isopropyl β-D-1-thiogalactopyranoside (IPTG) was added at a final concentration of 500 mM and bacteria were incubated for 3 h at 30 °C. The bacteria were pelleted at 4600 g for 10 min at 4 °C, the supernatant was discarded, and the pellet was washed once in ice-cold PBS. *E. coli* were lysed in ice-cold LBG buffer and sonicated three times for 15 s at 80% of maximum power. Afterwards, 1% Triton X-100 was added to the lysates and incubated on a roller for 15 min at 4 °C, followed by a centrifugation step at 17.000 g for 10 min at 4 °C. Glutathione agarose 4B, previously once washed with LBG buffer, was added to the *E. coli* supernatant and incubated on a rotator for 1 h at 4 °C. The mixture was centrifugated at 3200 g for 5 min at 4 °C and the supernatant was removed. After three washing steps with LBG buffer, the pelleted agarose was resuspended in 50% glycerol in LBG buffer, aliquoted and frozen at -80 °C.

7.3.4.2 GST-Raf-1 pulldown assay

Transfected HEK293T cells (see 7.2.1) were treated with different recombinant semaphorins in concentrations between 25 and 150 nM for 20 min at 37 °C or starved in FCS-free medium ON followed by stimulation. HEK293T cells were lysed using the ice-cold protein lysis buffer (PLB) containing protease inhibitors (Roche). The cell lysates were cleared by centrifugation at 17.000 g for 10 min at 4 °C and the supernatant was loaded on an aliquoted GST-Raf-1 agarose, after taking some µl for lysate control. After an incubation step on a rotator for 50 min at 4 °C, the samples were centrifuged at 17.000 g for 1 min and washed three times with PLB buffer. Lysates and GST-Raf-1 agarose were resuspended in Laemmli buffer and boiled for 5 min at 99 °C before continuing with SDS-PAGE (see 7.3.1). Alternatively, the Ras Pull-down Activation Assay Biochem Kit (Cytoskeleton, Inc.) was used according to manufacturer's instructions.

7.3.5 Co-Immunoprecipitation (CO-IP)

The Co-Immunoprecipitation (CO-IP) is a biochemical method to study protein-protein interactions. Cell lysates are incubated with agarose beads coupled to antibodies (similar to 7.3.4.2) that allow a pulldown of specific proteins with their

interaction partners. By performing a Western blot, other proteins, interacting with the precipitated protein, can be detected.

For this experiment, previously seeded, transfected and/or pre-treated HEK293T cells in 10 cm dishes were harvested by discarding the medium and adding an appropriate amount of lysis buffer (usually between 500-1000 µl). For this study, a stringent RIPA buffer and a less stringent NP-40 buffer containing protease and phosphatase inhibitors (Roche/ThermoFisher) were used depending on the interaction properties of the desired proteins. The lysates were transferred into an Eppendorf tube and incubated on a roller for 10 min at 4 °C followed by clearing of lysates at 17.000 g for 10 min at 4 °C. Meanwhile, 20 µl of Protein A/G agarose or ANTI-FLAG M2 Affinity Agarose Gel (Sigma) were washed once with ice-cold lysis buffer. After taking some lysate for total protein control, the supernatant was loaded onto the agarose. 2 µg of specific antibody was added to samples with Protein A/G agarose. After incubation on a roller for 90 min at 4 °C, the agarose beads were centrifuged at 10.000 g for 10 s at 4 °C and washed 4 times with ice-cold lysis buffer. Lysate control and agarose beads were resuspended in 4x/2x Laemmli buffer and boiled for 5 min at 99 °C before being loaded on an SDS-PAGE followed by a Western blot (see 7.3.3).

7.3.6 Mass spectrometry

Analyzation of interaction partners and post-translational modifications (PTM) of Rasal1 were performed in cooperation with Dr. Johannes Graumann (Max-Planck-Institute for Heart and Lung Research, Bad Nauheim). For this reason, HEK293T cells were transfected with cDNA plasmids for Rasal1-FLAG and VSV-Plexin-B1 and treated with Semaphorin 4D [25 nM]. Afterwards, an immunoprecipitation against Rasal1-FLAG was performed (see 7.3.5) and the samples were snap-frozen in liquid nitrogen before mass spectrometry analysis.

7.3.7 Production and purification of human Semaphorin 4D

Lec3.2.8.1 Chinese hamster ovary cells (CHO cells) that produce soluble histidine-tagged Semaphorin 4D (Davis et al. 1990; Love et al. 2003) were cultured in GMEM (Sigma Aldrich) with 20% FBS (Gibco) and GS supplement (Sigma Aldrich) until confluency. The medium was collected every other day and stored at 4 °C for two weeks. After medium collection, the supernatant was centrifugated at 3000 g for 10 min at 4 °C and filtered through a Filtropur V25 0,45 µM (Sarstedt). Then,

the medium was diluted 1:3 with PBS and 1M Tris-HCl (pH 8,0) was added to a final concentration of 10 mM. For each liter of medium, 2.5 ml of Ni-NTA agarose (Qiagen) was added and incubated on a rotator for 2 h at 4 °C. Afterwards, the Ni-NTA agarose was separated from the medium using an Econo-Column Funnel (BioRad). The agarose was washed with 20-50 ml of PBS containing 10 mM Tris-HCl (pH 8,0) followed by elution of histidine tag-bound Semaphorin 4D with 10-20 ml of histidine elution buffer. The eluate was concentrated in an Amicon Ultra-15 tube (Millipore) until the volume was less than 250 µl. In cooperation with Dr. Sabrina Sapski (Institute of Pharmacology, Max-Planck-Institute for Heart and Lung Research, Bad Nauheim), Semaphorin 4D was further purified in a gel filtration chromatography and fractionated. Appropriate fractions were afterwards pooled and the concentration of Semaphorin 4D was determined by performing a Coomassie Gel SDS-PAGE (see 7.3.2) and comparing amount of protein to a BSA standard.

7.3.8 Biotinylation of cell surface proteins

For the detection of membrane proteins, a method previously described by Elia 2012 and Pischedda et al. 2014 was used by covalently adding biotin to primary amines of proteins exposed extracellularly. After precipitation and antibody specific detection, the membrane-associated protein of interest could be encountered.
The biotinylation reaction of a 10 cm dish with previously seeded cells (see 7.1) was performed by washing the cells two times with ice-cold PBS followed by incubation with 8 ml of biotin-NHS (Sigma) in PBS (0,25 mg/ml) for 10 min at 4 °C with gentle shaking. Afterwards, the reaction was quenched by adding of 6 ml Tris-HCl (50 mM, pH 7,4) and the cells were scraped off the dish and collected in a 50 ml tube. Then, cells were pelleted at 3000 g for 5 min at 4 °C and washed 3 times with ice-cold PBS. The pellet was resuspended in 800 µl of lysis buffer containing protease inhibitors (Roche) and an immunoprecipitation was performed with 20 µl of Pierce Streptavidin Agarose against biotin as described in 7.3.5.

7.4 DNA cloning methods

7.4.1 Polymerase chain reaction (PCR)

The polymerase chain reaction (PCR) is a standard method to amplify specific DNA sequences by thermal cycling. The specificity can be obtained by primer design and annealing temperatures. Generally, a DNA template is denaturated and forward/reverse primers can anneal to the desired sequence and a heat-resistant DNA-dependent DNA polymerase can then synthesize the DNA fragment between the two primers. By cycling of these steps, the fragment is exponentially produced and can be used for further applications.

The standard reaction mixture for generating PCR products is shown in Table 13. For this purpose, the Phusion Hot Start High-Fidelity DNA Polymerase (Phusion) system (ThermoFisher) was used according to manufacturer's instructions. All primers for cloning are presented in Table 10 with their restriction sites and corresponding template (usually cDNA from pre-existing plasmids (Table 9)).

Table 13. Standard reaction mix for PCR with Phusion

Components	Amount [µl]
HF buffer	10
dNTP	1
Forward primer [10 µM]	1
Reverse primer [10 µM]	1
DMSO	1
cDNA Template [100 ng]	X
Phusion	0,2
ddH_2O [final volume 50 µl]	X

The PCR was performed in a FlexCycler^2 (analytikjena) according to a standard protocol (Table 14). The annealing temperature (T_A) was calculated from the respective primer melting temperatures (T_m, T_A=T_m-5). In addition, the extension time depended on the length of the PCR product (Phusion extension speed 15-30 s/kb) and the cycle number on the final PCR product amount.

Table 14. Standard protocol for Phusion PCR

Step	Temperature [°C]	Time [s]	
Denaturation	98	30	
Denaturation	98	10	25-35 cycles
Annealing	X	10	
Extension	72	X	
Final Extension	72	5	
Hold	4	∞	

7.4.2 Overlap PCR

To fuse two PCR products, an overlap PCR was performed. By designing a 20 bp overlap between the PCR products, annealing and creation of a new template was achieved, followed by thermal cycling amplification. The pipetting scheme for such an overlap PCR is presented in Table 15. The protocol used for the overlap PCR was the standard protocol for Phusion PCR (Table 14).

Table 15. Reaction mix for overlap PCR with Phusion

Components	Amount [µl]
HF buffer	10
dNTP	1
5' primer [1 µM]	1
3' primer [1 µM]	1
DMSO	1
PCR template 1 [200 ng]	X
PCR template 2 [200 ng]	X
Phusion	0,5
ddH_2O [final volume 50 µl]	X

7.4.3 Enzymatic digest of PCR products and cDNA plasmids

An enzymatic digest of DNA is needed to create sticky DNA ends, that are complementary to each other and allow a directed ligation between different pieces, e.g. ligate a PCR product into a vector backbone (see 7.4.5). A second application is the test digest, where cDNA plasmids are digested, loaded on an agarose gel (see 7.4.4) and checked for expected fragment sizes. This digest was

being conducted by restriction enzymes (ThermoFisher) that have a specific DNA sequence restriction site. Digests were performed with one or two enzymes depending on the application. Each combination of enzymes needed different buffer conditions. The right buffer was chosen by using the ThermoFisher Double Digest Calculator. A standard pipetting digest mix consisted of the respective buffers, the enzymes, the template (PCR product, cDNA plasmid) and ddH_2O (final volume 40 µl). Then, the digest was incubated for 1 h at 37 °C and loaded on an agarose gel for purification/analysis.

7.4.4 Agarose gel electrophoresis

To purify or isolate PCR products/vector backbones, samples were mixed with 10X DNA loading dye, loaded on agarose gels (0,8-2% agarose in TAE buffer) containing 1,25 µM ethidium bromide and run at 80-120 V for 1 h. Afterwards, the DNA bands were visualized and photographed under UV-light using the INFINITY gel documentation system (Peqlab). Specific bands were cut out with a scalpel and isolated with the NucleoSpin Gel and PCR clean-up kit (Macherey-Nagel) according to manufacturer's instructions.

7.4.5 Ligation

The PCR products were ligated into an expression vector backbone. The vector backbone and the PCR product were previously digested with restriction enzymes creating matching overlaps (see 7.4.3) and ligated using the T4 DNA ligase system (ThermoFisher). For ligation, PCR products were added in different molecular ratios (0:1, 1:1, 3:1, 5:1) to the backbone (100 ng) together with T4 DNA ligase buffer and ddH_2O to a final volume of 20 µl. The mix was incubated for 1 h at RT. Afterwards, 5 µl of the ligation were directly transformed into competent *E. coli* (see 7.4.7) or frozen for further use.

7.4.6 Mutagenesis

Mutagenesis of cDNA plasmids is a standard technique in molecular biology to introduce point mutations, switch nucleotides and to delete or insert base pairs. This can be achieved through standard cloning techniques like PCR amplification, digestion and ligation, by designing primers carrying the desired mutations or by

mutagenesis kits, that allow an in vitro site-directed mutagenesis. In this study, standard techniques and mutagenesis kits were used. For mutating Plexin-B2, the QuickChange XL Site-Directed Mutagenesis Kit (Agilent Technologies) was used according to manufacturer's instructions. All other constructs were mutated using standard cloning strategies (see 7.4 ff.)

7.4.7 Transformation and plasmid isolation

For the amplification of cDNA plasmids, constructs were transformed into competent One Shot Top10 Chemically Competent *E. coli* (ThermoFisher). According to the protocol, 6 µl of ligations or 200 µg of cDNA plasmids were mixed with 50 µl of chemo competent *E. coli* and kept on ice for 30 min. Then, the mixture was heat shocked for 45 s at 42 °C and again kept on ice for 5 min. Afterwards, bacteria were incubated with lysogeny broth (LB) medium without antibiotics on a shaker at 37 °C for 1 h followed by their cultivation at 37 °C ON an agarose plate containing selection antibiotics. The next day, colonies were picked and incubated on a shaker in 2 mL of LB medium with antibiotics at 37 °C ON, in order to perform a mini plasmid isolation of cloned construct using the NucleoSpin Plasmid Miniprep Kit (Macherey-Nagel) according to manufacturer's instructions. Further characterizations of the construct followed like test expression in eukaryotic cells (see 7.2.1), test digest (see 7.4.3) or sequencing using the Seqlab-Microsynth service (Balgach, Switzerland) followed by analyzing the results with the SnapGene Viewer (GSL Biotech, snapgene.com).
For preparative cDNA plasmid isolation, colonies were incubated in 2 ml of antibiotics containing LB medium on a shaker for 1 h at 37 °C. Pre-culture was added to an Erlenmeyer flask containing 250 ml of LB medium and antibiotics. The bacteria were incubated on a shaker at 37 °C ON. The day after, cDNA plasmids were isolated using the NucleoBond Xtra Midi Kit (Macherey-Nagel) according to manufacturer's instructions.

7.5 Molecular biological methods

7.5.1 RNA isolation and reverse transcription

To isolate RNA from the respective seeded cells in 6-well plates, 1 ml of peqGOLD TriFast (Peqlab) was added to the cells. After an incubation of 5 min at RT, the

lysate was transferred into an Eppendorf tube and 200 µl of chloroform were added, vortexed and incubated for another 5 min at RT. The mixture was centrifugated at 17.000 g for 15 min at 4 °C followed by a transfer of the aqueous upper phase into a new tube. To precipitate the RNA, 500 µl of isopropanol were added and vortexed. The precipitation was performed either for 15 min at RT or for 1 h at -20 °C. Afterwards, the RNA was pelleted by centrifugation at 17.000 g for 10 min at 4 °C, washed once with 70 % ethanol and air-dried. The RNA was resuspended in nuclease free water for 10 min at 55 °C. The concentration was measured using the NanoDrop 2000 Spectrophotometer (ThermoFisher) and samples were stored at -80 °C or directly used for reverse transcription. For reverse transcription, around 500-2000 ng of RNA were reversed transcribed into cDNA using the First Strand cDNA Synthesis kit (ThermoFisher) according to manufacturer's instructions.

If the cell number was too small or a DNAse treatment was necessary for absolute quantification of mRNA expression levels using RT-qPCR (see 7.5.3), the RNA isolation was performed using the Direct-zol RNA MicroPrep kit including DNAse I treatment (Zymo Research) according to manufacturer's instructions, followed by reverse transcription.

7.5.2 Reverse transcriptase polymerase chain reaction (RT-PCR)

The reverse transcriptase PCR (RT-PCR) is a non-quantitative method to determine the expression of specific genes. For this, previously reverse transcribed cDNA (see 7.5.1) was mixed with specific primers, deoxyribose nucleoside triphosphate (dNTP), dimethyl sulfoxide (DMSO), a 10x Taq buffer with KCl and Taq DNA Polymerase from ThermoFisher (see Table 16). The PCR program is presented in Table 17. After thermal cycling, the samples were loaded on an agarose gel and documented as described in 7.4.4. Glyceraldehyde 3-phosphate dehydrogenase (GAPDH) was amplified as a house-keeping gene for normalization of target genes.

Table 16. Standard reaction mix for PCR with Taq DNA Polymerase

Components	Amount [µl]
10x Taq Buffer with KCl	5
dNTP	1
Forward primer [10 µM]	3

Reverse primer [10 µM]	3
DMSO	1,5
cDNA Template [100 ng]	X
Taq DNA Polymerase	0,5
ddH_2O [final volume 50 µl]	X

Table 17. Standard protocol for Taq DNA Polymerase PCR

Step	Temperature [°C]	Time [s]	
Denaturation	95	120	
Denaturation	98	30	30 cycles
Annealing	T_M-5	30	
Extension	72	1 min/kb	
Final Extension	72	5	
Hold	4	∞	

7.5.3 Quantitative real-time RT-PCR (RT-qPCR)

The quantitative real-time RT-PCR (RT-qPCR) is a quantitative method to study gene expression in real-time by measuring the cycle-wise fluorescence intensity of SYBR Green, a dye that intercalates with double stranded DNA during PCR amplification. Its principle is based on the method of the PCR (see 7.4.1) and was performed with the iQ SYBR Green Supermix (BioRad) in a Real Time Quantitative Thermal Cycler (BioRad) according to manufacturer's instructions. Shortly, the cDNA was mixed with the respective forward/reverse primers and the IQ SYBR Green Supermix (see Table 18). The mix was then pipetted into a 96-well plate. The standard protocol for a RT-qPCR is presented in Table 19, used primers are listed in Table 11.

Table 18. Standard reaction mix for RT-qPCR.

Components	Amount [µl]
SYBR Green Supermix	12,5
Forward primer [10 µM]	0,25
Reverse primer [10 µM]	0,25
cDNA [20 ng]	5
ddH_2O [final volume 25 µl]	7

Table 19. Standard protocol for RT-qPCR

Step	Temperature [°C]	Time [s]	
Denaturation	95	180	
Denaturation	95	10	40 cycles
Annealing	60	30	
Extension	72	30	
Final Extension	72	120	
Melting	55 → 95	10	

For relative gene expression analysis, the ΔC_t [gene of interest] was normalized to ΔC_t [GAPDH] by subtraction and fold change calculation ($\Delta\Delta C_t$), equaling thr relative expression of the target gene in comparison to GAPDH.
This method can be also used to determine absolute expression of a target DNAse pre-treated RNA/cDNA transcript. To measure copy numbers of transcripts per ng of RNA, a standard expression curve of isolated genomic DNA (gDNA, see 7.5.4) is being measured and a conversion function is used to calculate an absolute copy number.

7.5.4 Genomic DNA isolation

Previously seeded cells in a 6-well plate were lysed in 1 ml gDNA isolation buffer with proteinase K (500 µg/ml) and incubated at 37 °C ON. The next day, the lysate was mixed with 0,5 ml Roti-phenol/chloroform/isoamyl alcohol (Roth) and was centrifuged at 17.000 g for 5 min at RT. The upper phase was transferred into a new Eppendorf tube and 0,5 ml of chloroform were added, the phases mixed and centrifuged at 17.000 g for 5 min at RT. Again, the upper phase was transferred into a new Eppendorf tube and mixed with 0,1 volume of 3M sodium acetate (NaOAc) and 2,5 volumes of ice-cold ethanol. After mixing, the tube was centrifuged at 17.000 g for 5 min at RT. The pelleted DNA was washed once in 70% ethanol (v/v), air-dried and resuspended in TE buffer. After measuring the concentration, the gDNA was used for absolute quantification of mRNA expression levels using RT-qPCR (see 7.5.3).

7.6 Immunofluorescence

7.6.1 COS-7 collapse assay

The COS-7 collapse assay enables to study semaphorin-dependent plexin signaling in vitro. COS-7 cells, overexpressing plexins, collapse after semaphorin stimulation similar to the axonal growth cone collapse, which is mediated by an integrin-dependent reorganization of the cytoskeleton that leads to retraction and compression of the cytoplasm (Turner and Hall 2006; Yukawa et al. 2010b).
For this assay, COS-7 cells were seeded on coverslips in a 24-well plate. These coverslips were treated with 1 M HCl ON, washed with ddH_2O and sterilized with UV-light. The next day, cells were transfected with the cDNA plasmids of choice (see 7.2.1). 24 h later, transfected COS-7 cells were treated with semaphorins (25-150 nM), either alone or together with BAPTA-AM (10 µM), ATP (50 µM) or starving medium for 1 h at 37 °C. Afterwards, the cells were stained with an immunofluorescence staining (see 7.6.2), microscopic images were taken and blinded quantitative analysis was performed using a Zeiss LSM 700.

7.6.2 Immunofluorescence staining

To stain specific proteins with fluorophore-tagged antibodies, previously seeded on coverslips, transfected and pre-treated cells were washed three times with PBS and fixed in 4% para-formaldehyde (PFA) for 20 min at 37 °C. Fixed cells were permeabilized wit 0,2% Triton X-100 in PBS for 20 min at RT, followed by a short blocking step with 1% BSA in PBS. Then, coverslips were incubated with antibodies in 1% BSA in PBS for 1 h at RT. After three washing steps with PBS, the firstly used antibody was marked with a fluorophore-conjugated second antibody and the DNA was stained with 4′,6-diamidino-2-phenylindole (DAPI; 3,6 µM) for 1 h at RT. Finally, the samples were washed four times with PBS and mounted on microscopic slights with DAKO fluorescence mounting medium (Agilent Technologies). Microscopic images were taken using a Zeiss LSM 700 microscope.

7.7 Live-cell imaging

7.7.1 Translocation studies of GFP-Rasal1

To investigate the localization of GFP-Rasal1 in the cell after application of different compounds, a live-cell imaging was performed. Therefore, HeLa cells were seeded in a µ-Slide 8 well plate (ibidi) and were transfected with the cDNA plasmid coding for GFP-Rasal1 according to 7.2.1. After 24 h, the slide was imaged with a Zeiss LSM 700 microscope over a time course of up to 5 min with one picture every 2 s. The cells were treated with Semaphorin 4D (50-150 nM) and/or histamine (100-400 µM) while the fluorescence intensity and localization of GFP-Rasal1 was measured (Walker et al. 2004; Liu et al. 2005). Different regions of interest (ROIs) were set in the cytoplasm of HeLa cells and the mean fluorescence intensity was quantified for different cells during the time course. The data analysis was made with ImageJ and Microsoft Excel 2016, calculating the relative translocation of GFP-Rasal1 normalized to the fluorescence background.

7.8 Pharmacological methods

7.8.1 Alkaline-Phosphatase (AP)-assay

A pharmacological approach to determine binding of a specific ligand to its receptor is a dose-dependent measurement of receptor occupancy. For this purpose, an assay was designed, in which Semaphorin 4C bound to its receptor Plexin-B2, can be detected in a colorimetric experiment, where a specific antibody against the F_c part of recombinant mouse Semaphorin 4C chimera protein (Rndsystems) is coupled to alkaline phosphatase (Flanagan and Leder 1990; Tamagnone et al. 1999; Deng et al. 2007). After adding 4-nitrophenyl phosphate disodium salt hexahydrate (phosphatase substrate, pNPP, Sigma Aldrich), an enzymatic reaction by the alkaline phosphatase to p-nitrophenol is taking place. The yellow, insoluble product can be detected with an iMark microplate reader (BioRad) by measuring the absorption at 415 nm. The experimental procedure starts with transfected COS-7 cells (6000 cells) previously seeded in a 96-well plate overexpressing Plexin-B2 constructs and/or siRNA against TMEM260. 24 h post transfection, the cells were treated with Semaphorin 4C in different concentrations together with an AP-conjugated antibody against mouse $F_{c\gamma}$ fragments (1:5000) for

90 min at 4 °C. Then, the cells were washed three times with cold Hank's balanced salt solution (HBSS) to wash-out excessive, unbound antibodies. This step was followed by incubation of pNPP in pNPP buffer for 10-15 min at 37 °C until yellow precipitate was visible, and the absorption was measured at 415 nm using an iMark microplate reader (BioRad). The analysis consisted of a background subtraction of untransfected control cells and an average calculation of dupli-/triplicates.

8 Results

8.1 The role of TMEM260 in plexin signaling

8.1.1 Functional characterization of TMEM260 knockdown in vitro

The IPT domains of plexins are not being O-mannosylated by POMT1/POMT2 or TMTC1-4 in comparison to other glycosylation sites of the cadherin superfamily, indicating the existence of a so far unknown candidate performing this glycosylations (Larsen et al. 2017a; Larsen et al. 2017b). Recent unpublished data from Adnan Halim and colleagues, University of Copenhagen, Denmark identified TMEM260 as a possible candidate for plexin O-mannosylation (Fig. 6A). TMEM260 is a protein with unknown function, that is encoded by the *TMEM260* gene. Truncated mutations in this locus cause a syndrome with neurodevelopmental, cardiac and renal symptoms (Ta-Shma et al. 2017). After the loss of TMEM260, the glycosylations at IPT domains are gone (unpublished data), suggesting, that TMEM260 may be involved in influencing semaphorin-plexin signaling, since glycosylations are important post-translational modifications (PTMs) for molecular trafficking/clearance, endocytosis and signal transduction (Ohtsubo and Marth 2006). To test this, different cell biological, biochemical and pharmacological assays were performed to characterize the role of TMEM260 in plexin signaling.

Initially, an siRNA knockdown of TMEM260 in COS-7 cells was established (Fig. 6B). Then, these cells overexpressing siRNA against TMEM260 were investigated concerning their ability to bind Semaphorin 4C. For this reason, an AP-assay was performed with COS-7 cells overexpressing Plexin-B2. The cells were incubated with different concentrations of Semaphorin 4C and the binding to Plexin-B2 was measured colorimetrically with an AP-tagged antibody against Semaphorin 4C as described above. It could be shown that the binding of Semaphorin 4C to Plexin-B2 was significantly higher after the knockdown of TMEM260 in comparison to the untreated or control siRNA expressing COS-7 cells (Fig. 6C).

Further, a biotinylation assay was performed to confirm, if this observation was due to abrogated expression levels of Plexin-B2. For this reason, COS-7 cells, engineered to express Plexin-B2, and transfected with control siRNA or siRNA directed against TMEM260, were treated with biotin, resulting in biotinylation of surface proteins. After precipitation of all biotinylated proteins, a Western blot was

performed against Plexin-B2 revealing a higher amount of membrane-associated Plexin-B2 in cells treated with siRNA against TMEM260 compared to the cells transfected with control siRNA (Fig. 6D).

Besides, a possible involvement in downstream signaling was examined with a COS-7 collapse assay. COS-7 cells were transfected with Plexin-B2 and either control siRNA or siRNA directed against TMEM260 and treated with Semaphorin 4C followed by an immunofluorescence staining (Fig. 6E). Collapsed cells were quantified and no difference in the downstream signaling ability between control siRNA or siRNA against TMEM260 transfected COS-7 cells could be observed (Fig. 6F).

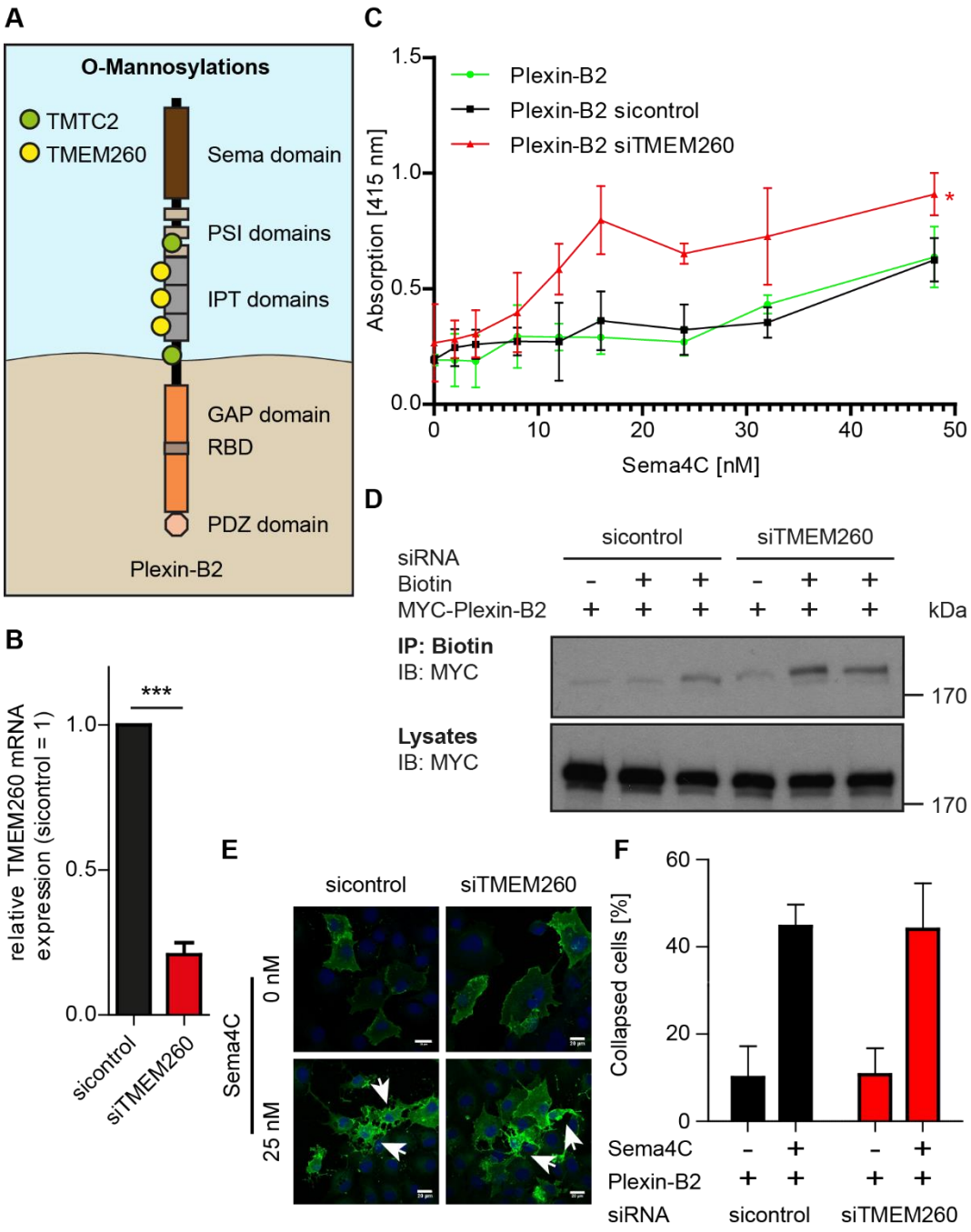

Figure 6. Knockdown of TMEM260 leads to elevated binding of Semaphorin 4C and increased plasma membrane localization of Plexin-B2 without altering downstream signaling. A) Plexin-B2 is O-mannosylated by transmembrane and TPR repeat-containing protein 2 (TMTC2) at the PSI domain and close to the transmembrane domain. O-mannosylations at the IPT domains are performed by TMEM260. B) Relative TMEM260 mRNA expression was quantified with RT-qPCR and sicontrol was used as relative control. COS-7 cells were transfected for 48 h with control siRNA (sicontrol) or siRNA directed against TMEM260 (siTMEM260) as described in Material and Methods. The values represent mean±SEM of 5 independent experiments, *** = p<0,001, two-sided t test. C) Alkaline phosphatase (AP)-assay of COS-7 cells overexpressing murine MYC-Plexin-B2 and either siRNAs sicontrol or siTMEM260. Cells were incubated with recombinant murine Semaphorin 4C (Sema4C) for 1 h at 4 °C. The absorption of antibody mediated AP activity of plexin-bound semaphorin was measured with 3 technical replicates at 415 nm and normalized to background

absorption. The values represent mean±SEM, * = p<0,05, one-way ANOVA, Dunnett test, Plexin-B2 sicontrol = control. D) Biotinylation assay of COS-7 cells overexpressing MYC-Plexin-B2 and siRNAs sicontrol or siTMEM260. Plasma membrane-associated proteins were biotinylated for 10 min at 4 °C and a precipitation for biotin was performed. MYC-Plexin-B2 was detected with Western blot analysis. E) COS-7 collapse assay of COS-7 cells overexpressing MYC-Plexin-B2 (green) and either siRNA sicontrol or siTMEM260 (DAPI (blue)). Cells were treated with 25 nM recombinant murine Semaphorin 4C for 1 h at 37 °C, followed by immunofluorescence staining and blinded quantification of collapsed cells, indicated with white arrows, scale bar 20 µm. F) Corresponding quantification of E) of three independent experiments. The values represent mean±SD.

8.1.2 Functional characterization of TMEM260 knockout in vitro

Additionally, the plasma membrane localization of endogenous Plexin-B2 was analyzed using HEK293 cells with a CRISPR-Cas9 mediated knockout of TMEM260 in order to elucidate the role of TMEM260 in protein targeting, with AC2 as a wildtype control and B1, D3 and F1 as TMEM260KO. These cells were kindly provided from Adnan Halim and colleagues and were firstly analyzed for their expression and localization of Plexin-B2 with immunofluorescence staining. As presented in Fig. 7A, all four cell lines had similar expression levels of endogenous Plexin-B2 and its localization to the plasma membrane at cell-cell contacts was not changed. Hence, a difference in expression levels or plasma membrane localization of Plexin-B2 could not be observed by comparing the control cell line AC2 with all TMEM260KO cell lines (B1, D3, F1). Furthermore, a Western blot for Plexin-B2 of total HEK293 lysates revealed bands in different intensities. While the WT control AC2 has a more intense band at 170 kDa and a less intense band at 250 kDa, all TMEM260KO cell lines (B1, D3 and F1) were reversed. These two bands represent full length (250 kDa) and the cleaved extracellular part of Plexin-B2 (170 kDa). Artigiani et al. 2003 provide strong evidence, that this cleaving process is performed by protein convertases at the cell surface and is necessary to increase ligand binding and induce signal transduction (Fig. 7B). Interestingly, a biotinylation assay of membrane-associated proteins showed more cleaved Plexin-B2 at the cell surface in all TMEM260KO cell lines (B1, D3, F1) in comparison to the WT (AC2) control (Fig. 7C).

In sum, these data indicate a role for TMEM260 in plasma membrane targeting and proteolytic processing of Plexin-B2 in siRNA and CRISPR mediated knockdown/knockout of TMEM260 in HEK293 cells. In the case of siRNA mediated knockdown, a significant increase in binding of Semaphorin 4C to Plexin-B2, without altering downstream signaling, could be noticed.

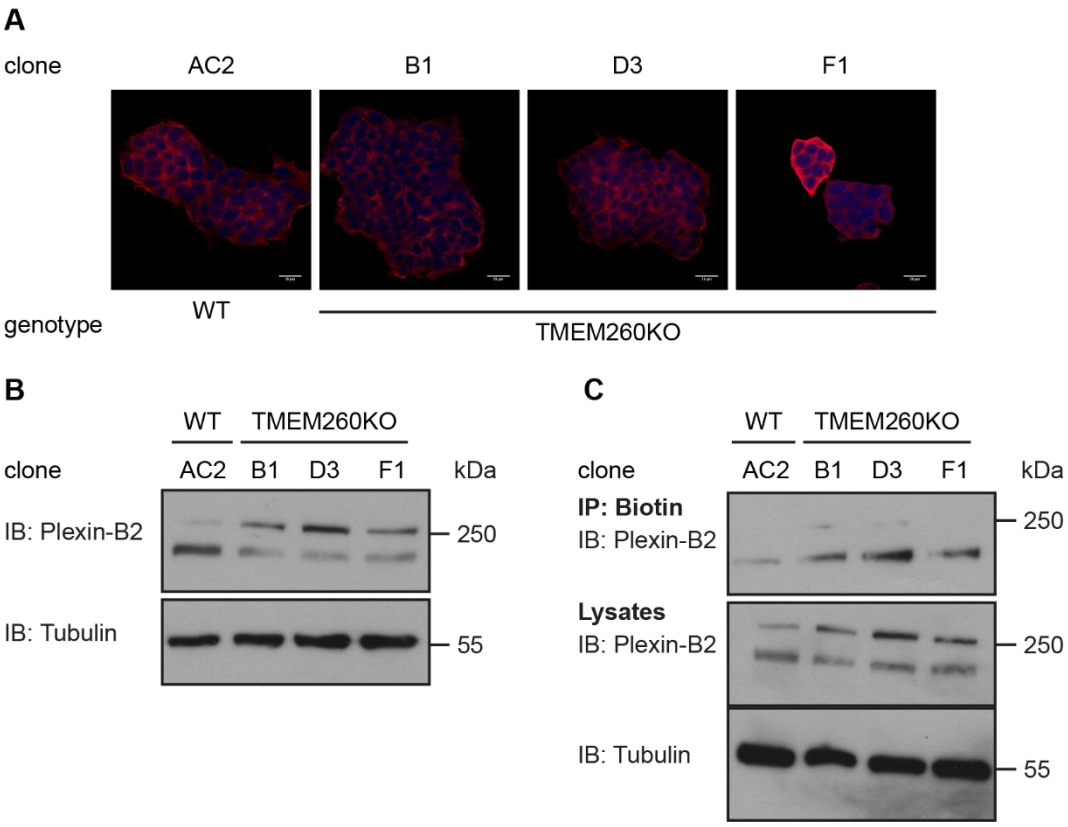

Figure 7. The knockout of TMEM260 in HEK293 cells leads to increased plasma membrane localization of Plexin-B2 and defective processing by protein convertases. A) Immunofluorescence staining of endogenous Plexin-B2 (red, DAPI (blue)) in HEK293 CRISPR cell lines AC2 (WT) and B1, D3, F1 (all TMEM260KO). B) Western blot analysis of Plexin-B2 expression in total lysates of HEK293 CRISPR cell lines AC2 (WT) and B1, D3, F1 (all TMEM260KO). C) Biotinylation assay of HEK293 CRISPR cell lines AC2 (WT) and B1, D3, F1 (all TMEM260KO). Membrane-associated proteins were biotinylated for 10 min at 4 °C and a precipitation for biotin was performed as described in Matherial & Methods. Plexin-B2 was detected with Western blot analysis.

8.2 The role of Rasal1 in plexin signaling

8.2.1 Are plexins GAPs? – An old controversy

Plexins have been described as semaphorin-dependent GAPs for R-Ras (Oinuma et al. 2004a), but direct GAP activity of isolated intracellular domains of plexins towards R-Ras could not be observed (Wang et al. 2012). The stimulation of Plexin-B1 with Semaphorin 4D leads to the deactivation of R-Ras that requires additional binding of Rnd1 to Plexin-B1, but the molecular mechanism is not understood (Fig. 8A). It is known that active, GTP-bound R-Ras can bind to the receptor Plexin-B1 in the presence of Rnd1 (Fig. 8B) and can be deactivated after application of Semaphorin 4D (Fig. 8C).

Here, this observation was confirmed in an overexpression system, where active R-Ras binds to Plexin-B1 in the presence of Rnd1. This effect is gone in absence of Rnd1 (Fig. 8B). Furthermore, the activity level of R-Ras was reduced after Semaphorin 4D application in comparison to the untreated control, or in cells not overexpressing VSV-Plexin-B1 (Fig. 8C).

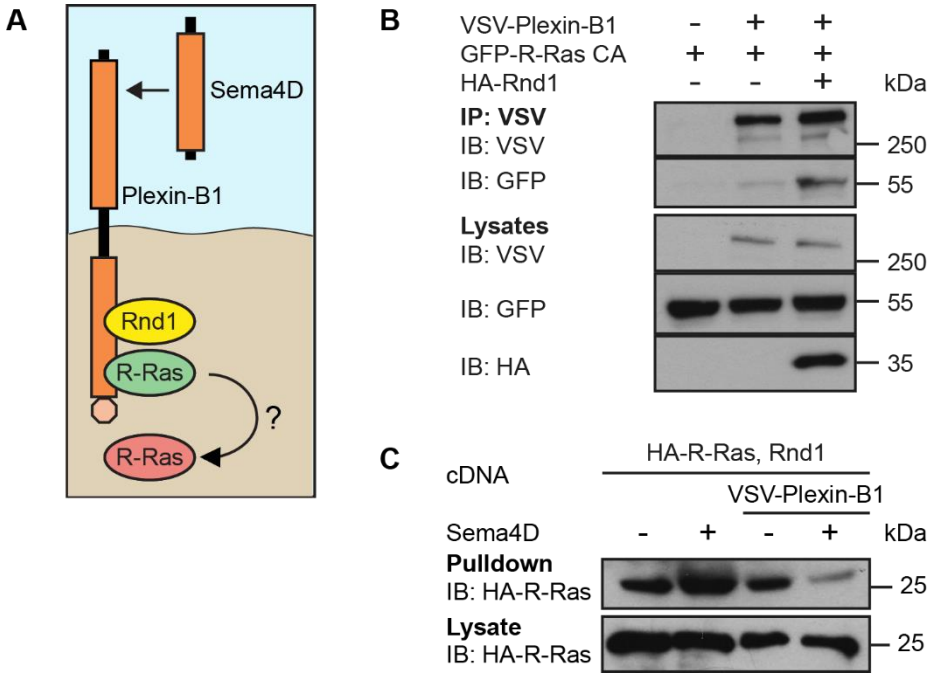

Figure 8. Active R-Ras binds to Plexin-B1 and gets deactivated after stimulation with Semaphorin 4D. A) Scheme of semaphorin-dependent R-Ras deactivation by Plexin-B1. Plexin-B1 binds Rnd1 (yellow) and active, GTP-bound R-Ras (green). Upon application of Semaphorin 4D (Sema4D), R-Ras is being deactivated (GDP-bound state, red), yet the exact mechanism is unclear. B) The binding of constitutively active R-Ras G38V (CA) to Plexin-B1 is dependent on the presence of Rnd1. HEK293T cells were transfected with the indicated cDNA constructs for 24 h at 37 °C. CO-

IP against VSV-Plexin-B1 was performed and the proteins were detected with Western blot analysis. C) GST-Raf1 pulldown for active, GTP-bound R-Ras. HEK293T cells were transfected with the indicated cDNA constructs for 24 h at 37 °C and active R-Ras levels were determined in dependency of Sema 4D treatment (50 nM for 20 min at 37 °C) with a GST-Raf1 pulldown followed by Western blot analysis.

8.2.2 Identification of Rasal1 as the GAP downstream of plexins

If on the one hand, plexins possess a direct GAP activity towards R-Ras, a knockdown of plexins would lead to an increase in active R-Ras, since the plexin mediated deactivation is not possible anymore. If on the other hand, plexins lack direct GAP activity towards R-Ras, another RasGAP could act downstream of plexins to mediate semaphorin-dependent R-Ras deactivation.

Interestingly, previously performed experiments by Thomas Worzfeld and Jakub M. Swiercz revealed, that after the knockdown of Plexin-B2 in HEK293 cells, the R-Ras activity was lowered, rather than increased, pointing to another RasGAP acting downstream of plexins, that can deactivate R-Ras in the absence of Plexin-B2 (Fig. 9A). This observation led to the assumption, that plexins may regulate R-Ras activity by an indirect mechanism. For this reason, they further screened for all possible RasGAPs with siRNA and GST-Raf1/Rho pulldown approaches to find possible candidates whose knockdown leads to the restoration of basal R-Ras activity. Therefore, a GST-Raf1 pulldown in HEK293 cells transfected with the indicated control siRNA or siRNAs against Plexin-B2 and possible RasGAPs was performed (Fig. 9A). Rap1GAP2 (GARNL4), IQGAP1, Neurofibromin (NF1), RAP1GAP and RASAL1 were the only candidates, where the simultaneous knockdown of Plexin-B2 and the corresponding RasGAP led to the restoration of basal R-Ras activity. To further characterize their role in downstream signaling of Plexin-B2, the semaphorin dependency of these five enzymes was investigated and only the knockdown of Rasal1 and IQGAP1 intercepted the decrease in R-Ras activity after Semaphorin 4C application (Fig. 9C).

Consequently, they assessed the question, how R-Ras-specific this effect is for Rasal1 and IQGAP1, since plexins also regulate the activity of Rho GTPases (Worzfeld and Offermanns 2014) and furthermore, wide-ranging interactions between Ras and Rho GTPases have been described (Bar-Sagi and Hall 2000). Hence, a RhoA pulldown revealed an unspecific role for IQGAP1 in mediating RhoA deactivation in absence of stimuli, validating Rasal1 as the only specific semaphorin dependent R-Ras deactivator (Fig. 9D). Thereupon, a universal role for Rasal1 downstream of all plexin subfamilies could be shown in a GST-Raf1

pulldown by knocking down Rasal1 with siRNA and application of Semaphorin 6C (Plexin-A1), Semaphorin 4C (Plexin-B2), Semaphorin 7A (Plexin-C1) or Semaphorin 3E (Plexin-D1) (Fig. 9B, E). Indeed, the knockdown of Rasal1 led to the loss of semaphorin sensitivity for all plexin subfamilies.

Concluding, these data show that Rasal1 is the only specific GAP downstream of plexins, that can mediate semaphorin-dependent R-Ras deactivation for all plexin subfamilies and can perform this action in a plexin-indirect mechanism.

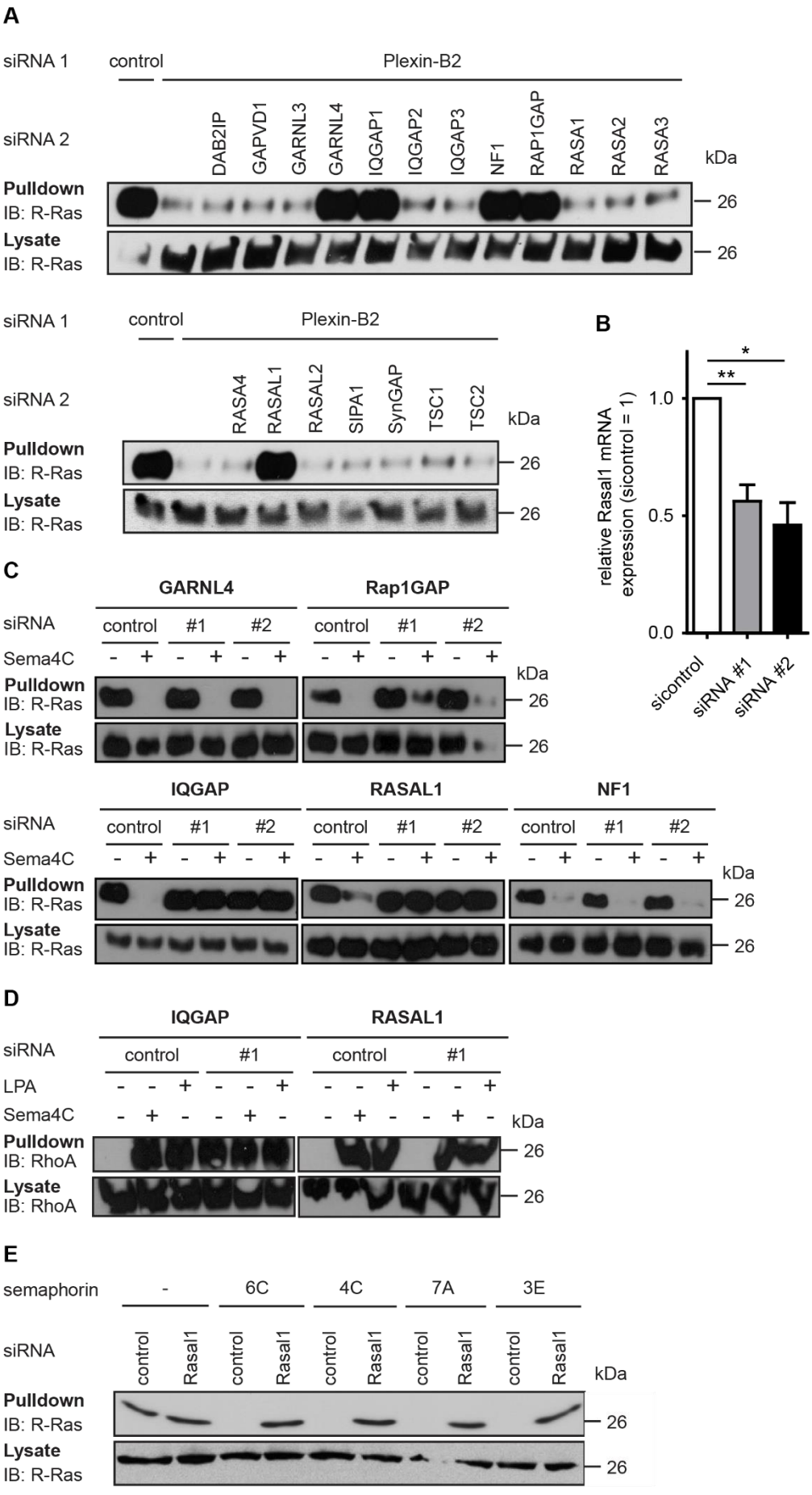
A
siRNA 1
control
Plexin-B2
siRNA 2
DAB2IP
GAPVD1
GARNL3
GARNL4
IQGAP1
IQGAP2
IQGAP3
NF1
RAP1GAP
RASA1
RASA2
RASA3
kDa
Pulldown
IB: R-Ras
Lysate
IB: R-Ras
26
26
siRNA 1
control
Plexin-B2
siRNA 2
RASA4
RASAL1
RASAL2
SIPA1
SynGAP
TSC1
TSC2
kDa
Pulldown
IB: R-Ras
Lysate
IB: R-Ras
26
26
B
relative Rasal1 mRNA expression (sicontrol = 1)
1.0
0.5
0.0
*
**
sicontrol
siRNA #1
siRNA #2
C
GARNL4
Rap1GAP
siRNA
control
#1
#2
control
#1
#2
Sema4C
- + - + - + - + - + - +
kDa
Pulldown
IB: R-Ras
Lysate
IB: R-Ras
26
26
IQGAP
RASAL1
NF1
siRNA
control
#1
#2
control
#1
#2
control
#1
#2
Sema4C
- + - + - + - + - + - + - + - + - +
kDa
Pulldown
IB: R-Ras
Lysate
IB: R-Ras
26
26
D
IQGAP
RASAL1
siRNA
control
#1
control
#1
LPA
- - + - - + - - + - - +
Sema4C
- + - - + - - + - - + -
kDa
Pulldown
IB: RhoA
Lysate
IB: RhoA
26
26
E
semaphorin
-
6C
4C
7A
3E
siRNA
control
Rasal1
control
Rasal1
control
Rasal1
control
Rasal1
control
Rasal1
kDa
Pulldown
IB: R-Ras
Lysate
IB: R-Ras
26
26

Figure 9. Rasal1 is a GAP downstream of plexins. A) GTPase activating protein (GAP) screen for all possible RasGAPs with glutathione S-transferase (GST)-Raf1 pulldown in HEK293 cells was performed. Cells were transfected with control siRNA (sicontrol) or siRNA directed against Plexin-B2 (siPlexin-B2) in combination with siRNAs directed against the indicated RasGAPs and active R-Ras was determined via Western blot analysis. B) Relative Rasal1 mRNA expression was quantified with RT-qPCR and sicontrol was used as relative control. HEK293T cells were transfected for 48 h with siRNAs sicontrol or siRNA #1/#2. The values represent mean±SEM of 3-5 independent experiments, * = p<0,05, ** = p<0,01, two-sided t test. C) Semaphorin (Sema) dependence of positive hits from A). GARNL4, Rap1GAP, IQGAP, RASAL1 and NF1 were investigated for their role in semaphorin dependent R-Ras activity levels by prefmoring GST-Raf1 pulldowns followed by Western blot analysis. HEK293 cells were transfected with sicontrol or two different siRNAs against the indicated RasGAP and were treated with the Plexin-B2 ligand Semaphorin 4C. D) RhoA activity levels of IQGAP and RASAL1 in HEK293 cells, transfected with sicontrol or siRNA for the indicated RasGAP, dependent on lysophosphatidic acid (LPA) or Semaphorin 4C application are shown. RhoA acitivity levels were measured with RhoA pulldown followed by Western blot analysis. E) HEK293 cells were transfected with sicontrol or siRasal1 and were treated with Semaphorin 6C, Semaphorin 4C, Semaphorin 7A and Semaphorin 3E as ligands for all plexin subfamilies (Plexin A-D). R-Ras activity levels were measured with GST-Raf1 pulldown followed by Western blot analysis. The experiments A and C-E were performed by Thomas Worzfeld and Jakub M. Swiercz.

8.2.3 Rasal1 deactivates R-Ras via its GAP domain

After the identification of Rasal1 as the only specific GAP for the deactivation of R-Ras downstream of plexins, the GAP function was analyzed with biochemical and cell biological assays on Rasal1 wildtype (WT) and Rasal1 lacking GAP activity (mutGAP).

The activity level of R-Ras was determined in an overexpression system in HEK293T cells with a GST-Raf1 pulldown followed by Western blot analysis (Fig. 10A). As described above, the application of Semaphorin 4D leads to a decrease in active R-Ras, that can be intensified by the overexpression of Rasal1 WT. In cells transfected with Rasal1 mutGAP, application of Semaphorin 4D does not lower R-Ras activity. The same is being observed when Rasal1 WT, but not the receptor Plexin-B1, is overexpressed.

In conclusion, the semaphorin-mediated deactivation of R-Ras is executed by Rasal1, specifically its GAP domain, and depends on Plexin-B1 to exert semaphorin-dependent function.

Furthermore, the influence of Rasal1 was characterized with a COS-7 collapse assay, which serves as a functional readout for semaphorin-plexin signaling. For this purpose, COS-7 cells were transfected with the indicated cDNA constructs as well as shRNA against Rasal1 (Fig. 10B) and their role in inducing signaling ability

of cellular collapse was examined as described above (Fig. 10C). Further, the percentage of collapsed COS-7 cells was quantified (Fig. 10D) and a significantly lower collapse efficiency was observed in cells overexpressing constitutively active R-Ras, Rasal1 mutGAP or shRNA against Rasal1 (around 45%) in comparison to the control groups overexpressing only Plexin-B1 or Plexin-B1 together with Rasal1 WT (around 60%). Cells showed in the absence of Semaphorin 4D, independently of their transfected cDNA construct, around 15% of collapse and in untransfected COS-7 cells no collapse was detectable. The lower collapse efficiency in cells overexpressing Rasal1 mutGAP strengthens the importance of the GAP domain of Rasal1 in this signaling mechanism and phenocopied the knockdown of Rasal1 and the overexpression of constitutively active R-Ras, in which Rasal1 was not able to deactivate R-Ras after semaphorin application.

Taken these data together, the necessity of the GAP domain of Rasal1 to exert R-Ras deactivation was shown, and therefore confirmed the role of Rasal1 as a specific GAP in semaphorin-plexin signaling.

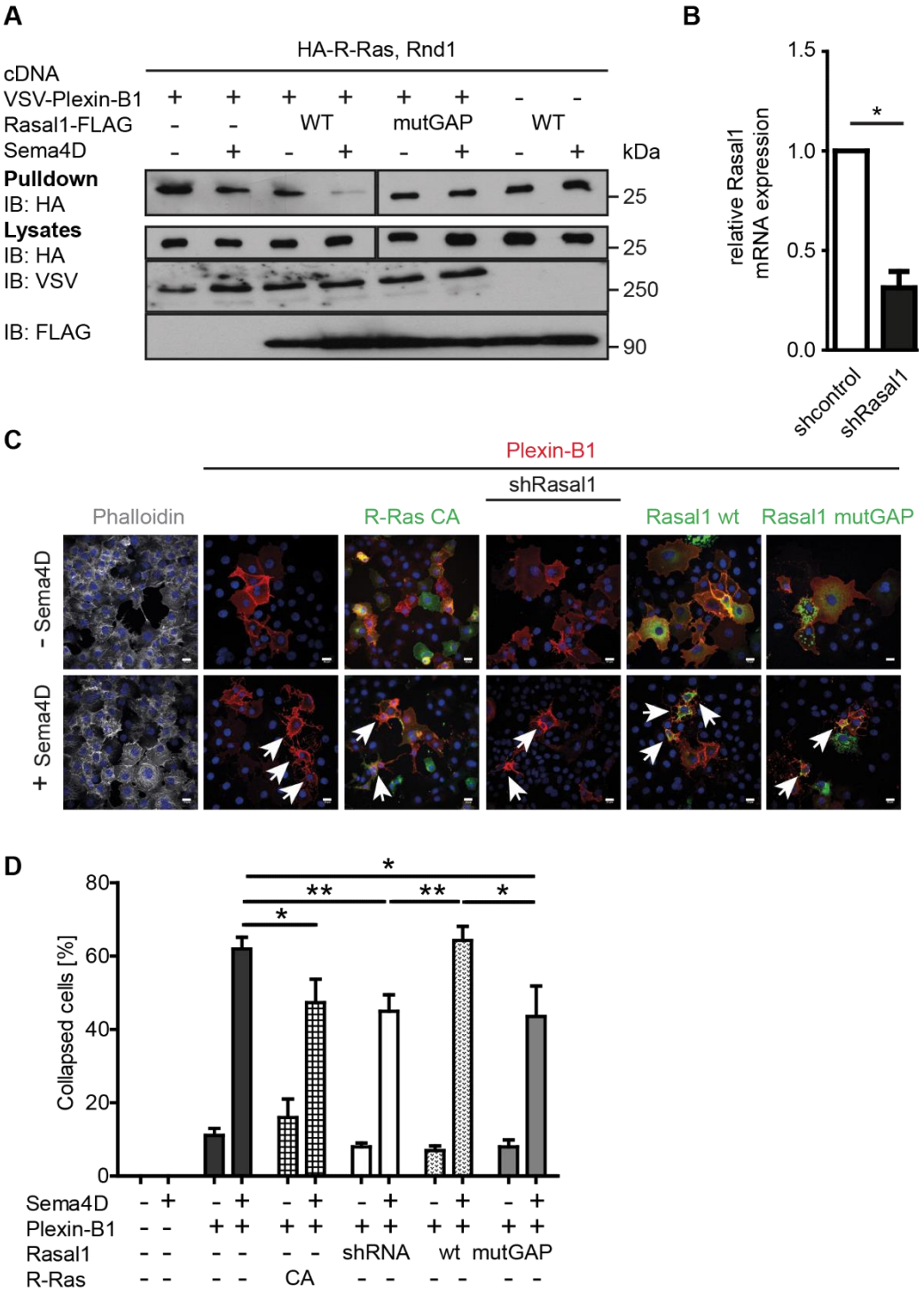

Figure 10. Rasal1 signals downstream of plexins via its GAP domain. A) GST-Raf1 pulldown of HEK293T cells transfected with the cDNA constructs Ha-R-Ras, Rnd1, VSV-Plexin-B1 and Rasal1-FLAG for 24 h at 37 °C. After application of Semaphorin 4D (Sema4D) for 20 min, a GST-Raf1 pulldown for active R-Ras, followed by Western blot analysis, was performed. B) Relative Rasal1 mRNA expression was quantified with RT-qPCR and shcontrol was used as relative control. COS-7 cells were stably transduced with shRNAs shcontrol or shRasal1 as described in Material and Methods. The values represent mean±SEM of 3 independent experiments, * = p<0,05, two-sided t test. C) Collapse assay of COS-7 cells transfected with cDNA constructs encoding VSV-Plexin-B1, HA-R-Ras G38V (constitutively active, CA), Rasal1-FLAG wildtype (WT), Rasal1-FLAG lacking GAP

activity (mutGAP) or with stably transduced shRNA against Rasal1 (shRasal1). 24 h after transfection, the cells were treated with Semaphorin 4D (25 nM) for 1 h at 37 °C and a collapse assay, followed by immunofluorescence staining, was performed. White arrows indicate collapsed cells, scale bar 20 µm. D) Corresponding quantification of C) of 3-8 independent experiments. The values represent mean±SEM, * = p<0,05, ** = p<0,01, two-sided t test.

8.2.4 Rasal1 may interact with plexins

To elucidate, whether Rasal1 directly interacts with plexins and whether this interaction is semaphorin-dependent, CO-immunoprecipitations (CO-IPs) were performed against Rasal1-FLAG or Rasal2-FLAG, serving as a negative specificity control.

As shown in Fig. 11A, HEK293T cells were transfected with the indicated cDNA constructs, Semaphorin 4D was applicated and a CO-IP was performed. Together with Rasal1, Plexin-B1 precipitated, indicating an interaction between these two partners. The interaction was not influenced by semaphorin application and was specific as compared to VSV-Plexin-B1 that did not precipitate with Rasal2.

Then, the semaphorin dependency of this interaction with cDNA constructs for different Rasal1 mutations (Fig. 11B) was tested. VSV-Plexin-B1 was overexpressed in HEK293T cells together with Rasal1 wildtype (WT), mutated GAP domain lacking activity (mutGAP) or a deletion mutant missing the two C2 domains of Rasal1 (dC) and checked for interaction with Plexin-B1 in a CO-IP as described above.

A comparable degree of interaction of Rasal1 WT and mutGAP with the receptor Plexin-B1 was observed that was not influenced by semaphorin application confirming the results of Fig. 11A. Therefore, the functionality of the Rasal1 GAP domain is not necessary for the binding to Plexin-B1. Interestingly, the interaction between Plexin-B1 and Rasal1 dC was increased in comparison to the other Rasal1 constructs. Even though this interaction was also not semaphorin-dependent, the stronger interaction could point towards a possible role of the C2 domains by negatively regulating interaction with the plexin signaling complex.

Moreover, CO-IPs in HEK293T cells were performed to study the interaction of Rasal1-FLAG with different mutants of Plexin-B2 (Fig. 11C). The experiments were performed as described above and the mutants used here were a triple mutation of arginines in the Plexin-B2 GAP domain, which is important for the binding of R-Ras (RA), the semaphorin binding deficient mutant (E369G) and Plexin-B2 lacking the whole intracellular domain (dIC). As a result, Rasal1 interacted with Plexin-B2 wildtype, Plexin-B2 RA and Plexin-B2 dIC with similar intensities, whereas Plexin-

B2 E369G had an increased interaction in comparison to the wildtype. The ability of Rasal1 to interact with Plexin-B2 RA suggests a R-Ras independent mechanism, while the interaction with Plexin-B2 E369G is phenocopying the wildtype condition. Beyond that, the deletion of the intracellular domain of Plexin-B2 does not prevent interaction with Rasal1, which suggests that the detected interaction might be unspecific or indirect.

Taken together, Rasal1 may interact with plexins in a possible indirect mechanism and this interaction seemed to be neither influenced by semaphorin application, nor by the binding of R-Ras to plexins or a non-functional GAP domain of Rasal1.

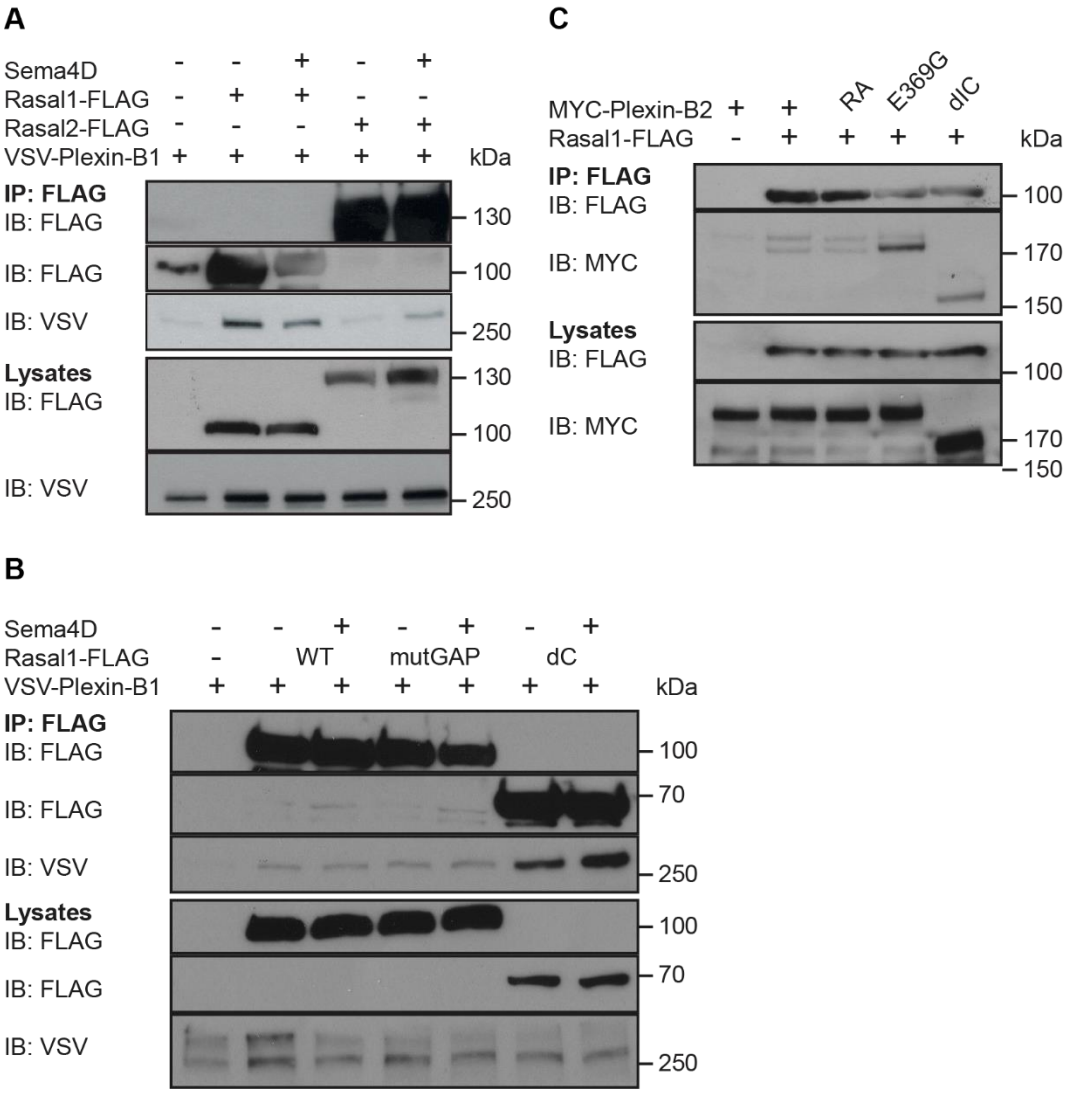

Figure 11. Rasal1 interacts with plexins in a semaphorin independent manner. A)-C) CO-immunoprecipitations (CO-IPs) against FLAG. HEK293T cells were transfected with the indicated cDNA constructs and incubated for 24 h at 37 °C followed by application of 25 nM Semaphorin 4D (Sema4D) for 20 min at 37 °C (A) and B)) and a CO-IP against Rasal1-FLAG/Rasal-2-FLAG. Interaction partners were identified via Western blot analysis. The abbreviated cDNA constructs are Rasal1-FLAG wildtype (WT), Rasal1-FLAG lacking GTPase activating protein (GAP) activity

(mutGAP), Rasal1-FLAG lacking the two C2 domains (dC) or MYC-Plexin-B2 mutants with a binding deficiency of R-Ras (RA), a binding deficiency of semaphorins (E369G) or lacking the complete intracellular domain (dIC).

8.2.5 Calcium-dependency of Rasal1 activity

Rasal1 has been shown to oscillate between the cytoplasm and the plasma membrane in a calcium-dependent manner (Walker et al. 2004). This translocation is necessary for the functionality of this RasGAP and is mediated, in the case of Rasal1, by two N-terminal C2 domains (Sot et al. 2013), while the C-terminal PH domain is believed to be non-functional (Liu et al. 2005).

To test in how far calcium plays a role in the context of semaphorin-induced plexin signaling, this question was approached by live-cell imaging of EGFP-Rasal1 in HeLa cells and with COS-7 assays to analyze semaphorin-plexin signal transduction (Fig. 12A).

As shown in Fig. 12B and D, HeLa cells were transfected with EGFP-Rasal1, and the localization of Rasal1 over a time course was imaged with application of Semaphorin 4D and/or histamine to induce intracellular calcium release via the histamine receptor H1. By measuring the fluorescence intensity (FI), the translocation of EGFP-Rasal1 to the plasma membrane was quantified over a matter of time (Fig. 12C, E).

As described by Walker et al. 2004, EGFP-Rasal1 oscillates with calcium spikes after histamine application (Fig. 12B, C). In the same setup, Semaphorin 4D was added to the cells and no translocation to the plasma membrane upon application was observed. The same cells were then stimulated with histamine as a positive control (Fig. 12 D, E).

To investigate whether treatment with Semaphorin 4D influences the histamine-induced effect on Rasal1 plasma membrane localization, a translocation assay of EGFP-Rasal1 in HeLa cells was performed similar to Fig. 12B-E and the retainment of Rasal1 at the plasma membrane was quantified after histamine application, performed with or without Semaphorin 4D pre-treatment. In Fig. 12F the mean percentage of plasma membrane retained EGFP-Rasal1 (around 15%) is displayed and it did not show any difference whether pre-treated with Semaphorin 4D or not. This indicates, that the Semaphorin 4D pre-treatment does not have an additional effect on Rasal1 membrane retainment after histamine application (Fig. 12E).

In consequence, application of semaphorins does not induce plasma membrane translocation of Rasal1 and does not augment the retainment of Rasal1 at the plasma membrane after calcium-induced translocation.

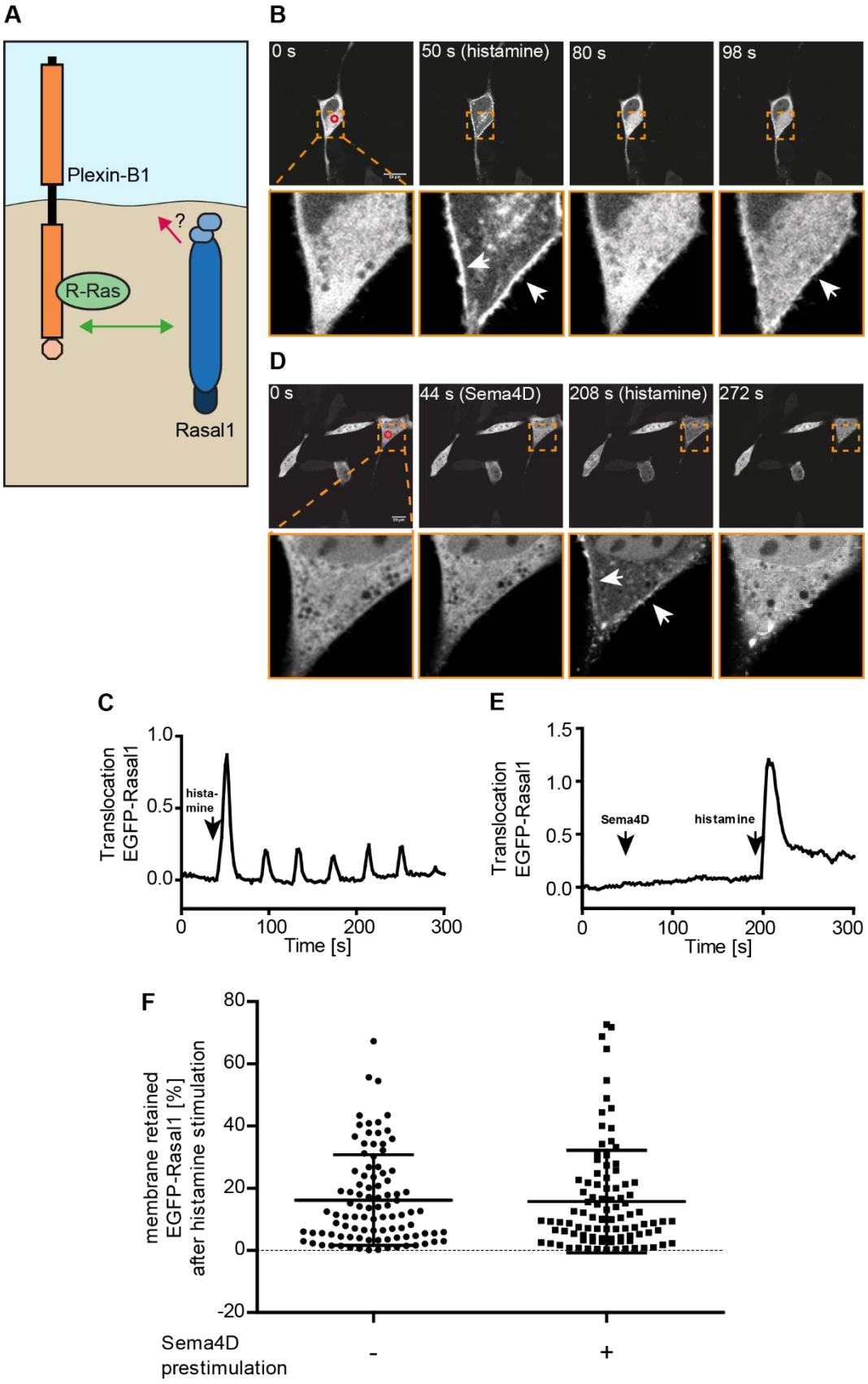

Figure 12. Semaphorin 4D application does not lead to translocation of Rasal1 to the plasma membrane. A) Scheme of R-Ras bound Plexin-B1 interacting with Rasal1 (green arrow), the necessity of calcium-dependent plasma membrane translocation of Rasal1 for GAP function in semaphorin-plexin signaling is not known (red arrow). B) EGFP-Rasal1 translocation assay. HeLa

cells were transfected with EGFP-Rasal1 for 24 h at 37 °C and stimulated with histamine (100 µM) in a live-cell imaging setup. Upper lane: time frame (0, 50, 80, 96 s) with histamine application at 50 s, red circle represents the region of interest (ROI) set for quantification. Lower lane: magnification of cytoplasm, white arrows show plasma membrane translocation of EGFP-Rasal1. C) Corresponding quantification of B), the fluorescence intensity (FI) of the ROI was quantified and the translocation of EGFP-Rasal1 was calculated as translocation = $1/(FI_{ROI}-FI_{background})$. D) EGFP-Rasal1 translocation assay. HeLa cells were transfected as described in B) and treated with Semaphorin 4D (Sema4D, 50 nM at 44 s) followed by histamine (100 µM at 208 s). Upper lane: time frame (0, 44, 208, 272 s), red circle represents the ROI set for quantification. Lower lane: magnification of cytoplasm, white arrows show plasma membrane translocation of EGFP-Rasal1. E) Quantification of D) was performed as described in C). F) Quantification of plasma membrane retainment of EGFP-Rasal1 after histamine (100 µM) application with or without Semaphorin 4D pre-treatment (50 nM). For quantification, ROIs were set in the cytoplasm of HeLa cells transfected with EGFP-Rasal1 for 24 h at 37 °C and the FI was calculated during time lapse. The maximal intensity (Max) and the recovery of cytoplasmic EGFP-Rasal1 after histamine application (Rec), as well as the background intensity (Low), were determined. The percentage of plasma membrane retained EGFP-Rasal1 was calculated as retainment = 100/(Max-Low)*(Rec-Low), n=96-97, mean±SD.

Next, the influence of calcium on the signaling ability of the semaphorin-plexin system was tested with COS-7 assays to quantify the contribution of calcium to cellular collapse. Therefore, COS-7 cells were transfected with cDNA constructs encoding for Plexin-B1 and Rasal1 mutants, lacking either the PH domain (dPH) or the two C2 domains (dC). Other cells, overexpressing Plexin-B1, were starved ON with 0% FCS or were pre-treated with adenosine triphosphate (ATP) (50 µM), an agonist of the purinergic receptor P2 leading to intracellular calcium release, or BAPTA-AM (10 µM), where calcium was intracellularly complexed, and were then examined concerning their signaling ability after Semaphorin 4D induced cellular collapse as described above (Fig. 13A). Then, the percentage of collapsed COS-7 cells was quantified and similar percentages of collapse in the absence of Semaphorin 4D (around 15%) were detected for all conditions as displayed in Fig. 13B. The control cells, overexpressing only Plexin-B1, had a collapse efficiency of around 65% and therefore showed similar properties like the cells overexpressing Rasal1 dPH (70%) additionally. A significant reduction of collapsed cells in comparison to the control condition was observed upon overexpression of Rasal1 dC (50%). The pretreatment with ATP had an additional (80%) and not significant effect on collapse efficiency but was significantly higher in comparison to the BAPTA-AM pre-treated cells (60%). Similar to the effect of BAPTA-AM or the overexpression of Rasal1 dC, was the starving of COS-7 cells performed with 0% FCS, which points towards a general decrease in semaphorin-plexin signaling that may not be calcium specific. Thus, the signaling ability of Rasal1 in semaphorin-

plexin signaling is not dependent on the PH domain but in contrast, the two C2 domains play a pivotal role in signal transduction. A calcium dependency could also be observed by stimulating calcium release (ATP) or blocking intracellular calcium (BAPTA-AM), which either induced or reduced collapse efficiency, respectively. Nevertheless, this effect was not prominent in comparison to the control cells, only implicating a partly functional calcium dependence mediated by the calcium sensitive C2 domains.

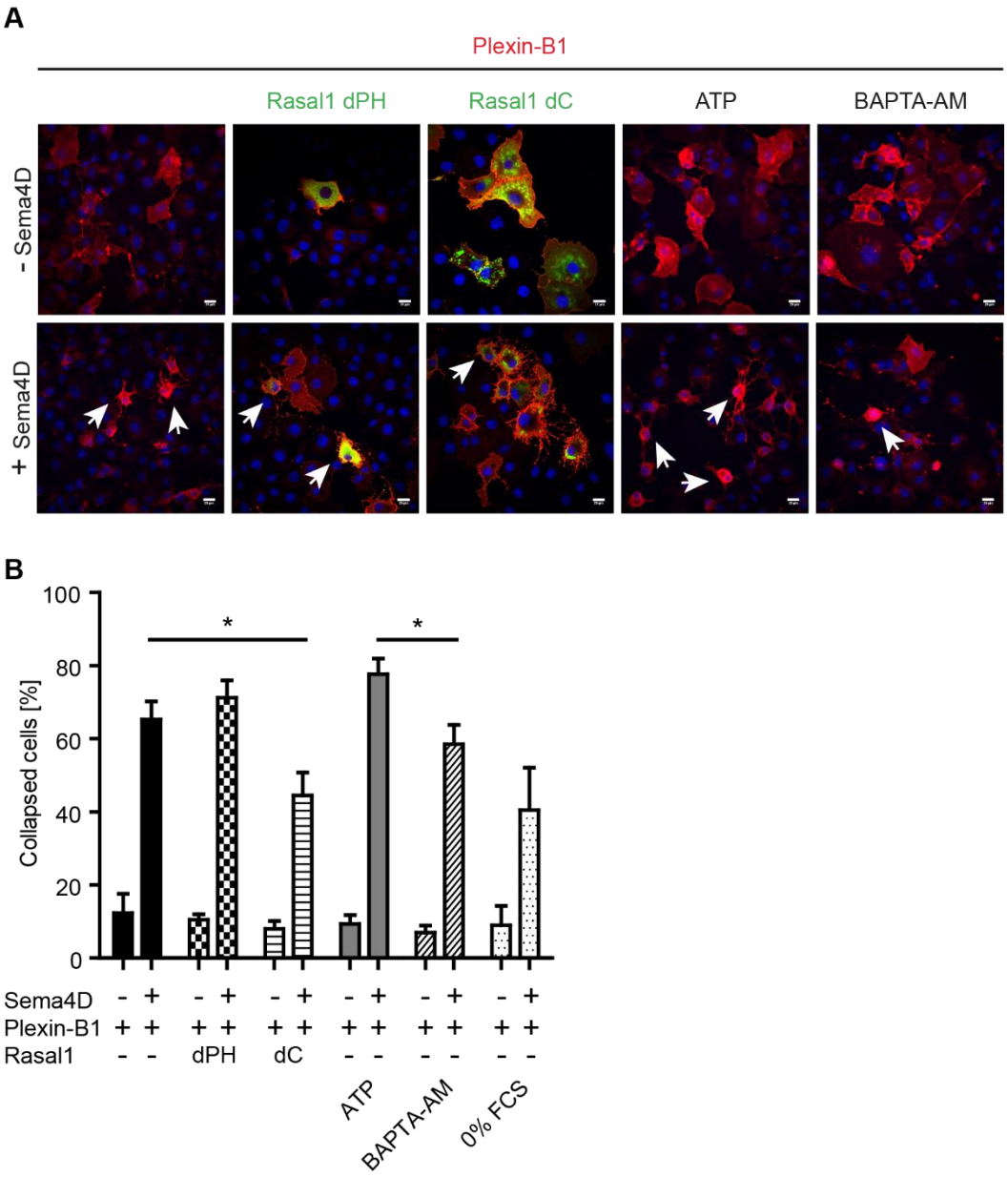

Figure 13. The C2 domains of Rasal1 are important for signaling. A) Collapse assay of COS-7 cells transfected with cDNA constructs encoding VSV-Plexin-B1, Rasal1-FLAG lacking the PH domain (dPH) or the two C2 domains (dC). After 24 h, some cells were pre-treated for 1 h at 37 °C with adenosine triphosphate (ATP) (50 µM), BAPTA-AM (10 µM) or were starved with 0% fetal calf serum (FCS) for 16 h at 37 °C. Then, all conditions were treated with Semaphorin 4D (Sema4D, 25

nM) for 1 h at 37 °C and collapse assay followed by immunofluorescence was performed. White arrows indicate collapsed cells, scale bar 20 µm. B) Corresponding quantification of A) of 3-5 independent experiments. The values represent mean±SEM, * = p<0,05, two-sided t test.

8.2.6 Plexins are sequestering active R-Ras

Subsequently, the next analysis aimed at a better understanding of how semaphorins impact the interactions between Plexin-B1, R-Ras and Rasal1. Therefore, it was hypothesized, that plexins could sequester active R-Ras protecting it from deactivation by Rasal1. Consequently, the application of semaphorins could lead to a release of R-Ras from plexins, being then deactivated by Rasal1.

To test this, investigations on interactions between Rasal1 and R-Ras were performed in collaboration with Dominique Brandt irrespective of the activation level of R-Ras (Fig. 14A). In a CO-IP experiment, HEK293T cells were transfected with Rasal1 and wildtype, constitutively active or dominant negative R-Ras. The CO-IP was performed against Rasal1 and in a Western blot analysis, interactions with R-Ras mutants were examined. As presented in Fig. 14A, Rasal1 can interact with R-Ras independent of its activity state: The interaction was observable equally for wildtype, constitutively active and dominant negative R-Ras and its specificity was confirmed by the negative control, overexpressing R-Ras and lacking Rasal1. Next, the question was addressed, whether the shown interaction of Rasal1 and R-Ras is dependent on the two C2 domains or the PH domain and if a functional GAP domain is needed for this binding. In Fig. 14B, the result of a CO-IP similar to Fig. 14A is presented. HEK293T cells were transfected with Rasal1 wildtype, Rasal1 lacking the two C2 domains (dC), the PH domain (dPH) or lacking GAP activity (mutGAP) and R-Ras wildtype. By co-immunoprecipitating R-Ras with different Rasal1 mutants, no loss of the binding ability of Rasal1 towards R-Ras was noticed. Moreover, the GAP domain of Rasal1 was able to bind R-Ras regardless of its functionality or by deletion of the two C2 domains or the PH domain.

These data indicate that the binding of R-Ras to Rasal1 is only dependent on its GAP domain and that loss of either the two C2 domains, or the PH domain does neither inhibit nor stimulate R-Ras binding.

Furthermore, it has been shown that Plexin-B1 can bind active R-Ras in the presence of Rnd1 (Fig. 8B). To test a possible influence of this interaction by the overexpression of Rasal1, HEK293T cells were transfected with different amounts

of Rasal1-Flag cDNA and were checked for Plexin-B1 R-Ras interaction in a CO-IP (Fig. 14C). With increasing amount of Rasal1, the interaction of Plexin-B1 with R-Ras remained constant, while Rasal1 binding increased. By noticing that Plexin-B1 can only bind active R-Ras, this result points towards a mechanism, in which Plexin-B1 binds active R-Ras and protects it from semaphorin-independent deactivation by Rasal1.

This observation was further investigated by examining the interaction of Rasal1 with R-Ras and analyzed whether an increasing amount of Plexin-B1 can disrupt this binding (Fig. 14D). It could be shown that the interaction of Rasal1 with R-Ras was decreased with increasing amounts of overexpressed Plexin-B1, confirming the results of Fig. 14C, that Plexin-B1 is sequestering active R-Ras.

Summarizing, the binding of Rasal1 to R-Ras was characterized being exclusively dependent on the Rasal1 GAP domain that can besides interact with R-Ras regardless of its activation status and it was further shown, that Plexin-B1 is sequestering active R-Ras.

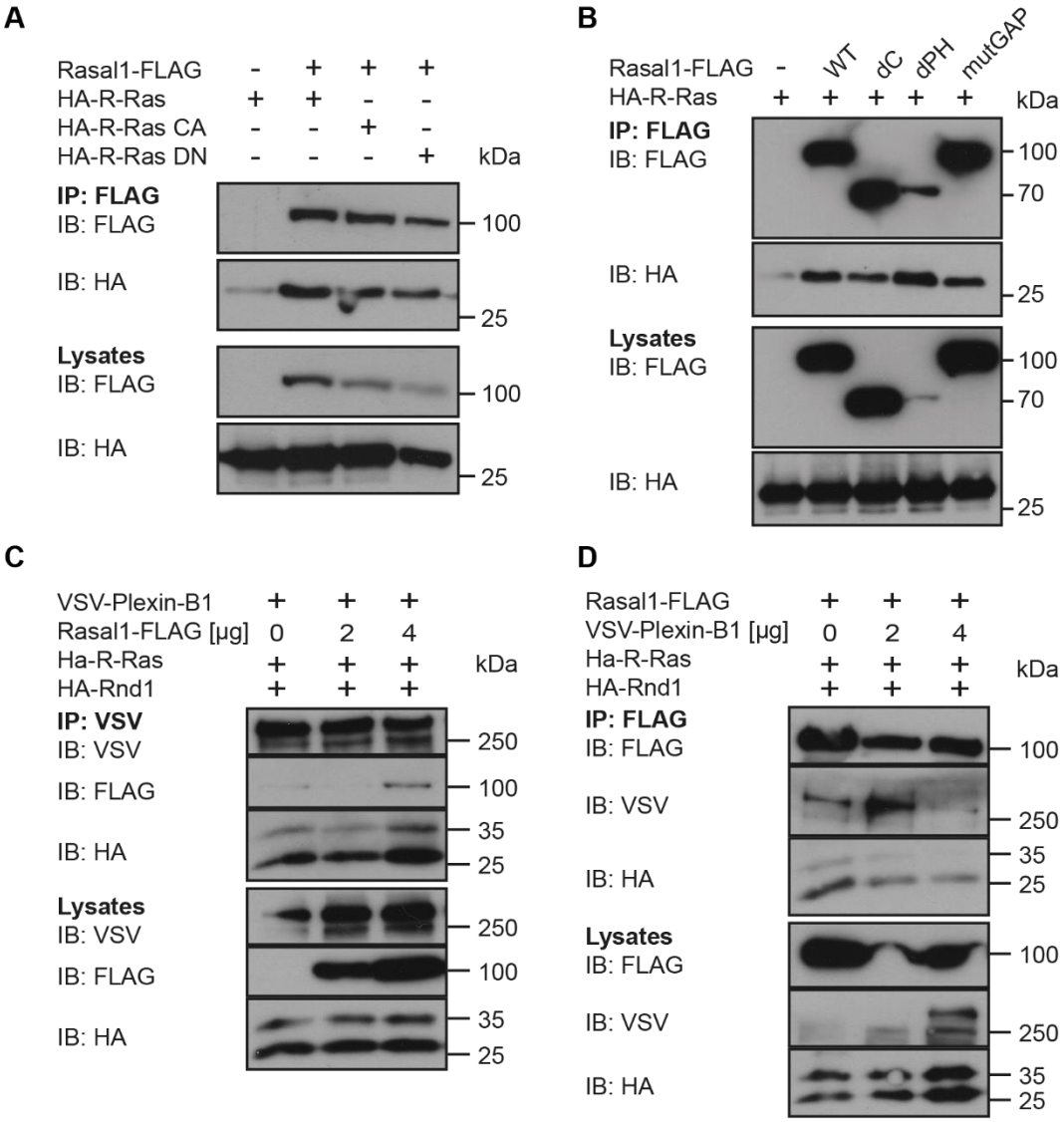

Figure 14. Plexin-B1 is sequestering R-Ras and protects it from interaction with Rasal1. A) CO-IP against Rasal1-FLAG. HEK293T cells were transfected with Rasal1-FLAG and HA-R-Ras wildtype, HA-R-Ras G38V (constitutively active, CA) or HA-R-Ras S43N (dominant negative, DN) for 24 h at 37 °C and CO-IP, followed by Western blot analysis was performed. B) CO-IP against FLAG. HEK293T cells were transfected for 24 h at 37 °C with Rasal1-FLAG wildtype (WT), Rasal1-FLAG lacking the two C2 domains (dC), the PH domain (dPH) or lacking GAP activity (mutGAP) and HA-R-Ras wildtype and a CO-IP, followed by Western blot analysis was performed. Experiments A) and B) were performed by D. Brandt. C) Titration of Rasal1-FLAG in a CO-IP against VSV-Plexin-B1. HEK293T cells were transfected with VSV-Plexin-B1, HA-R-Ras, HA-Rnd1 and different amounts of Rasal1-FLAG wildtype (0, 2, 4 µg) for 24 h at 37 °C and a CO-IP, followed by Western blot analysis was performed. D) Titration of VSV-Plexin-B1 in a CO-IP against Rasal1-FLAG. HEK293T cells were transfected with Rasal1-FLAG, HA-R-Ras, HA-Rnd1 and different amounts of VSV-Plexin-B1 (0, 2, 4 µg) for 24 h at 37 °C and a CO-IP, followed by Western blot analysis was performed.

8.2.7 R-Ras is released from plexins after semaphorin application

Given the observation, that plexins bind active R-Ras and sequester it from deactivation by Rasal1, an application of semaphorins should lead to a release of R-Ras from plexins, followed by the deactivation of R-Ras by Rasal1 in response. To test this hypothesis, a CO-IP for VSV-Plexin-B1 was performed and its interaction was investigated with constitutively active R-Ras with or without application of Semaphorin 4D and Semaphorin 7A, serving as a negative and specificity control since Semaphorin 7A binds to the endogenously low expressed receptor Plexin-C1 (Fig. 15A).

As expected, the specific interaction of R-Ras CA with Plexin-B1 was only observable in the presence of Rnd1, as described by Oinuma et al. After application of Semaphorin 4D, less interaction was observed similar to the level of the negative control overexpressing only R-Ras CA, or the condition without Rnd1. This decrease was not observable after the application of Semaphorin 7A.

Hence, these data suggest on the one hand a semaphorin-mediated release of active R-Ras from plexins and on the other hand an increase in the interaction of Rasal1 and R-Ras consequently followed by R-Ras deactivation.

Summarizing, the following mechanism for Rasal1 mediated deactivation of R-Ras downstream of plexins is proposed:

Without semaphorin application, plexins bind active R-Ras and sequester it from deactivation by Rasal1. After the binding of semaphorins, initiating plexin signaling, active R-Ras is being released by plexins and is then deactivated by Rasal1 (Fig. 15B).

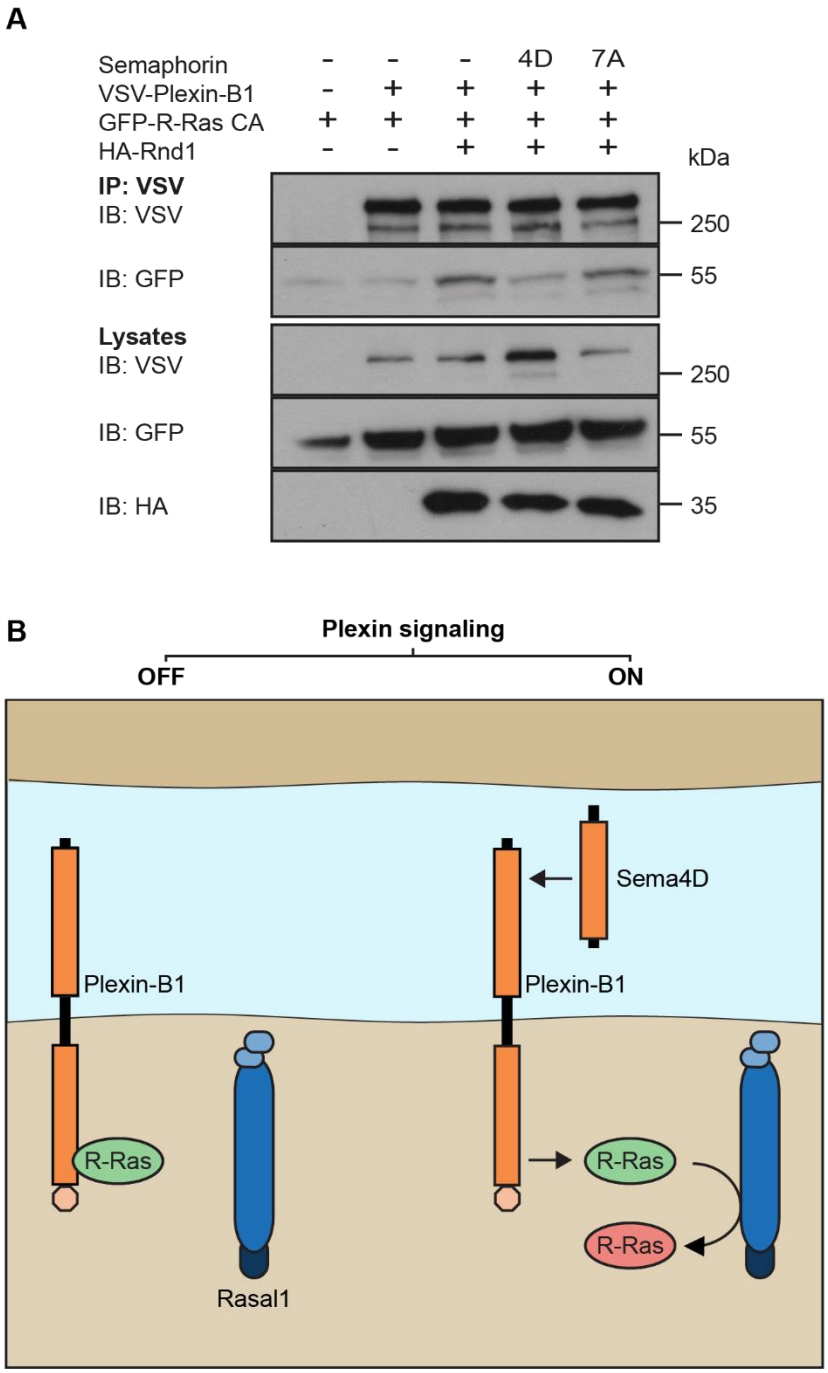

Figure 15. Semaphorin application leads to a release of active R-Ras from plexins. A) CO-IP against VSV-Plexin-B1. HEK293T cells were transfected with VSV-Plexin-B1, HA-Rnd1 and GFP-R-Ras G38V (constitutively active, CA) for 24 h at 37 °C, treated with Semaphorin 4D [50 nM] or Semaphorin 7A [50 nM] for 20 min at 37 °C and CO-IP, followed by Western blot analysis was performed. B) Signaling mechanism of Rasal1 downstream of plexins. Plexin-B1 is sequestering active R-Ras (green). The binding of Semaphorin 4D to Plexin-B1 induces the release of active R-Ras from Plexin-B1, leading to the deactivation of R-Ras (red) by Rasal1.

8.3 Plexin signaling controls Gastrin expression

8.3.1 Gastrin expression is controlled by R-Ras

Since Rasal1 has been identified as the key player in the regulation of R-Ras activity downstream of plexins, a possible functional relevance of this pathway in physiology and hence, its influence in the development of diseases seems feasible. The expression of gastrin, a peptide hormone responsible for the production of gastric acid, has been shown to be regulated by K-Ras (Nakata et al. 1998; Hori et al. 2003). Therefore, the question was assessed, in how far its homologue R-Ras could be involved in the regulation of gastrin expression as well. For the investigations, the murine intestinal neuroendocrine tumor cell line STC-1 was chosen for experiments, which expresses both Plexin-B1, Rasal1, R-Ras and gastrin as analyzed in Fig. 16A.

Next, the relative Gastrin mRNA expression in STC-1 cells was checked via RT-qPCR as described before. These cells were transfected with constitutively active R-Ras or K-Ras and set in relation to the untransfected control. Thus, it could be shown that R-Ras can induce gastrin mRNA expression similar to K-Ras and could therefore be involved in regulating gastrin expression (Fig. 16B).

On top of that, the semaphorin dependence of R-Ras mediated gastrin expression was elucidated by application of Semaphorin 4D to STC-1 cells and gastrin mRNA expression was analyzed with RT-qPCR relative to control cells in the absence of Semaphorin 4D (Fig. 16C).

A significant downregulation of gastrin expression (around 80%) was observed upon Semaphorin 4D application, indicating an involvement of the semaphorin-plexin system in gastrin expression.

In summary, R-Ras can upregulate gastrin expression, while the application of Semaphorin 4D leads to a downregulation of gastrin expression.

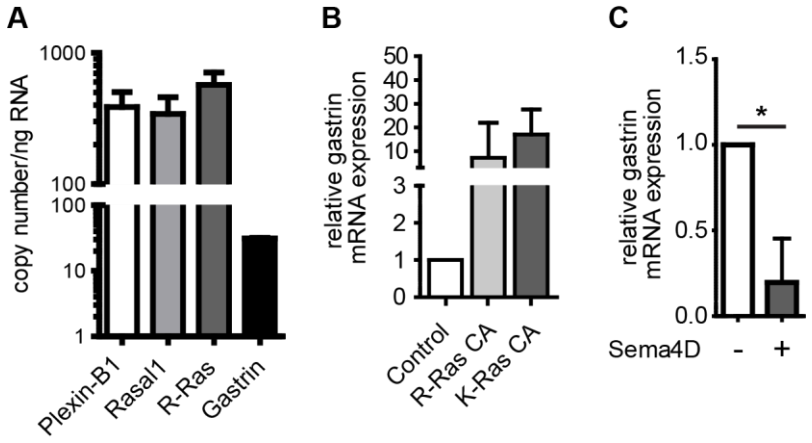

Figure 16. Gastrin expression is controlled by R-Ras in STC-1 cells. A) Plexin-B1, Rasal1, R-Ras and gastrin are expressed in STC-1 cells. Absolute quantification of mRNA expression levels using RT-qPCR for Plexin-B1, Rasal1, R-Ras and Gastrin in STC-1 cells. RNA and genomic DNA were isolated, and absolute quantification of mRNA expression levels via RT-qPCR was performed. The values represent mean±SD of 2-4 independent experiments. B) Relative gastrin mRNA expression was quantified with RT-qPCR and untransfected cells were used as relative control. STC-1 cells were transfected with cDNA constructs encoding for constitutively active R-Ras G38V (R-Ras CA) or constitutively active K-Ras G12V (K-Ras CA). The values represent mean±SEM of 3-6 independent experiments. C) Relative gastrin mRNA expression was quantified with RT-qPCR. STC-1 cells were treated with 50 nM of Semaphorin 4D (Sema4D) for 20 min at 37 °C, followed by RNA isolation and cDNA synthesis. The values represent mean±SD of 5 independent experiments, * = $p<0,05$, two-sided t test.

8.3.2 Semaphorin 4B can act as a ligand for Plexin-B1

Our laboratory analyzed the expression patterns of semaphorins in the stomach epithelium (data not shown) and did not detect expression of Semaphorin 4D, while Semaphorin 4B was strongly expressed. This led to the hypothesis, that membrane-bound Semaphorin 4B, may act as a ligand for Plexin-B1 in the stomach.

The ability of Semaphorin 4B to induce collapse in COS-7 cells overexpressing Plexin-B1 or Plexin-B2 was tested, serving as a functional readout for semaphorin-plexin signaling (Fig. 17A).

Hence, either Semaphorin 4D or conditioned medium of HEK293T cells previously transfected with a cDNA construct for Semaphorin 4B were added to COS-7 cells and the collapse efficiency was quantified (Fig. 17B).

Semaphorin 4D treated COS-7 cells overexpressing Plexin-B1 (collapse around 60%) and COS-7 cells overexpressing Plexin-B2 with application of Semaphorin 4B conditioned media were used (collapse around 40%) as positive controls, since

Plexin-B2 has been described as a ligand for Semaphorin 4B (Xia and Worzfeld 2016).

Interestingly, also Plexin-B1 overexpressing COS-7 cells, that were incubated with Semaphorin 4B conditioned medium, were collapsed in around 50% of the cases, exceeding Plexin-B2 overexpressing COS-7 cells with Semaphorin 4B conditioned medium application (40%).

Taken together, Semaphorin 4B serves as a ligand for Plexin-B1 and could therefore regulate gastrin expression in the stomach epithelium.

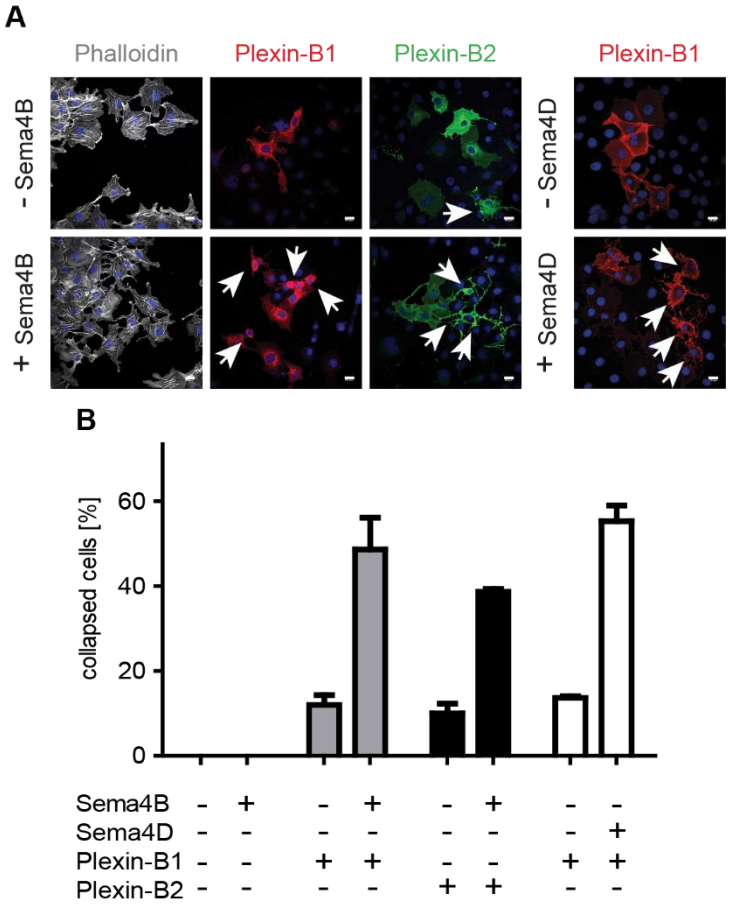

Figure 17. Semaphorin 4B signals via Plexin-B1. A) Collapse assay of COS-7 cells transfected with cDNA constructs encoding VSV-Plexin-B1 or MYC-Plexin-B2. 24 h post transfection, cells were treated for 1 h at 37 °C with either Semaphorin 4D (Sema4D, 25 nM) or with supernatant of HEK293T cells, which were transfected for 24 h at 37 °C with a Semaphorin 4B (Sema4B) cDNA construct, and collapse assay, followed by immunofluorescence was performed. White arrows indicate collapsed cells, scale bar 20 µm. B) Corresponding quantification of A) of 3 independent experiments. The values represent mean±SEM.

8.4 Functional characterization of Plexin-B2 mutations

The kidney expresses several semaphorins and plexins during organogenesis, that are also involved in adult renal pathophysiology like glomerular diseases or acute kidney injury (Xia and Worzfeld 2016). In fact, elevated semaphorin-plexin signaling reduces kidney function in diabetic nephropathy (Mohamed et al. 2014; Aggarwal et al. 2015) and promotes tubular damage and apoptosis of tubular epithelial cells in acute kidney injury (Ranganathan et al. 2014; Jayakumar et al. 2013; Tian et al. 2018).

Another pathological condition, the congenital anomalies of the kidney and urinary tract (CAKUT), is the most common cause of kidney disorders in the first three decades of life, that manifest in different clinical characteristics and is associated with abnormal renal development (van der Ven et al. 2018a). In particular, CAKUT is caused in 5-20% of patients by different monogenic gene mutations (van der Ven et al. 2018a; van der Ven et al. 2018b), while the other percentage may have epigenetic and environmental factors (Nicolaou et al. 2015). Consequently, enormous effort was invested in next-generation sequencing methods to identify novel mutations contributing to CAKUT. And so, Friedhelm Hildebrandt and colleagues (Boston Children's Hospital, Harvard Medical School, Boston, USA) identified different mutations in Plexin-B2 with a possible involvement in CAKUT emergence (unpublished data), since Plexin-B2 has been shown to play a role in ureteric branching during murine kidney development (Perälä et al. 2011).

In cooperation with Friedhelm Hildebrandt and colleagues the question was assessed, if and how these mutations of Plexin-B2 found in CAKUT patients have a physiological role in plexin signaling. Therefore, three point mutations (T79M, T1355M and T1726M, Fig. 18A) were characterized, that are located in the extracellular Sema domain and in the intracellular GAP domain by cell biological and pharmacological approaches.

First, the membrane localization was investigated of cDNA constructs of the corresponding conserved murine Plexin-B2 mutations (Fig. 18B), that have been determined by whole-exome sequencing (van der Ven et al. 2018a), and the mutation E369G, a semaphorin-binding deficient mutant serving as a negative control for functional readouts. For this purpose, HEK293T cells were transfected with cDNA constructs encoding for Plexin-B2 wildtype and Plexin-B2 mutations and expression levels were checked with immunofluorescence staining. The plasma membrane targeting as well as the general expression level of all cDNA

constructs was comparable. Plexin-B2 translocated to plasma membranes at cell-cell contacts independently of mutations.

Furthermore, the binding ability of recombinant murine Semaphorin 4C to Plexin-B2 mutants was examined with an AP-assay (Fig. 18C). COS-7 cells, overexpressing the introduced Plexin-B2 cDNA constructs, were incubated with different concentrations of Semaphorin 4C and the binding to Plexin-B2 was measured colorimetrically with an AP-tagged antibody as described before. As a result, the sema-binding deficient mutant E369G was unable to bind Semaphorin 4C and had a binding profile similar to the untransfected control. The Plexin-B2 mutations T79M, T1359M and T1730M had no significantly different binding in comparison to Plexin-B2 wildtype, indicating that the binding of the ligand Semaphorin 4C to the receptor Plexin-B2 is not affected by these mutations.

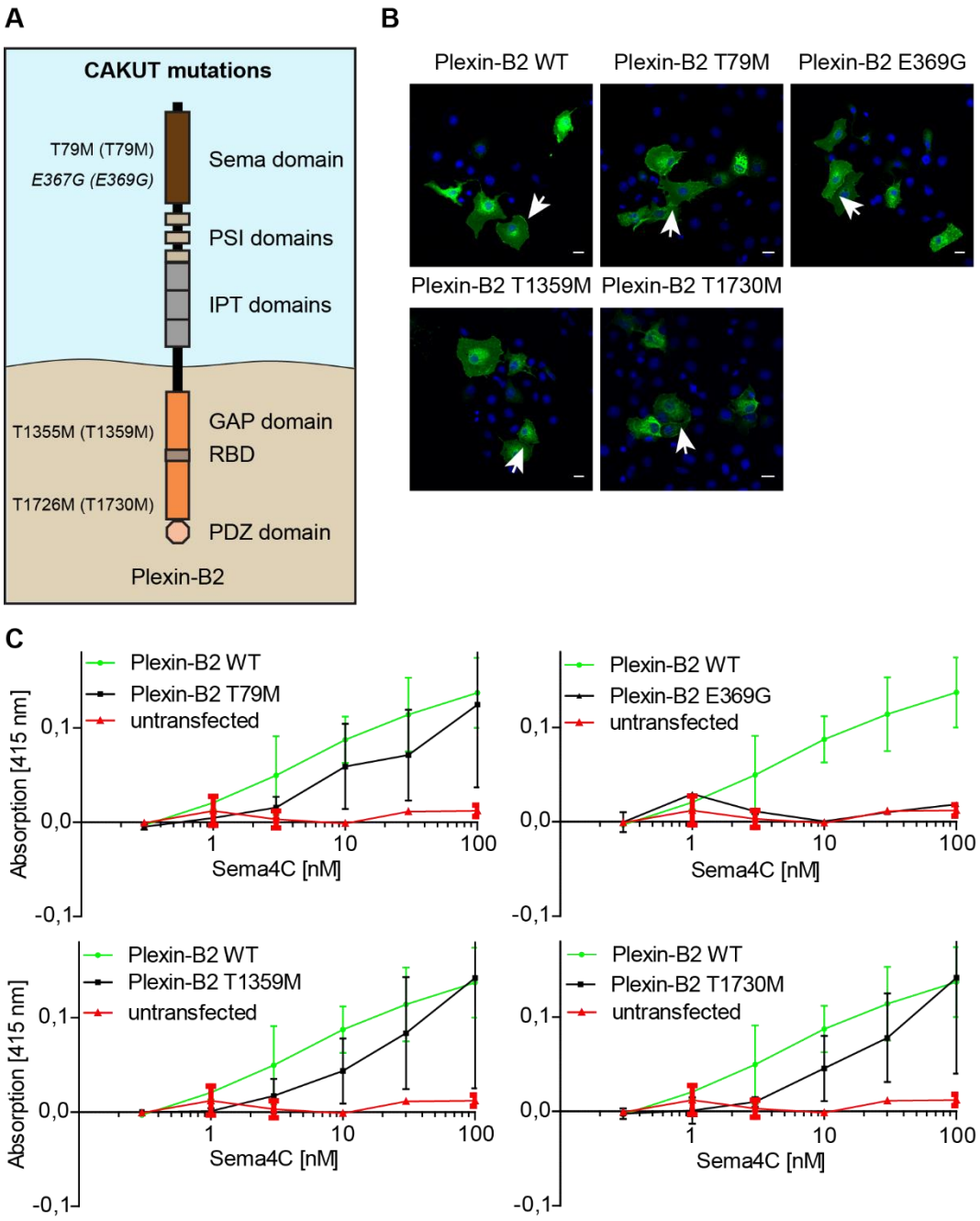

Figure 18. Mutations of Plexin-B2 found in CAKUT patients do not change plasma membrane localization or binding of Semaphorin 4C. A) Schematic image of the domain organisation of Plexin-B2 with point mutations T79M, T1355M and T1726M occuring in CAKUT patients. The indicated mutations in brackets are the corresponding murine positions. Mutation E367G (E369G) is a semaphorin-binding deficient mutant and serves as a negative control. B) Overexpression and immnofluorescence staining of murine MYC-Plexin-B2 cDNA wildtype (WT) and mutants in HEK293T cells (green, DAPI (blue)). Arrows indicate plasma membrane localization of murine MYC-Plexin-B2 WT and mutants at cell-cell contacts. C) Alkaline phosphatase (AP)-assay of COS-7 cells, overexpressing murine MYC-Plexin-B2 mutants incubated with increasing concentrations of recombinant murine Semaphorin 4C (Sema4C) for 1 h at 4 °C. The absorption of antibody-mediated

AP activity of plexin-bound semaphorin was measured with 2-3 technical replicates at 415 nm and normalized to background absorption. The values represent mean±SEM, scale bar 20 µm.

Moreover, the extracellular mutation in the murine sema domain T79M and the intracellular mutation in the GAP domain T1730M of Plexin-B2 were chosen for further investigations due to their potentially interesting localization in important regions for signal transduction. Hence, the binding of recombinant Semaphorin 4C to these mutants was checked in the range between 0 and 64 nM of Semaphorin 4C with more replicates (Fig. 19A). Similar to the findings in Fig. 18C, the binding of Semaphorin 4C to Plexin-B2 T79M and T1730M did not change in comparison to the Plexin-B2 wildtype control, while the binding of Semaphorin 4C to Plexin-B2 E369G was completely suppressed.

To check for abrogated signaling of these two Plexin-B2 mutations, the COS-7 collapse assay was used as a functional readout for semaphorin-plexin-mediated signal transduction (Fig. 19B), since semaphorin treated cells react with a collapse of the cytoplasm. COS-7 cells were transfected with the indicated cDNA constructs and Semaphorin 4C was applicated followed by immunofluorescence staining. Collapsed cells were counted blinded and quantified (Fig. 19C). Indeed, the collapse efficiency of Plexin-B2 T79M was significantly reduced in comparison to the wildtype control, while the collapse efficiency of Plexin-B2 T1730M did not change.

Taken these data together, mutations of Plexin-B2 found in CAKUT patients do not have a changed binding to the ligand, but the downstream signaling ability is, at least in the case of mutation T79M, reduced.

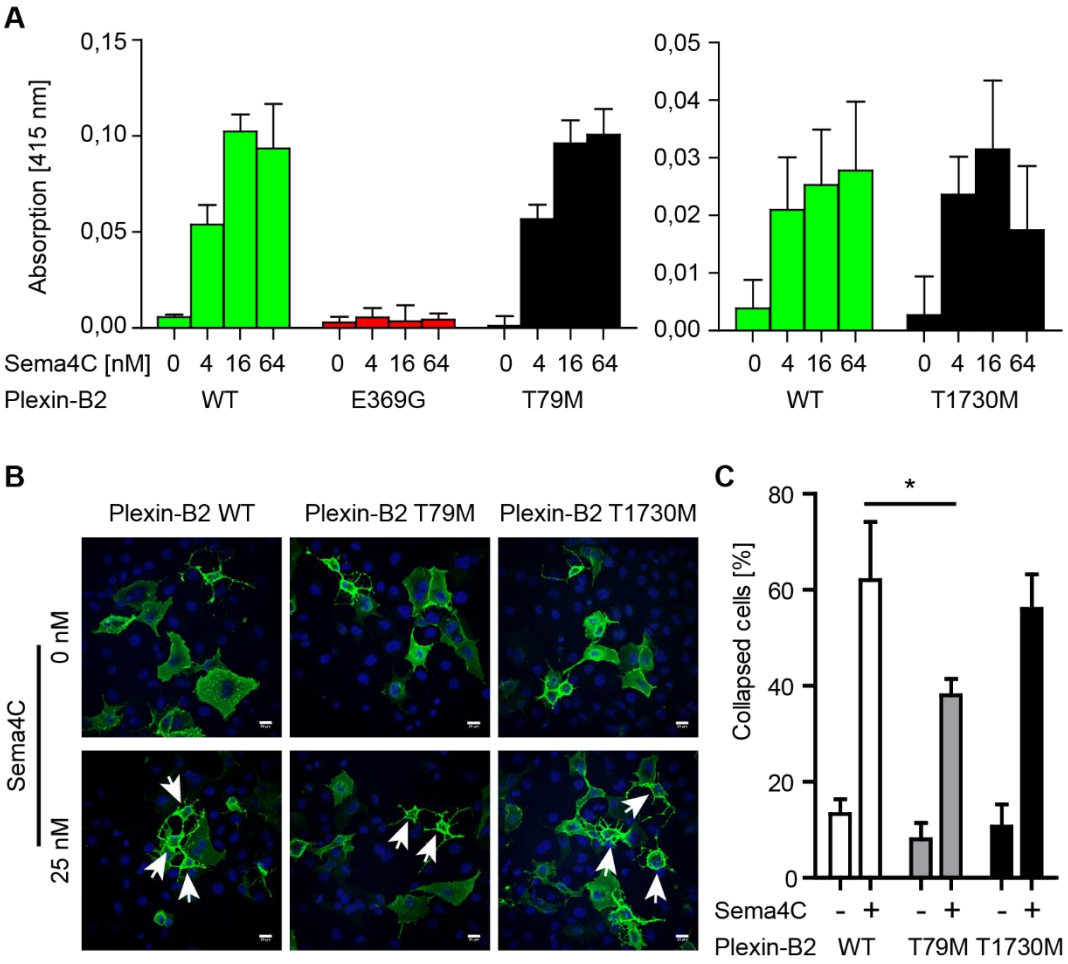

Figure 19. Plexin-B2 mutation T79M negatively influences downstream signaling of Plexin-B2. A) AP-assay of COS-7 cells overexpressing murine MYC-Plexin-B2 wildtype (WT), E369G, T79M or T1730M, incubated with recombinant murine Semaphorin 4C (Sema4C) for 1 h at 4 °C. The absorption of antibody-mediated alkaline phophatase (AP) activity of plexin-bound semaphorin was measured with 5-6 technical replicates at 415 nm and normalized to background absorption. B) Collapse assay of COS-7 cells overexpressing MYC-Plexin-B2 WT, T79M or T1730M (green, DAPI (blue)). Cells were treated with 25 nM recombinant murine Semaphorin 4C for 1 h at 37 °C, followed by immunofluorescence staining and blinded quantification of collapsed cells. White arrows indicate collapsed cells, scale bar 20 µm. C) Corresponding quantification of the COS-7 collapse assay from B) of three independent experiments. The values represent mean±SD, * = p<0,05, two-sided t test.

9 Discussion

This study elucidated the so far unknown mechanism of plexin-mediated R-Ras deactivation and validated Rasal1 as the missing GAP downstream of plexins. In addition to that, the influence of different mutations in Plexin-B2 and the role of TMEM260 in semaphorin-plexin signaling was characterized.

9.1 TMEM260 is involved in plexin processing

Glycosylations are posttranslational modifications that participate in different biological processes including cell adhesion, endocytosis and signal transduction (Ohtsubo and Marth 2006). Joshi et al. summarized O-glycosylation pathways across kingdoms, showing O-mannosylation is taking place in vertebrates, yeast and fungi. In metazoans particularly, plexins are being O-mannosylated at five different positions: the mannosylations at the PSI domain and close to the transmembrane region of Plexin-B2 are being performed by TMTC2 (Larsen et al. 2017a). Furthermore, Plexin-B2 is mannosylated at three additional amino acids in the IPT domains (Fig. 6A, unpublished data). Adnan Halim and colleagues (University of Copenhagen, Denmark) provide strong evidence, that the IPT domain mannosylations are performed by TMEM260 (unpublished data).

So far, little is known about the role of TMEM260 in a physiological context, but mutations in the *TMEM260* gene were shown to lead to a syndrome with diverse symptoms affecting the neuronal, cardiac and renal system (Ta-Shma et al. 2017) and are involved in normal brain development in mice (Wang et al. 2020). Similar pathophysiological (Xia and Worzfeld 2016; Pasterkamp and Giger 2009; Gu and Giraudo 2013) and developmental (Worzfeld et al. 2014; Perälä et al. 2011) phenotypes have also been reported for abrogated semaphorin-plexin signaling and confirm a possible involvement of TMEM260-mediated mannosylation in plexin-dependent physiology.

In an siRNA approach for TMEM260, more binding of Semaphorin 4C after knockdown of TMEM260 was observed and more Plexin-B2 was located at the plasma membrane, while the downstream signaling was not changed in comparison to the wildtype control (Fig. 6). In accordance with that, CRISPR-mediated knockout of TMEM260 resulted in the same effects (Fig. 7). Interestingly, whole cell lysates for Plexin-B2 revealed a defect in protein processing by protein convertases in cells lacking TMEM260. In 2003, Artigiani et al. described the

necessity of the cleavage of the extracellular domain of Plexin-B1/B2 at the plasma membrane by protein convertases to induce semaphorin-mediated signal transduction. After the knockout of TMEM260, less cleaved and therefore less active Plexin-B2 was found in comparison to the wildtype control, leading to the assumption that TMEM260 plays a role in protein processing and hence signal transduction. It has been known for decades, that glycosylations can influence correct protein folding, protein-protein interactions and stimulate signal transduction (Rudd and Dwek 1997; Wormald et al. 2002), while IPT domains have been identified as important regulators in ligand-binding and protein processing (Ma et al. 2010). Taken these findings together, O-mannosylations at plexins may facilitate processing by protein convertases and help to correctly fold the extracellular domain.

Even though compensatory effects of remaining TMEM260 in siRNA knockdown cells cannot be excluded, more Plexin-B2 was targeted to the plasma membrane in comparison to the wildtype control in siRNA and CRISPR treated cells. These data show an involvement of TMEM260 in membrane targeting of plexins.

More Plexin-B2 (cleaved and uncleaved) was found at the plasma membrane after TMEM260 knockdown/knockout in comparison to the wildtype control leading to an increase in Semaphorin 4C binding, while total Plexin-B2 unveiled deficient protein cleavage. It was estimated that the overall expression of Plexin-B2 is higher in cells lacking TMEM260 due to redeeming effects: missing TMEM260-mediated O-mannosylation leads to abrogated trafficking and processing by protein convertases being (over-)compensated by increased Plexin-B2 expression.

To address this hypothesis, further experiments investigating Plexin-B2 promotor activity, signal transduction in CRISPR cell lines, as well as structural analysis and tracking of Plexin-B2 trafficking should be performed in the future.

9.2 Physiological diversity of Ras proteins and RasGAPs

The functionality of the plexin GAP domain in deactivating R-Ras has been controversial. Initially, Plexin-B1 was described as a direct GAP for R-Ras (Oinuma et al. 2004a), while Wang et al. (2012) did not observe a direct GAP activity on isolated intracellular domains of plexins. Indeed, all publications showing GAP activity towards R-Ras have been performed with whole cells or isolated membranes (Oinuma et al. 2004a; Worzfeld et al. 2012; Uesugi et al. 2009),

indicating that other membrane-associated proteins might be involved in mediating GAP activity.

This study contributes to unravel this controversy by validatingRasal1 as the only specific regulator of R-Ras activity downstream of plexins, acting as a GAP following semaphorin stimulation.

So far, it is known that active, GTP-bound, R-Ras binds to plexins in the presence of Rnd1 and is deactivated upon stimulation with semaphorins (Fig. 8, Oinuma et al. 2004b; Oinuma et al. 2004a).

R-Ras is a non-classical isoform of the oncogene Ras, a major player in cell proliferation, migration and differentiation (Drosten et al. 2010). Ras proteins are mutated in around 30% of all human cancers (Prior et al. 2012), underlining the need of tight activity regulation under physiological conditions and the importance of controlling R-Ras in semaphorin-plexin signaling. Due to low intrinsic GAP activity, Ras proteins need GAPs for their GTP hydrolysis (Wennerberg et al. 2005; Bernards and Settleman 2004). Hence, the regulation of Ras by RasGAPs suggests an oncogenic relevance in conducting this signaling pathway on an additional level. Several mutations in RasGAPs have been described, corroborating their pathophysiological role in Ras signaling, among them NF1 in neurofibromatosis type I (Dasgupta et al. 2003), RASA1 in blood vessel growth (Lapinski et al. 2012), RASA4 in epithelial cell transformation (Westbrook et al. 2005), disabled homolog 2-interacting protein (DAB2IP) in prostate cancer (Min et al. 2010) and Rasal2 in ovarian/breast cancer (Huang et al. 2014; Feng et al. 2014). The existence of different Ras isoforms and RasGAPs with diverse, tissue-specific and non-redundant functions elucidates the complexity and vast pathophysiological potential of Ras signaling, especially during carcinogenesis (Colicelli 2004; King et al. 2013; Malumbres and Barbacid 2003).

9.3 Rasal1 – the missing GAP downstream of plexins

It could be shown in Fig. 9 and 10, that Rasal1 acts specifically as a GAP in semaphorin-plexin signaling and exerts its function via its GAP domain. These data could also confirm the hypothesis of an indirect mechanism of semaphorin-mediated R-Ras deactivation by plexins, since the knockdown of the plexin receptor phenocopied R-Ras activation levels after semaphorin stimulation. Furthermore, the universality of Rasal1 in semaphorin-plexin signaling was shown to be true for all plexin subfamilies. Due to the lack of appropriate antibodies for

Rasal1 or Plexin-B1 in Western blot analysis, pulldown and CO-IP assays with overexpressed cDNA constructs had to be performed. During these studies, the simultaneous overexpression of three or more constructs in HEK293T cells was were difficult heading in qualitative results, that made a reference to endogenous conditions complicated. For example, in Fig. 10A, a lack of Plexin-B1 should lead to a deactivation of R-Ras by Rasal1 wildtype as can be seen after the siRNA-mediated knockdown of Plexin-B2 in Fig. 9. Since this is not the case, secondary compensatory mechanisms regulating cDNA construct expression, localization or activity and defective stoichiometry of signaling partners could explain this discrepancy.

To confirm the involvement of Rasal1 as a GAP downstream of plexins, the COS-7 collapse assay as a functional readout for semaphorin-plexin signaling was performed. Despite the fact, that the collapse efficiency only partially depends on R-Ras (overexpression of constitutively active R-Ras phenocopied Rasal1 knockdown or overexpression of Rasal1 mutGAP) and the quantified differences were fairly low, this assay was the method of choice to quantify semaphorin-plexin signaling and elaborate the influence of different signaling partners. Furthermore, it has been discovered that the collapse of COS-7 cells not only depends on R-Ras but also on Rap1 (data not shown), contradicting observations of Oinuma et al. (2010) and Yukawa et al. (2010b).

Moreover, this thesis provides evidence that Rasal1, but not Rasal2, interacts with plexins independent of semaphorin stimulation and R-Ras binding (Fig. 11). This interaction was detected between Plexin-B1 and Rasal1 lacking the two C2 domains, as well as for Plexin-B2 lacking the intracellular domain and Rasal1. Two different reflections could contribute to these observations: (1) the interaction is unspecific or (2) the interaction is indirect and mediated by other proteins. To assess possibility (1), the binding domain of Rasal1 to plexins was tried to identify by cloning different deletion mutants and characterizing their interaction with plexins (data not shown). Unfortunately, all mutants were co-immunoprecipitated with Plexin-B1 and therefore it was not possible to identify the responsible domain of Rasal1, pointing to rather unspecific interactions. On top of that, the plexin signaling complex involves further binding of different proteins including ErbB-2 and Met, resulting in phosphorylation and cross-activation (Swiercz et al. 2008; Worzfeld et al. 2012; Conrotto et al. 2005). Therefore, an indirect mechanism as hypothesized in possibility (2) seems reasonable and might be mediated by the extracellular domain of plexins interacting with other membrane receptors, and by

this means bringing Rasal1 close to the intracellular domain of plexins. Unfortunately, it was not possible to identify an interaction between Rasal1 and ErbB-2 or Met due to lacking availability or specificity of antibodies.
In addition to that, a phosphorylation-dependent regulation of interaction and activity of Rasal1 seems conceivable in the case of ErbB-2 and Met phosphorylating Plexin-B1, that is necessary for RhoA signaling as described by Swiercz et al. (2008). Interestingly, ErbB-2 conducted phosphorylation results in activation of RhoA, while Met mediated phosphorylation inhibits RhoA activation (Swiercz et al. 2004; Swiercz et al. 2008). It was tried to identify possible phosphorylation sites of Rasal1 with Mass spectrometry, but ambiguous results were obtained that were not conclusive, and therefore this analysis was stopped. Finding the exact interaction mechanism between plexins, Rasal1 and other players in semaphorin-plexin signaling remains a challenging task to address in a future study.

Rasal1 displays GAP activity only when bound to the plasma membrane, while purified protein does not show GAP activity for Ras (Walker et al. 2004). The unique feature of Rasal1 is its ability to oscillate between the cytoplasm and the plasma membrane with increasing calcium spikes and distinguishes it from permanently translocated RasGAPs like Rasa4. The calcium-dependent translocation is mediated via the two C2 domains of Rasal1, while the PH domain is non-functional (Walker et al. 2004; Liu et al. 2005; Lockyer et al. 2001).
This study revealed, that semaphorin application does not induce intracellular calcium release and plasma membrane translocation of Rasal1 (Fig. 12), but that Rasal1 activity is still dependent on the C2 domains and the availability of calcium in the cell. This correlation has been shown by overexpressing Rasal1 mutants lacking the two C2 domains and by blocking intracellular calcium signaling with BAPTA-AM in COS-7 collapse assays (Fig. 13). These observations led to the assumption that Rasal1 decodes two different, partially unconnected signals: (1) the deactivation of R-Ras downstream of plexins and (2) a calcium regulated activation of RasGAP activity. Physiological intracellular calcium concentrations seem to be enough to mediate semaphorin-induced R-Ras deactivation as estimated in (1). It is therefore tempting to assume that regulation of Rasal1 activity by increasing calcium-spikes as described in (2), adds additional signaling potential to the deactivation of R-Ras after semaphorin stimulation, by increasing activity and availability of Rasal1 at the plasma membrane. An increase in intracellular calcium could possibly result from cross-activation of other receptors

after activation of plexin signaling and might not have been observable in the experiments due to the overexpression of EGFP-Rasal1, making it difficult to detect small amounts of translocation (Fig. 12).

Since Rasal1 acts as a negative regulator of Ras activity and is calcium sensitive, it seems conceivable that under certain conditions RasGAPs can act as tumor suppressors by regulating Ras activity, since a link between calcium influence and cell proliferation has been described a long time ago (Boynton et al. 1976). Furthermore, Swiercz et al. (2009) have depicted the recruitment of PLCγ into the Plexin-B1 receptor complex to regulate RhoGEF activity without altering R-Ras signaling, and in this way regulating cell migration. Even though, lipase activity of PLCγ is not needed for RhoA activation, the binding of PLCγ to Plexin-B1 could connect semaphorin-plexin signaling to a calcium release from the endoplasmic reticulum upon co-activation of RTKs like ErbB-2, leading to the activation of different calcium-dependent pathways and therefore possibly influencing RasGAP activity (Worzfeld et al. 2012).

In other contexts, plexins can act as adhesion molecules in the presence of calcium via homophilic binding mechanisms (Ohta et al. 1995) and can serve as mechanosensors in endothelial cells, leading to intracellular calcium increase after force application (Mehta et al. 2020).

Despite the role of plexins as adhesion and mechanosensation molecules, it might be conceivable that calcium potentiates plexin signaling in a semaphorin-independent manner by increasing membrane localization of plexins or cross-activating additional signaling pathways, as shown in the case of Rab46, a calcium sensitive GTPase, integrating G protein signaling for trafficking and cargo release of Weibel-Palade bodies (Miteva et al. 2019).

Thereupon, additional experiments must elucidate the specific role of calcium in the regulation of Rasal1-mediated R-Ras activity, to investigate other calcium-dependent roles of plexins in development, as well as under physiological and pathophysiological conditions.

Analyzing the exact mechanism of R-Ras deactivation by Rasal1, it has been shown that the GAP domain of plexins binds active R-Ras and sequesters it from the deactivation by Rasal1 (Fig. 14). This concept of Ras GTPase binding without changing the activity level has as well been observed for the GAP IQGAP, that lacks necessary arginine residues to perform GTP hydrolysis (Maertens and Cichowski 2014). In the light of these findings, binding of semaphorins leads to the release of active R-Ras, possibly due to the dimerization of the plexin receptor

followed by conformational changes (Fig. 15). It is not known yet, whether this release is caused by a change in affinity of R-Ras to plexins and whether this mechanism is induced by Rasal1 or other players in the signaling complex, e.g. Rnd1, but results in binding of R-Ras to Rasal1 and hence deactivation. It is imaginable, that M-Ras and Rap1 are deactivated by the same mechanism, since Rasal1 exerts GAP activity to Ras and Rap (Sot et al. 2010). Recently, Cuellar et al. (2017) presented crystal structures of the Rasal1 domain topology, explaining the dual specificity of Rasal1 to Ras and Rap. Moreover, Rap1 is a homologue of Ras and a redundant or additive function of these two proteins in plexin signaling seems conceivable. In addition to that, further experiments confirming GAP activity of Rasal1 towards R-Ras are needed to prove enzymatic function of Rasal1 in a plexin signaling context.

There are 14 encoded RasGAPs in the human genome and their expression and activity level is tissue- and context-specific (Maertens and Cichowski 2014).
Due to their highly similar function in deactivating Ras GTPases, it seems likely, that other RasGAPs could be involved in the deactivation of R-Ras downstream of plexins under certain conditions, that arise from the aforementioned differences in the tissue- and context-specific expression and activity regulation. Especially Rasa4, a member of the GAP1^{m} family like Rasal1, is structurally and functionally very closely related to Rasal1 (King et al. 2013; Liu et al. 2005) and could be one of these candidates. Since the concept of the involvement of GAPs for R-Ras deactivation in plexin signaling is new, further experiments for the RasGAP specificity must confirm the universal role of Rasal1 in different tissues and under different cellular situations.
Moreover, RasGAPs can have Ras-independent functions as in the case of DAB2IP-dependent nuclear factor-kappaB activation (Min et al. 2010), of IQGAP1 acting as a scaffold protein (White et al. 2012), of Tagap regulating GTPase interactions with Plexin-D1 in thymocytes (Duke-Cohan et al. 2018) and of Rasal1 negatively regulating T-cell activity by association with the T-cell receptor (Thaker et al. 2019).
This versatility in activity regulation of Ras arising from numerous GAPs and their diverse expression pattern coupled with additional signaling functions elucidates the complexity beyond the Ras oncogene and the necessity to characterize their oncogenic influence in carcinogenesis and consequently use GAPs as potentially therapeutic targets. Since it is pharmacologically easier to design antagonists than activating proteins for therapy, the focus on exploiting RasGAPs in

pathophysiology should be lay on (epi-)genetic regulation of RasGAP expression and the localization, stability or activity mediated by the cellular interactome.

9.4 Rasal1 is a negative regulator of gastric acid production

Finally, evidence is provided that the semaphorin-plexin-Rasal1-R-Ras signaling axis is negatively controlling gastrin expression in STC-1 cells (Fig. 16) and mouse models, by identifying Rasal1 as an inhibitor of gastric acid production and a protective player in peptic ulcers disease, since gastric acid leads to lesions of the stomach epithelium (submitted manuscript). Rasal1 could act as a tumor suppressor in the stomach, due to its negative influence on R-Ras dependent gastrin expression and could consequently protect the stomach from gastrin-mediated cell proliferation contributing to gastric cancer (Chen et al. 2014; Lee et al. 2005).

In addition to that, Semaphorin 4B was found to be a functional ligand for Plexin-B1 in the stomach epithelium for this newly characterized pathway (Fig. 17). Moreover, Semaphorin 4D, the classical ligand of Plexin-B1 also exists in a soluble and cleaved form that could be delivered via the blood stream into the gastric epithelium, representing an additional level of gastrin expression regulation by inter-organ communication (Delaire et al. 2001).

Another player in gastric acid production is histamine, that gets released by ECL cells upon gastrin stimulation and can induce, like gastrin , gastric acid production in parietal cells (Engevik et al. 2020). It is conceivable, that secreted histamine could also act on G cells in a negative feedback loop by inducing calcium dependent Rasal1 activation, resulting in lower gastrin expression.

For current standard treatment of peptic ulcers disease, proton pump inhibitors (PPIs) are used to prevent the release of gastric acid into the gastric lumen. The long-term effects of PPI treatment include structural and functional changes of the gastric mucosa, ECL cell hyperplasia and hypergastrinaemia inter alia correlated to elevated gastrin levels (Malfertheiner et al. 2017). The activation of the plexin-Rasal1-R-Ras signaling pathway could therefore be a desirable approach, since the regulation of gastrin production could lead to the prevention of gastrin-related adverse effects occurring during PPI medication. But due to relatively low side effects, the long-term experience and the easy oral application, the current standard treatment with PPIs has a clear advantage in comparison to a possible new therapy based on the semaphorin-plexin system.

9.5 Proposed mechanism of Rasal1-mediated gastrin regulation

In addition to the provided data on the Rasal1-mediated signaling mechanism of semaphorins and plexins and their role in the regulation of gastrin expression, further in vivo and ex vivo experiments were performed in collaboration with Dr. Rui Xu, that give strong evidence for the involvement of this pathway in the expression of gastrin and in the production of gastric acid in vivo (data not shown, submitted manuscript). In sum, it could be shown that the application of semaphorins to murine and human gastric organoids led to a downregulation of gastrin mRNA expression. Using different genetic mouse models, the role of the semaphorin-plexin-Rasal1 signaling axis that controls gastrin mRNA expression, gastrin plasma concentrations and gastric acid production was confirmed. Finally, it could be shown that this signaling pathway had a protective effect in nonsteroidal anti-inflammatory drug (NSAID)-induced gastric lesions.

The proposed in vivo mechanism of Rasal1-mediated regulation of gastrin expression is presented in Fig. 20: Plexin-B1, expressed in the stomach epithelium, binds active R-Ras and sequesters it from the deactivation by GAPs. Upon stimulation by binding of Semaphorin 4D or Semaphorin 4B to Plexin-B1, active R-Ras gets released from Plexin-B1 and is then being deactivated by Rasal1.

R-Ras is a GTPase activating downstream effector that can upregulate gastrin mRNA expression in G cells of the gastric epithelium. After R-Ras induced gastrin release by G cells, it signals via the CCK2 receptor on parietal cells that produce gastric acid in response and secrete it into the gastric lumen.

The semaphorin-plexin-Rasal1 signaling pathway is consequently a negative regulator of gastrin expression and can therefore protect the stomach epithelium from peptic ulcers disease.

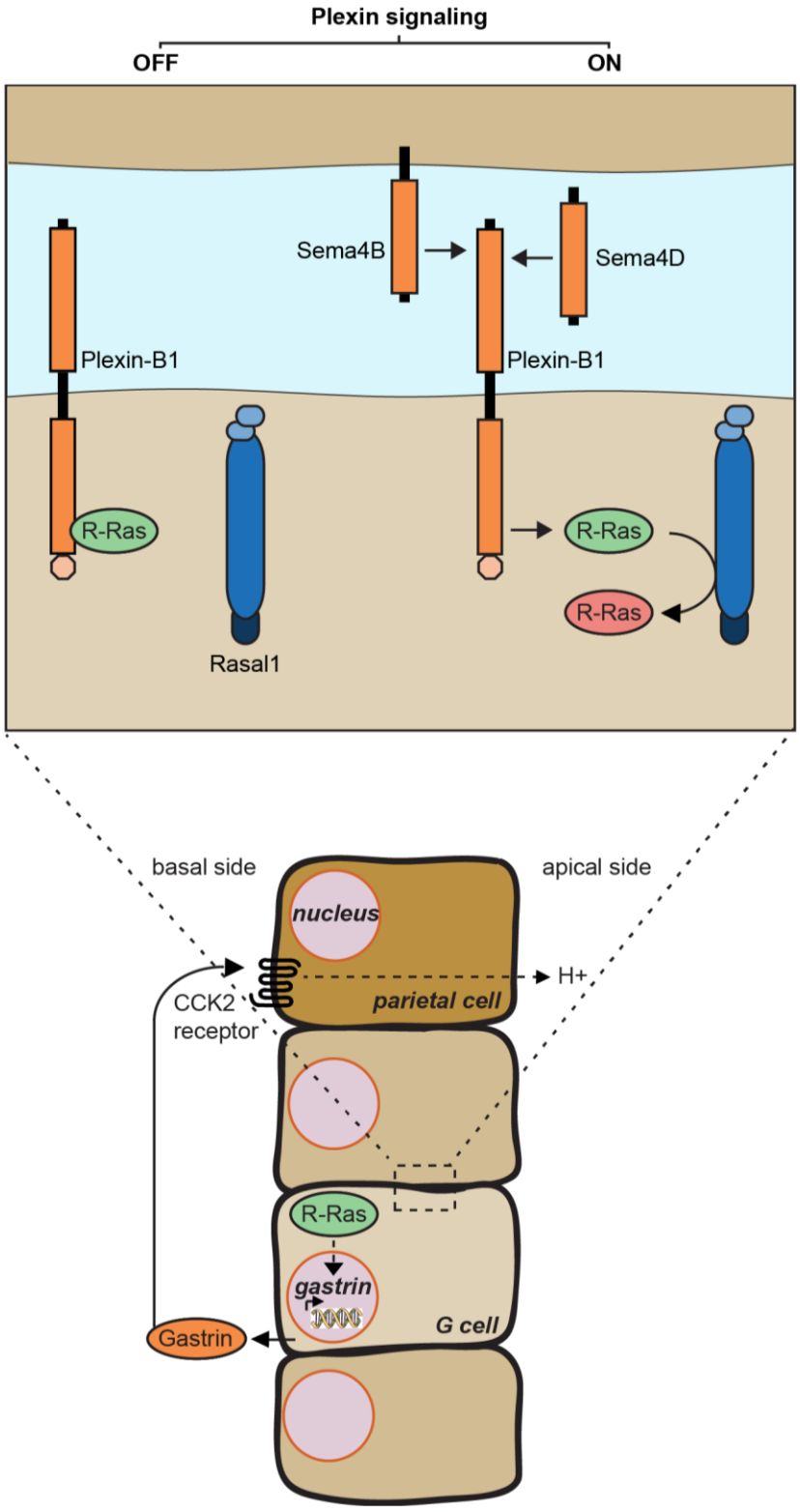

Figure 20. Rasal1 negatively regulates gastrin expression in the stomach. In the stomach epithelium, gastrin expression is regulated by R-Ras. The release of gastrin by G cells leads to the stimulation of parietal cells via the CCK2 receptor and thereby the production of gastric acid. Rasal1 is a negative regulator of gastrin expression. Plexin-B1 sequesters active R-Ras (green) from deactivation by Rasal1. After the binding of Semaphorin 4D (Sema4D) or Semaphorin 4B (Sema4B), active R-Ras is being released and then deactivated by Rasal1 (red), negatively regulating gastric acid production.

9.6 Human Plexin-B2 mutation affects plexin-signaling

In the kidney, the semaphorin-plexin system plays a role in organogenesis and pathophysiology (Xia and Worzfeld 2016). Elevated levels of semaphorins and plexins have been shown to result in various kidney diseases (Mohamed et al. 2014; Ranganathan et al. 2014) and B-plexins were identified to be involved in mitotic spindle orientation, with defective morphogenesis and repair in the kidney (Xia et al. 2015). Further publications describe Plexin-B1/Semaphorin 4D and Plexin-B2/Semaphorin 4C to be involved in development and organogenesis of various tissues and organs, like branching morphogenesis in the developing kidney (Korostylev et al. 2008; Perälä et al. 2011). In addition to that, Plexin-B1 was found to be downregulated in renal cell carcinomas (Gómez Román et al. 2008). These data underline the complexity and versatility of semaphorin-plexin signaling and its different functions in distinct organs or under physiological and pathophysiological conditions.

The data of Plexin-B2 mutations found in CAKUT patients have revealed an involvement of mutation T79M in plexin signaling, while the expression level, localization or binding of Semaphorin 4C were not influenced by any of these mutations (Fig. 18 and 19). In 2014, Rodriguez has reviewed the broad symptoms of patients with CAKUT, ranging from asymptomatic to severe, life-threatening malformations of the kidney and the urinary tract. Connecting the malformations of CAKUT patients to the role of Plexin-B1/Plexin-B2 in kidney morphogenesis, it is tempting to assume that germline mutations of plexins are involved in the emergence of CAKUT.

The sema domain of plexins is involved in binding of semaphorins and neuropilins that lead to dimerization of plexins and hence downstream signaling (Wang et al. 2012; Takahashi and Strittmatter 2001). The mutation T79M in the sema domain of Plexin-B2 opens therefore at least two possibilities for its involvement in the semaphorin-plexin system: (1) the binding of Semaphorin 4C is abrogated due to less membrane-bound receptor/binding or (2) the signal-transduction is defective. According to the investigations concerning the binding measurements of Semaphorin 4C to Plexin-B2, possibility (1) seems unlikely, since neither the localization of Plexin-B2 nor the binding of Semaphorin 4C were significantly changed in HEK293T cells overexpressing Plexin-B2 mutation T79M in comparison to Plexin-B2 wildtype. Given the fact, that binding of semaphorins is essential for the dimerization of plexins and hence downstream signaling, the lower

signaling ability of Plexin-B2 mutation T79M could be caused by less dimerization of the receptor, pointing towards possibility (2). Even though, no mutations of the sema domain of plexins have been described so far, the sema domain of Met, a receptor tyrosine kinase, was shown to be responsible for dimerization and activation (Kong-Beltran et al. 2004) and here, mutation V370D led to defective dimerization and therefore less receptor activation (Miao et al. 2019). This example of a mutation in the sema domain of Met, that influences receptor activation, offers a concept that could be interesting to investigate in the context of Plexin-B2 mutation T79M in further experiments.

In conclusion, the results add information to the general involvement of semaphorin-plexin signaling in CAKUT and revealed that Plexin-B2 mutation T79M negatively influences Plexin-B2 activation.

Still, in the future more data on the activation of Plexin-B2 carrying mutations need to be acquired, e.g. with Ras/Rho pulldowns, to confirm these observations. In addition to this, an approach to visualize abrogated dimerization would be desirable.

All in all, this study enlightens central previously unknown mechanisms in semaphorin-plexin signaling and helps understanding the influence and importance of this versatile pathway in physiological and pathophysiological conditions on a molecular level. Furthermore, an old controversy about the GAP function of plexins was deciphered by validating Rasal1 as the only specific regulator of R-Ras activity downstream of plexins. In the future, these findings might add expertise to the treatment of different diseases, but still, various further investigations are needed to address some of the previously discussed open questions and thereby help to better use these findings in the context of disease development.

10 Summary

Semaphorins, a class of soluble and membrane-bound ligands, and their corresponding receptors, plexins, play a pivotal role in organogenesis, physiology of different tissues and organ systems, as well as in the development of diseases. Plexins exert diverse signaling functions via their intracellular domain. One of these functions is the deactivation of R-Ras, a non-classical isoform of the oncogene Ras. So far, the exact mechanism of this plexin-mediated R-Ras deactivation is unknown.

In this thesis, the yet unidentified mechanism is elucidated, recently discovered players in the semaphorin-plexin system are investigated and mutations of plexins are characterized for their role in ligand-binding and downstream signaling. For this purpose, molecular biological, biochemical, cell biological and pharmacological methods were combined.

It could be shown that mutations of Plexin-B2 occurring in patients with congenital anomalies of the kidney and urinary tract impair the plexin-mediated signaling ability. Moreover, TMEM260, a protein with so far unknown function, serves as an O-mannosyltransferase for plexins and a role for these protein-mediated Plexin-B2 mannosylations was identified in membrane targeting and proteolytic processing.

Additionally, Rasal1 was validated and characterized as a GTPase activating protein downstream of plexins, that deactivates R-Ras. In this mechanism plexins bind active R-Ras, without influencing its activity. The binding of semaphorins to plexins induces the release of R-Ras from plexin binding and R-Ras then gets deactivated by Rasal1.

Finally, these findings were set in a translational context by identifying a role of the semaphorin-plexin-Rasal1-R-Ras signaling axis in the negative regulation of gastrin gene expression in vitro, a peptide hormone that stimulates gastric acid production.

Concluding, these findings illuminate new mechanistic insights into plexin signaling, uncover new molecular functions of plexins in pathophysiology and clear up the controversy about the function of the plexin GTPase activating protein domain in the regulation of R-Ras activity.

11 Zusammenfassung

Semaphorine, eine Klasse von löslichen und membrangebundenen Liganden, und ihre zugehörigen Rezeptoren, Plexine, spielen eine bedeutende Rolle in der Organogenese, der Physiologie verschiedener Gewebe und Organsysteme, sowie bei der Entstehung von Krankheiten. Plexine vermitteln ihre vielfältigen Signalfunktionen durch ihre intrazelluläre Domäne. Eine dieser Funktionen ist die Deaktivierung von R-Ras, einer nicht-klassischen Isoform des Ras-Onkogens. Bis jetzt ist der exakte Mechanismus dieser Plexin-regulierten R-Ras Deaktivierung unklar.

In der vorliegenden Dissertation wird dieser Mechanismus aufgeklärt, weitere neu-entdeckte Akteure im Semaphorin-Plexin System charakterisiert und Mutationen in Plexinen hinsichtlich ihrer Ligandenbindung und Signalweiterleitung untersucht. Hierfür wurden molekularbiologische, biochemische, zellbiologische und pharmakologische Methoden kombiniert.

Es wurde herausgefunden, dass Mutationen im Plexin-B2-Gen bei Patienten, die an kongenitalen Anomalien der Nieren und ableitenden Harnwege leiden, die Plexin-vermittelte Signalweiterleitung beeinträchtigen. Darüber hinaus ist TMEM260, ein Protein unbekannter Funktion, welches als O-Mannosyltransferase für Plexine identifiziert wurde, verantwortlich für die Membranlokalisation und proteolytischer Prozessierung von Plexin-B2.

Des Weiteren wurde Rasal1 als ein den Plexinen nachgeschaltetes GTPase-aktivierendes Protein validiert und charakterisiert, welches R-Ras deaktiviert. Der zugrundeliegende Mechanismus konnte in dieser Arbeit aufgeklärt und gezeigt werden, dass Plexine aktives R-Ras binden, ohne dessen Aktivität zu beeinflussen. Nach der Bindung von Semaphorinen an Plexine, wird aktives R-Ras aus der Bindung von Plexinen freigesetzt und durch Rasal1 deaktiviert.

Zuletzt wurden diese Erkenntnisse in einen translationalen Kontext gesetzt, der eine wichtige Rolle der Semaphorin-Plexin-Rasal1-R-Ras Signalachse bei der negativen Regulation der Transkription des Gastrin-Gens in vitro aufzeigt, einem Peptidhormon, welches die Magensäureproduktion anregt.

Zusammengefasst geben diese Ergebnisse neue mechanistische Einblicke in den Plexinsignalweg, decken neue, molekulare und pathophysiologische Funktionen von Plexinen auf, und lösen die Kontroverse über die Funktionalität der GTPase-aktivierenden Proteindomäne bei der Regulierung der R-Ras Aktivität.

12 References

Abid, A., Ismail, M., Mehdi, S. Q., Khaliq, S., 2006. Identification of novel mutations in the SEMA4A gene associated with retinal degenerative diseases. Journal of medical genetics 43 (4): 378–381. 10.1136/jmg.2005.035055.

Aggarwal, P. K., Veron, D., Thomas, D. B., Siegel, D., Moeckel, G., Kashgarian, M., Tufro, A., 2015. Semaphorin3a promotes advanced diabetic nephropathy. Diabetes 64 (5): 1743–1759. 10.2337/db14-0719.

Ahmadian, M. R., Stege, P., Scheffzek, K., Wittinghofer, A., 1997. Confirmation of the arginine-finger hypothesis for the GAP-stimulated GTP-hydrolysis reaction of Ras. Nature structural biology 4 (9): 686–689.

Alto, L. T., Terman, J. R., 2017. Semaphorins and their Signaling Mechanisms. Methods in molecular biology (Clifton, N.J.) 1493: 1–25. 10.1007/978-1-4939-6448-2_1.

Ardito, F., Giuliani, M., Perrone, D., Troiano, G., Lo Muzio, L., 2017. The crucial role of protein phosphorylation in cell signaling and its use as targeted therapy (Review). International Journal of Molecular Medicine 40 (2): 271–280. 10.3892/ijmm.2017.3036.

Artigiani, S., Barberis, D., Fazzari, P., Longati, P., Angelini, P., van de Loo, J.-W., Comoglio, P. M., Tamagnone, L., 2003. Functional regulation of semaphorin receptors by proprotein convertases. The Journal of biological chemistry 278 (12): 10094–10101. 10.1074/jbc.M210156200.

Aurandt, J., Li, W., Guan, K.-L., 2006. Semaphorin 4D activates the MAPK pathway downstream of plexin-B1. The Biochemical journal 394 (Pt 2): 459–464. 10.1042/BJ20051123.

Aurandt, J., Vikis, H. G., Gutkind, J. S., Ahn, N., Guan, K.-L., 2002. The semaphorin receptor plexin-B1 signals through a direct interaction with the Rho-specific nucleotide exchange factor, LARG. Proceedings of the National Academy of Sciences of the United States of America 99 (19): 12085–12090. 10.1073/pnas.142433199.

Balakrishnan, A., Penachioni, J. Y., Lamba, S., Bleeker, F. E., Zanon, C., Rodolfo, M., Vallacchi, V., Scarpa, A., Felicioni, L., Buck, M., Marchetti, A., Comoglio, P. M., Bardelli, A., Tamagnone, L., 2009. Molecular profiling of the "plexinome" in melanoma and pancreatic cancer. Human mutation 30 (8): 1167–1174. 10.1002/humu.21017.

Bar-Sagi, D., Hall, A., 2000. Ras and Rho GTPases: a family reunion. Cell 103 (2): 227–238. 10.1016/s0092-8674(00)00115-x.

Basile, J. R., Afkhami, T., Gutkind, J. S., 2005. Semaphorin 4D/plexin-B1 induces endothelial cell migration through the activation of PYK2, Src, and the phosphatidylinositol 3-kinase-Akt pathway. Molecular and cellular biology 25 (16): 6889–6898. 10.1128/MCB.25.16.6889-6898.2005.

Basile, J. R., Gavard, J., Gutkind, J. S., 2007. Plexin-B1 utilizes RhoA and Rho kinase to promote the integrin-dependent activation of Akt and ERK and endothelial cell motility. The Journal of biological chemistry 282 (48): 34888–34895. 10.1074/jbc.M705467200.

Battistini, C., Tamagnone, L., 2016. Transmembrane semaphorins, forward and reverse signaling: have a look both ways. Cellular and molecular life sciences CMLS 73 (8): 1609–1622. 10.1007/s00018-016-2137-x.

Bechtel, W., McGoohan, S., Zeisberg, E. M., Müller, G. A., Kalbacher, H., Salant, D. J., Müller, C. A., Kalluri, R., Zeisberg, M., 2010. Methylation determines fibroblast activation and fibrogenesis in the kidney. Nature medicine 16 (5): 544–550. 10.1038/nm.2135.

Bernards, A., Settleman, J., 2004. GAP control: regulating the regulators of small GTPases. Trends in cell biology 14 (7): 377–385. 10.1016/j.tcb.2004.05.003.

Boynton, A. L., Whitfield, J. F., Isaacs, R. J., 1976. The different roles of serum and calcium in the control of proliferation of BALB/c 3T3 mouse cells. In vitro 12 (2): 120–123. 10.1007/bf02796358.

Bradford, M. M., 1976. A rapid and sensitive method for the quantitation of microgram quantities of protein utilizing the principle of protein-dye binding. Analytical biochemistry 72: 248–254. 10.1006/abio.1976.9999.

Britton, S., Dernoncourt, E., Delteil, C., Froment, C., Schiltz, O., Salles, B., Frit, P., Calsou, P., 2014. DNA damage triggers SAF-A and RNA biogenesis factors exclusion from chromatin coupled to R-loops removal. Nucleic acids research 42 (14): 9047–9062. 10.1093/nar/gku601.

Brtva, T. R., Drugan, J. K., Ghosh, S., Terrell, R. S., Campbell-Burk, S., Bell, R. M., Der, C. J., 1995. Two distinct Raf domains mediate interaction with Ras. The Journal of biological chemistry 270 (17): 9809–9812. 10.1074/jbc.270.17.9809.

Bryant, L., Lozynska, O., Han, G., Morgan, J. I. W., Gai, X., Maguire, A. M., Aleman, T., Bennett, J., 2018. On variants and disease-causing mutations: Case studies of a SEMA4A variant identified in inherited blindness. Ophthalmic genetics 39 (1): 144–146. 10.1080/13816810.2017.1354384.

Burnette, W. N., 1981. "Western blotting": electrophoretic transfer of proteins from sodium dodecyl sulfate--polyacrylamide gels to unmodified nitrocellulose and radiographic detection with antibody and radioiodinated protein A. Analytical biochemistry 112 (2): 195–203. 10.1016/0003-2697(81)90281-5.

Calvisi, D. F., Ladu, S., Conner, E. A., Seo, D., Hsieh, J.-T., Factor, V. M., Thorgeirsson, S. S., 2011. Inactivation of Ras GTPase-activating proteins promotes unrestrained activity of wild-type Ras in human liver cancer. Journal of hepatology 54 (2): 311–319. 10.1016/j.jhep.2010.06.036.

Chen, H., Cheng, Z.-Y., Pan, Y., Wang, Z., Liu, Y., Zhang, J.-Q., 2014. RASAL1 influences the proliferation and invasion of gastric cancer cells by regulating the RAS/ERK signaling pathway. Human cell 27 (3): 103–110. 10.1007/s13577-014-0090-2.

Cohen, P., 2002. The origins of protein phosphorylation. Nature cell biology 4 (5): E127-30. 10.1038/ncb0502-e127.

Colicelli, J., 2004. Human RAS superfamily proteins and related GTPases. Science's STKE signal transduction knowledge environment 2004 (250): RE13. 10.1126/stke.2502004re13.

Conrotto, P., Valdembri, D., Corso, S., Serini, G., Tamagnone, L., Comoglio, P. M., Bussolino, F., Giordano, S., 2005. Sema4D induces angiogenesis through Met recruitment by Plexin B1. Blood 105 (11): 4321–4329. 10.1182/blood-2004-07-2885.

Cuellar, J., Valpuesta, J. M., Wittinghofer, A., Sot, B., 2017. Domain topology of human Rasal. Biological chemistry 399 (1): 63–72. 10.1515/hsz-2017-0159.

Dasgupta, B., Dugan, L. L., Gutmann, D. H., 2003. The neurofibromatosis 1 gene product neurofibromin regulates pituitary adenylate cyclase-activating polypeptide-mediated signaling in astrocytes. The Journal of neuroscience the official journal of the Society for Neuroscience 23 (26): 8949–8954.

Davis, H. E., Morgan, J. R., Yarmush, M. L., 2002. Polybrene increases retrovirus gene transfer efficiency by enhancing receptor-independent virus adsorption on target cell membranes. Biophysical chemistry 97 (2-3): 159–172. 10.1016/s0301-4622(02)00057-1.

Davis, S. J., Ward, H. A., Puklavec, M. J., Willis, A. C., Williams, A. F., Barclay, A. N., 1990. High level expression in Chinese hamster ovary cells of soluble forms of CD4 T lymphocyte glycoprotein including glycosylation variants. The Journal of biological chemistry 265 (18): 10410–10418.

Deb Roy, A., Yin, T., Choudhary, S., Rodionov, V., Pilbeam, C. C., Wu, Y. I., 2017. Optogenetic activation of Plexin-B1 reveals contact repulsion between

osteoclasts and osteoblasts. Nature communications 8: 15831. 10.1038/ncomms15831.

Delaire, S., Billard, C., Tordjman, R., Chédotal, A., Elhabazi, A., Bensussan, A., Boumsell, L., 2001. Biological activity of soluble CD100. II. Soluble CD100, similarly to H-SemaIII, inhibits immune cell migration. Journal of immunology (Baltimore, Md. 1950) 166 (7): 4348–4354. 10.4049/jimmunol.166.7.4348.

Deng, S., Hirschberg, A., Worzfeld, T., Penachioni, J. Y., Korostylev, A., Swiercz, J. M., Vodrazka, P., Mauti, O., Stoeckli, E. T., Tamagnone, L., Offermanns, S., Kuner, R., 2007. Plexin-B2, but not Plexin-B1, critically modulates neuronal migration and patterning of the developing nervous system in vivo. The Journal of neuroscience the official journal of the Society for Neuroscience 27 (23): 6333–6347. 10.1523/JNEUROSCI.5381-06.2007.

Drosten, M., Dhawahir, A., Sum, E. Y. M., Urosevic, J., Lechuga, C. G., Esteban, L. M., Castellano, E., Guerra, C., Santos, E., Barbacid, M., 2010. Genetic analysis of Ras signalling pathways in cell proliferation, migration and survival. The EMBO journal 29 (6): 1091–1104. 10.1038/emboj.2010.7.

Duke-Cohan, J. S., Ishikawa, Y., Yoshizawa, A., Choi, Y.-I., Lee, C.-N., Acuto, O., Kissler, S., Reinherz, E. L., 2018. Regulation of thymocyte trafficking by Tagap, a GAP domain protein linked to human autoimmunity. Science signaling 11 (534). 10.1126/scisignal.aan8799.

Elia, G., 2012. Cell surface protein biotinylation for SDS-PAGE analysis. Methods in molecular biology (Clifton, N.J.) 869: 361–372. 10.1007/978-1-61779-821-4_29.

Engevik, A. C., Kaji, I., Goldenring, J. R., 2020. The Physiology of the Gastric Parietal Cell. Physiological reviews 100 (2): 573–602. 10.1152/physrev.00016.2019.

Feng, J., Petersen, C. D., Coy, D. H., Jiang, J.-K., Thomas, C. J., Pollak, M. R., Wank, S. A., 2010. Calcium-sensing receptor is a physiologic multimodal chemosensor regulating gastric G-cell growth and gastrin secretion. Proceedings of the National Academy of Sciences of the United States of America 107 (41): 17791–17796. 10.1073/pnas.1009078107.

Feng, M., Bao, Y., Li, Z., Li, J., Gong, M., Lam, S., Wang, J., Marzese, D. M., Donovan, N., Tan, E. Y., Hoon, D. S. B., Yu, Q., 2014. RASAL2 activates RAC1 to promote triple-negative breast cancer progression. The Journal of clinical investigation 124 (12): 5291–5304. 10.1172/JCI76711.

Fisher, T. L., Reilly, C. A., Winter, L. A., Pandina, T., Jonason, A., Scrivens, M., Balch, L., Bussler, H., Torno, S., Seils, J., Mueller, L., Huang, H.,

Klimatcheva, E., Howell, A., Kirk, R., Evans, E., Paris, M., Leonard, J. E., Smith, E. S., Zauderer, M., 2016. Generation and preclinical characterization of an antibody specific for SEMA4D. mAbs 8 (1): 150–162. 10.1080/19420862.2015.1102813.

Flanagan, J. G., Leder, P., 1990. The kit ligand: a cell surface molecule altered in steel mutant fibroblasts. Cell 63 (1): 185–194. 10.1016/0092-8674(90)90299-t.

Ford, M. G., Valle, J. D., Soroka, C. J., Merchant, J. L., 1997. EGF receptor activation stimulates endogenous gastrin gene expression in canine G cells and human gastric cell cultures. The Journal of clinical investigation 99 (11): 2762–2771. 10.1172/JCI119466.

Franco, M., Tamagnone, L., 2008. Tyrosine phosphorylation in semaphorin signalling: shifting into overdrive. EMBO reports 9 (9): 865–871. 10.1038/embor.2008.139.

Giordano, S., Corso, S., Conrotto, P., Artigiani, S., Gilestro, G., Barberis, D., Tamagnone, L., Comoglio, P. M., 2002. The semaphorin 4D receptor controls invasive growth by coupling with Met. Nature cell biology 4 (9): 720–724. 10.1038/ncb843.

Gómez Román, J. J., Garay, G. O., Saenz, P., Escuredo, K., Sanz Ibayondo, C., Gutkind, S., Junquera, C., Simón, L., Martínez, A., Fernández Luna, J. L., Val-Bernal, J. F., 2008. Plexin B1 is downregulated in renal cell carcinomas and modulates cell growth. Translational research the journal of laboratory and clinical medicine 151 (3): 134–140. 10.1016/j.trsl.2007.12.003.

Graham, F. L., van der Eb, A. J., 1973. A new technique for the assay of infectivity of human adenovirus 5 DNA. Virology 52 (2): 456–467. 10.1016/0042-6822(73)90341-3.

Gu, C., Giraudo, E., 2013. The role of semaphorins and their receptors in vascular development and cancer. Experimental cell research 319 (9): 1306–1316. 10.1016/j.yexcr.2013.02.003.

Gunawardhana, N., Jang, S., Choi, Y. H., Hong, Y. A., Jeon, Y.-E., Kim, A., Su, H., Kim, J.-H., Yoo, Y.-J., Merrell, D. S., Kim, J., Cha, J.-H., 2017. Helicobacter pylori-Induced HB-EGF Upregulates Gastrin Expression via the EGF Receptor, C-Raf, Mek1, and Erk2 in the MAPK Pathway. Frontiers in cellular and infection microbiology 7: 541. 10.3389/fcimb.2017.00541.

Gurrapu, S., Franzolin, G., Fard, D., Accardo, M., Medico, E., Sarotto, I., Sapino, A., Isella, C., Tamagnone, L., 2019. Reverse signaling by semaphorin 4C

elicits SMAD1/5- and ID1/3-dependent invasive reprogramming in cancer cells. Science signaling 12 (595). 10.1126/scisignal.aav2041.

Gurrapu, S., Pupo, E., Franzolin, G., Lanzetti, L., Tamagnone, L., 2018. Sema4C/PlexinB2 signaling controls breast cancer cell growth, hormonal dependence and tumorigenic potential. Cell death and differentiation 25 (7): 1259–1275. 10.1038/s41418-018-0097-4.

Hanchate, N. K., Giacobini, P., Lhuillier, P., Parkash, J., Espy, C., Fouveaut, C., Leroy, C., Baron, S., Campagne, C., Vanacker, C., Collier, F., Cruaud, C., Meyer, V., García-Piñero, A., Dewailly, D., Cortet-Rudelli, C., Gersak, K., Metz, C., Chabrier, G., Pugeat, M., Young, J., Hardelin, J.-P., Prevot, V., Dodé, C., 2012. SEMA3A, a gene involved in axonal pathfinding, is mutated in patients with Kallmann syndrome. PLoS genetics 8 (8): e1002896. 10.1371/journal.pgen.1002896.

He, Z., Tessier-Lavigne, M., 1997. Neuropilin Is a Receptor for the Axonal Chemorepellent Semaphorin III. Cell 90 (4): 739–751. 10.1016/S0092-8674(00)80534-6.

Hoffmann, W., 2015. Current Status on Stem Cells and Cancers of the Gastric Epithelium. International journal of molecular sciences 16 (8): 19153–19169. 10.3390/ijms160819153.

Hori, H., Nakata, H., Iguchi, G., Yamada, H., Chihara, K., Baba, H., 2003. Oncogenic ras induces gastrin/CCKB receptor gene expression in human colon cancer cell lines LoVo and Colo320HSR. Journal of Laboratory and Clinical Medicine 141 (5): 335–341. 10.1016/S0022-2143(03)00021-0.

Hota, P. K., Buck, M., 2012. Plexin structures are coming: opportunities for multilevel investigations of semaphorin guidance receptors, their cell signaling mechanisms, and functions. Cellular and molecular life sciences CMLS 69 (22): 3765–3805. 10.1007/s00018-012-1019-0.

Huang, Y., Zhao, M., Xu, H., Wang, K., Fu, Z., Jiang, Y., Yao, Z., 2014. RASAL2 down-regulation in ovarian cancer promotes epithelial-mesenchymal transition and metastasis. Oncotarget 5 (16): 6734–6745. 10.18632/oncotarget.2244.

Ito, Y., Oinuma, I., Katoh, H., Kaibuchi, K., Negishi, M., 2006. Sema4D/plexin-B1 activates GSK-3beta through R-Ras GAP activity, inducing growth cone collapse. EMBO reports 7 (7): 704–709. 10.1038/sj.embor.7400737.

Janssen, B. J. C., Robinson, R. A., Pérez-Brangulí, F., Bell, C. H., Mitchell, K. J., Siebold, C., Jones, E. Y., 2010. Structural basis of semaphorin-plexin signalling. Nature 467 (7319): 1118–1122. 10.1038/nature09468.

Jayakumar, C., Ranganathan, P., Devarajan, P., Krawczeski, C. D., Looney, S., Ramesh, G., 2013. Semaphorin 3A is a new early diagnostic biomarker of experimental and pediatric acute kidney injury. PloS one 8 (3): e58446. 10.1371/journal.pone.0058446.

Jin, H., Wang, X., Ying, J., Wong, A. H. Y., Cui, Y., Srivastava, G., Shen, Z.-Y., Li, E.-M., Zhang, Q., Jin, J., Kupzig, S., Chan, A. T. C., Cullen, P. J., Tao, Q., 2007. Epigenetic silencing of a Ca(2+)-regulated Ras GTPase-activating protein RASAL defines a new mechanism of Ras activation in human cancers. Proceedings of the National Academy of Sciences of the United States of America 104 (30): 12353–12358. 10.1073/pnas.0700153104.

Joshi, H. J., Narimatsu, Y., Schjoldager, K. T., Tytgat, H. L. P., Aebi, M., Clausen, H., Halim, A., 2018. SnapShot: O-Glycosylation Pathways across Kingdoms. Cell 172 (3): 632-632.e2. 10.1016/j.cell.2018.01.016.

Kang, S., Kumanogoh, A., 2013. Semaphorins in bone development, homeostasis, and disease. Seminars in cell & developmental biology 24 (3): 163–171. 10.1016/j.semcdb.2012.09.008.

King, P. D., Lubeck, B. A., Lapinski, P. E., 2013. Nonredundant functions for Ras GTPase-activating proteins in tissue homeostasis. Science signaling 6 (264): re1. 10.1126/scisignal.2003669.

Klostermann, A., Lohrum, M., Adams, R. H., Püschel, A. W., 1998. The chemorepulsive activity of the axonal guidance signal semaphorin D requires dimerization. The Journal of biological chemistry 273 (13): 7326–7331. 10.1074/jbc.273.13.7326.

Kolfschoten, I. G. M., van Leeuwen, B., Berns, K., Mullenders, J., Beijersbergen, R. L., Bernards, R., Voorhoeve, P. M., Agami, R., 2005. A genetic screen identifies PITX1 as a suppressor of RAS activity and tumorigenicity. Cell 121 (6): 849–858. 10.1016/j.cell.2005.04.017.

Kolodkin, A. L., Levengood, D. V., Rowe, E. G., Tai, Y. T., Giger, R. J., Ginty, D. D., 1997. Neuropilin is a semaphorin III receptor. Cell 90 (4): 753–762. 10.1016/s0092-8674(00)80535-8.

Kolodkin, A. L., Matthes, D. J., Goodman, C. S., 1993. The semaphorin genes encode a family of transmembrane and secreted growth cone guidance molecules. Cell 75 (7): 1389–1399. 10.1016/0092-8674(93)90625-z.

Kong-Beltran, M., Stamos, J., Wickramasinghe, D., 2004. The Sema domain of Met is necessary for receptor dimerization and activation. Cancer cell 6 (1): 75–84. 10.1016/j.ccr.2004.06.013.

Korostylev, A., Worzfeld, T., Deng, S., Friedel, R. H., Swiercz, J. M., Vodrazka, P., Maier, V., Hirschberg, A., Ohoka, Y., Inagaki, S., Offermanns, S., Kuner, R., 2008. A functional role for semaphorin 4D/plexin B1 interactions in epithelial branching morphogenesis during organogenesis. Development (Cambridge, England) 135 (20): 3333–3343. 10.1242/dev.019760.

Kötting, C., Kallenbach, A., Suveyzdis, Y., Wittinghofer, A., Gerwert, K., 2008. The GAP arginine finger movement into the catalytic site of Ras increases the activation entropy. Proceedings of the National Academy of Sciences of the United States of America 105 (17): 6260–6265. 10.1073/pnas.0712095105.

Kumanogoh, A., Kikutani, H., 2013. Immunological functions of the neuropilins and plexins as receptors for semaphorins. Nature reviews. Immunology 13 (11): 802–814.

Kupzig, S., Deaconescu, D., Bouyoucef, D., Walker, S. A., Liu, Q., Polte, C. L., Daumke, O., Ishizaki, T., Lockyer, P. J., Wittinghofer, A., Cullen, P. J., 2006. GAP1 family members constitute bifunctional Ras and Rap GTPase-activating proteins. The Journal of biological chemistry 281 (15): 9891–9900. 10.1074/jbc.M512802200.

Laemmli, U. K., 1970. Cleavage of structural proteins during the assembly of the head of bacteriophage T4. Nature 227 (5259): 680–685. 10.1038/227680a0.

Lalani, S. R., Safiullah, A. M., Molinari, L. M., Fernbach, S. D., Martin, D. M., Belmont, J. W., 2004. SEMA3E mutation in a patient with CHARGE syndrome. Journal of medical genetics 41 (7): e94. 10.1136/jmg.2003.017640.

Lanas, A., Chan, F. K. L., 2017. Peptic ulcer disease. The Lancet 390 (10094): 613–624. 10.1016/S0140-6736(16)32404-7.

Lapinski, P. E., Kwon, S., Lubeck, B. A., Wilkinson, J. E., Srinivasan, R. S., Sevick-Muraca, E., King, P. D., 2012. RASA1 maintains the lymphatic vasculature in a quiescent functional state in mice. The Journal of clinical investigation 122 (2): 733–747. 10.1172/JCI46116.

Larsen, I. S. B., Narimatsu, Y., Joshi, H. J., Siukstaite, L., Harrison, O. J., Brasch, J., Goodman, K. M., Hansen, L., Shapiro, L., Honig, B., Vakhrushev, S. Y., Clausen, H., Halim, A., 2017a. Discovery of an O-mannosylation pathway selectively serving cadherins and protocadherins. Proceedings of the National Academy of Sciences of the United States of America 114 (42): 11163–11168. 10.1073/pnas.1708319114.

Larsen, I. S. B., Narimatsu, Y., Joshi, H. J., Yang, Z., Harrison, O. J., Brasch, J., Shapiro, L., Honig, B., Vakhrushev, S. Y., Clausen, H., Halim, A., 2017b.

Mammalian O-mannosylation of cadherins and plexins is independent of protein O-mannosyltransferases 1 and 2. The Journal of biological chemistry 292 (27): 11586–11598. 10.1074/jbc.M117.794487.

Lee, H. K., Lee, H.-J., Hur, K., Lee, H. S., Kim, W. H., Michaeli, D., Choe, K. J., Yang, H.-K., 2005. Growth effect of gastrin on gastric cancer and its clinical implications for gastric cancer surgery. Oncology reports 14 (2): 383–388.

Liu, D., Yang, C., Bojdani, E., Murugan, A. K., Xing, M., 2013. Identification of RASAL1 as a major tumor suppressor gene in thyroid cancer. Journal of the National Cancer Institute 105 (21): 1617–1627. 10.1093/jnci/djt249.

Liu, Q., Walker, S. A., Gao, D., Taylor, J. A., Dai, Y.-F., Arkell, R. S., Bootman, M. D., Roderick, H. L., Cullen, P. J., Lockyer, P. J., 2005. CAPRI and RASAL impose different modes of information processing on Ras due to contrasting temporal filtering of Ca2+. The Journal of cell biology 170 (2): 183–190. 10.1083/jcb.200504167.

Lockyer, P. J., Kupzig, S., Cullen, P. J., 2001. CAPRI regulates Ca(2+)-dependent inactivation of the Ras-MAPK pathway. Current biology CB 11 (12): 981–986. 10.1016/s0960-9822(01)00261-5.

Love, C. A., Harlos, K., Mavaddat, N., Davis, S. J., Stuart, D. I., Jones, E. Y., Esnouf, R. M., 2003. The ligand-binding face of the semaphorins revealed by the high-resolution crystal structure of SEMA4D. Nature structural biology 10 (10): 843–848. 10.1038/nsb977.

Luo, Y., Raible, D., Raper, J. A., 1993. Collapsin: a protein in brain that induces the collapse and paralysis of neuronal growth cones. Cell 75 (2): 217–227. 10.1016/0092-8674(93)80064-l.

Luzón-Toro, B., Fernández, R. M., Torroglosa, A., Agustín, J. C. de, Méndez-Vidal, C., Segura, D. I., Antiñolo, G., Borrego, S., 2013. Mutational spectrum of semaphorin 3A and semaphorin 3D genes in Spanish Hirschsprung patients. PloS one 8 (1): e54800. 10.1371/journal.pone.0054800.

Ma, Q., Zhang, K., Guin, S., Zhou, Y.-Q., Wang, M.-H., 2010. Deletion or insertion in the first immunoglobulin-plexin-transcription (IPT) domain differentially regulates expression and tumorigenic activities of RON receptor Tyrosine Kinase. Molecular cancer 9: 307. 10.1186/1476-4598-9-307.

Maertens, O., Cichowski, K., 2014. An expanding role for RAS GTPase activating proteins (RAS GAPs) in cancer. Advances in biological regulation 55: 1–14. 10.1016/j.jbior.2014.04.002.

Malfertheiner, P., Kandulski, A., Venerito, M., 2017. Proton-pump inhibitors: understanding the complications and risks. Nature reviews. Gastroenterology & hepatology 14 (12): 697–710. 10.1038/nrgastro.2017.117.

Malumbres, M., Barbacid, M., 2003. RAS oncogenes: the first 30 years. Nature reviews. Cancer 3 (6): 459–465. 10.1038/nrc1097.

Masuda, T., Taniguchi, M., 2015. Congenital diseases and semaphorin signaling: overview to date of the evidence linking them. Congenital anomalies 55 (1): 26–30. 10.1111/cga.12095.

Mehta, V., Pang, K.-L., Rozbesky, D., Nather, K., Keen, A., Lachowski, D., Kong, Y., Karia, D., Ameismeier, M., Huang, J., Fang, Y., Del Rio Hernandez, A., Reader, J. S., Jones, E. Y., Tzima, E., 2020. The guidance receptor plexin D1 is a mechanosensor in endothelial cells. Nature 578 (7794): 290–295. 10.1038/s41586-020-1979-4.

Merchant, J. L., 2000. EGF receptor activation of the human gastrin gene: a tale of two zinc finger transcription factor families. The Keio journal of medicine 49 (3): 106–110.

Miao, W., Sakai, K., Sato, H., Imamura, R., Jangphattananont, N., Takagi, J., Nishita, M., Minami, Y., Matsumoto, K., 2019. Impaired ligand-dependent MET activation caused by an extracellular SEMA domain missense mutation in lung cancer. Cancer science 110 (10): 3340–3349. 10.1111/cas.14142.

Michos, O., 2009. Kidney development: from ureteric bud formation to branching morphogenesis. Current opinion in genetics & development 19 (5): 484–490. 10.1016/j.gde.2009.09.003.

Min, J., Zaslavsky, A., Fedele, G., McLaughlin, S. K., Reczek, E. E., Raedt, T. de, Guney, I., Strochlic, D. E., Macconaill, L. E., Beroukhim, R., Bronson, R. T., Ryeom, S., Hahn, W. C., Loda, M., Cichowski, K., 2010. An oncogene-tumor suppressor cascade drives metastatic prostate cancer by coordinately activating Ras and nuclear factor-kappaB. Nature medicine 16 (3): 286–294. 10.1038/nm.2100.

Miteva, K. T., Pedicini, L., Wilson, L. A., Jayasinghe, I., Slip, R. G., Marszalek, K., Gaunt, H. J., Bartoli, F., Deivasigamani, S., Sobradillo, D., Beech, D. J., McKeown, L., 2019. Rab46 integrates Ca2+ and histamine signaling to regulate selective cargo release from Weibel-Palade bodies. The Journal of cell biology 218 (7): 2232–2246. 10.1083/jcb.201810118.

Mittal, R., Ahmadian, M. R., Goody, R. S., Wittinghofer, A., 1996. Formation of a transition-state analog of the Ras GTPase reaction by Ras-GDP,

tetrafluoroaluminate, and GTPase-activating proteins. Science (New York, N.Y.) 273 (5271): 115–117. 10.1126/science.273.5271.115.

Mohamed, R., Ranganathan, P., Jayakumar, C., Nauta, F. L., Gansevoort, R. T., Weintraub, N. L., Brands, M., Ramesh, G., 2014. Urinary semaphorin 3A correlates with diabetic proteinuria and mediates diabetic nephropathy and associated inflammation in mice. Journal of molecular medicine (Berlin, Germany) 92 (12): 1245–1256. 10.1007/s00109-014-1209-3.

Nagy, G. N., Suardíaz, R., Lopata, A., Ozohanics, O., Vékey, K., Brooks, B. R., Leveles, I., Tóth, J., Vértessy, B. G., Rosta, E., 2016. Structural Characterization of Arginine Fingers: Identification of an Arginine Finger for the Pyrophosphatase dUTPases. Journal of the American Chemical Society 138 (45): 15035–15045. 10.1021/jacs.6b09012.

Nakata, H., Wang, S. L., Chung, D. C., Westwick, J. K., Tillotson, L. G., 1998. Oncogenic ras induces gastrin gene expression in colon cancer. Gastroenterology 115 (5): 1144–1153. 10.1016/s0016-5085(98)70085-x.

Nazaryan-Petersen, L., Oliveira, I. R., Mehrjouy, M. M., Mendez, J. M. M., Bak, M., Bugge, M., Kalscheuer, V. M., Bache, I., Hancks, D. C., Tommerup, N., 2019. Multigenic truncation of the semaphorin-plexin pathway by a germline chromothriptic rearrangement associated with Moebius syndrome. Human mutation 40 (8): 1057–1062. 10.1002/humu.23775.

Negishi-Koga, T., Shinohara, M., Komatsu, N., Bito, H., Kodama, T., Friedel, R. H., Takayanagi, H., 2011. Suppression of bone formation by osteoclastic expression of semaphorin 4D. Nature medicine 17 (11): 1473–1480. 10.1038/nm.2489.

Nicolaou, N., Renkema, K. Y., Bongers, E. M. H. F., Giles, R. H., Knoers, N. V. A. M., 2015. Genetic, environmental, and epigenetic factors involved in CAKUT. Nature reviews. Nephrology 11 (12): 720–731. 10.1038/nrneph.2015.140.

Nogi, T., Yasui, N., Mihara, E., Matsunaga, Y., Noda, M., Yamashita, N., Toyofuku, T., Uchiyama, S., Goshima, Y., Kumanogoh, A., Takagi, J., 2010. Structural basis for semaphorin signalling through the plexin receptor. Nature 467 (7319): 1123–1127. 10.1038/nature09473.

Ohta, K., Mizutani, A., Kawakami, A., Murakami, Y., Kasuya, Y., Takagi, S., Tanaka, H., Fujisawa, H., 1995. Plexin: a novel neuronal cell surface molecule that mediates cell adhesion via a homophilic binding mechanism in the presence of calcium ions. Neuron 14 (6): 1189–1199. 10.1016/0896-6273(95)90266-x.

Ohta, K., Takagi, S., Asou, H., Fujisawa, H., 1992. Involvement of neuronal cell surface molecule B2 in the formation of retinal plexiform layers. Neuron 9 (1): 151–161. 10.1016/0896-6273(92)90230-b.

Ohta, M., Seto, M., Ijichi, H., Miyabayashi, K., Kudo, Y., Mohri, D., Asaoka, Y., Tada, M., Tanaka, Y., Ikenoue, T., Kanai, F., Kawabe, T., Omata, M., 2009. Decreased expression of the RAS-GTPase activating protein RASAL1 is associated with colorectal tumor progression. Gastroenterology 136 (1): 206–216. 10.1053/j.gastro.2008.09.063.

Ohtsubo, K., Marth, J. D., 2006. Glycosylation in cellular mechanisms of health and disease. Cell 126 (5): 855–867. 10.1016/j.cell.2006.08.019.

Oinuma, I., Ishikawa, Y., Katoh, H., Negishi, M., 2004a. The Semaphorin 4D receptor Plexin-B1 is a GTPase activating protein for R-Ras. Science (New York, N.Y.) 305 (5685): 862–865. 10.1126/science.1097545.

Oinuma, I., Ito, Y., Katoh, H., Negishi, M., 2010. Semaphorin 4D/Plexin-B1 stimulates PTEN activity through R-Ras GTPase-activating protein activity, inducing growth cone collapse in hippocampal neurons. The Journal of biological chemistry 285 (36): 28200–28209. 10.1074/jbc.M110.147546.

Oinuma, I., Katoh, H., Negishi, M., 2004b. Molecular dissection of the semaphorin 4D receptor plexin-B1-stimulated R-Ras GTPase-activating protein activity and neurite remodeling in hippocampal neurons. The Journal of neuroscience the official journal of the Society for Neuroscience 24 (50): 11473–11480. 10.1523/JNEUROSCI.3257-04.2004.

Oinuma, I., Katoh, H., Negishi, M., 2006. Semaphorin 4D/Plexin-B1-mediated R-Ras GAP activity inhibits cell migration by regulating beta(1) integrin activity. The Journal of cell biology 173 (4): 601–613. 10.1083/jcb.200508204.

Paldy, E., Simonetti, M., Worzfeld, T., Bali, K. K., Vicuña, L., Offermanns, S., Kuner, R., 2017. Semaphorin 4C Plexin-B2 signaling in peripheral sensory neurons is pronociceptive in a model of inflammatory pain. Nature communications 8 (1): 176. 10.1038/s41467-017-00341-w.

Pan, G.-Q., Ren, H.-Z., Zhang, S.-F., Wang, X.-M., Wen, J.-F., 2009. Expression of semaphorin 5A and its receptor plexin B3 contributes to invasion and metastasis of gastric carcinoma. World journal of gastroenterology 15 (22): 2800–2804. 10.3748/wjg.15.2800.

Pascoe, H. G., Wang, Y., Zhang, X., 2015. Structural mechanisms of plexin signaling. Progress in biophysics and molecular biology 118 (3): 161–168. 10.1016/j.pbiomolbio.2015.03.006.

Pasterkamp, R. J., 2012. Getting neural circuits into shape with semaphorins. Nature reviews. Neuroscience 13 (9): 605–618. 10.1038/nrn3302.

Pasterkamp, R. J., Giger, R. J., 2009. Semaphorin function in neural plasticity and disease. Current opinion in neurobiology 19 (3): 263–274. 10.1016/j.conb.2009.06.001.

Peacock, J. W., Takeuchi, A., Hayashi, N., Liu, L., Tam, K. J., Al Nakouzi, N., Khazamipour, N., Tombe, T., Dejima, T., Lee, K. C., Shiota, M., Thaper, D., Lee, W. C., Hui, D. H., Kuruma, H., Ivanova, L., Yenki, P., Jiao, I. Z., Khosravi, S., Mui, A. L.-F., Fazli, L., Zoubeidi, A., Daugaard, M., Gleave, M. E., Ong, C. J., 2018. SEMA3C drives cancer growth by transactivating multiple receptor tyrosine kinases via Plexin B1. EMBO molecular medicine 10 (2): 219–238. 10.15252/emmm.201707689.

Perälä, N., Jakobson, M., Ola, R., Fazzari, P., Penachioni, J. Y., Nymark, M., Tanninen, T., Immonen, T., Tamagnone, L., Sariola, H., 2011. Sema4C-Plexin B2 signalling modulates ureteric branching in developing kidney. Differentiation; research in biological diversity 81 (2): 81–91. 10.1016/j.diff.2010.10.001.

Pischedda, F., Szczurkowska, J., Cirnaru, M. D., Giesert, F., Vezzoli, E., Ueffing, M., Sala, C., Francolini, M., Hauck, S. M., Cancedda, L., Piccoli, G., 2014. A cell surface biotinylation assay to reveal membrane-associated neuronal cues: Negr1 regulates dendritic arborization. Molecular & cellular proteomics MCP 13 (3): 733–748. 10.1074/mcp.M113.031716.

Prior, I. A., Lewis, P. D., Mattos, C., 2012. A comprehensive survey of Ras mutations in cancer. Cancer research 72 (10): 2457–2467. 10.1158/0008-5472.CAN-11-2612.

Ranganathan, P., Jayakumar, C., Mohamed, R., Weintraub, N. L., Ramesh, G., 2014. Semaphorin 3A inactivation suppresses ischemia-reperfusion-induced inflammation and acute kidney injury. American journal of physiology. Renal physiology 307 (2): F183-94. 10.1152/ajprenal.00177.2014.

Reily, C., Stewart, T. J., Renfrow, M. B., Novak, J., 2019. Glycosylation in health and disease. Nature reviews. Nephrology 15 (6): 346–366. 10.1038/s41581-019-0129-4.

Repasky, G. A., Chenette, E. J., Der, C. J., 2004. Renewing the conspiracy theory debate: does Raf function alone to mediate Ras oncogenesis? Trends in cell biology 14 (11): 639–647. 10.1016/j.tcb.2004.09.014.

Rettenberger, A. T., Schulze, W., Breer, H., Haid, D., 2015. Analysis of the protein related receptor GPR92 in G-cells. Frontiers in physiology 6: 261. 10.3389/fphys.2015.00261.

Rodriguez, M. M., 2014. Congenital Anomalies of the Kidney and the Urinary Tract (CAKUT). Fetal and pediatric pathology 33 (5-6): 293–320. 10.3109/15513815.2014.959678.

Rohm, B., Ottemeyer, A., Lohrum, M., Püschel, A. W., 2000. Plexin/neuropilin complexes mediate repulsion by the axonal guidance signal semaphorin 3A. Mechanisms of development 93 (1-2): 95–104. 10.1016/s0925-4773(00)00269-0.

Rudd, P. M., Dwek, R. A., 1997. Glycosylation: heterogeneity and the 3D structure of proteins. Critical reviews in biochemistry and molecular biology 32 (1): 1–100. 10.3109/10409239709085144.

Saito, Y., Oinuma, I., Fujimoto, S., Negishi, M., 2009. Plexin-B1 is a GTPase activating protein for M-Ras, remodelling dendrite morphology. EMBO reports 10 (6): 614–621. 10.1038/embor.2009.63.

Sakurai, A., Doçi, C. L., Doci, C., Gutkind, J. S., 2012. Semaphorin signaling in angiogenesis, lymphangiogenesis and cancer. Cell research 22 (1): 23–32. 10.1038/cr.2011.198.

Sakurai, A., Gavard, J., Annas-Linhares, Y., Basile, J. R., Amornphimoltham, P., Palmby, T. R., Yagi, H., Zhang, F., Randazzo, P. A., Li, X., Weigert, R., Gutkind, J. S., 2010. Semaphorin 3E initiates antiangiogenic signaling through plexin D1 by regulating Arf6 and R-Ras. Molecular and cellular biology 30 (12): 3086–3098. 10.1128/MCB.01652-09.

Schachter, H., 2000. The joys of HexNAc. The synthesis and function of N- and O-glycan branches. Glycoconjugate journal 17 (7-9): 465–483. 10.1023/a:1011010206774.

Schmidt, A., Hall, A., 2002. Guanine nucleotide exchange factors for Rho GTPases: turning on the switch. Genes & development 16 (13): 1587–1609. 10.1101/gad.1003302.

Schubert, M. L., 2016. Gastric acid secretion. Current opinion in gastroenterology 32 (6): 452–460. 10.1097/MOG.0000000000000308.

Schulz, E., Klampfl, P., Holzapfel, S., Janecke, A. R., Ulz, P., Renner, W., Kashofer, K., Nojima, S., Leitner, A., Zebisch, A., Wölfler, A., Hofer, S., Gerger, A., Lax, S., Beham-Schmid, C., Steinke, V., Heitzer, E., Geigl, J. B., Windpassinger, C., Hoefler, G., Speicher, M. R., Boland, C. R., Kumanogoh, A., Sill, H., 2014. Germline variants in the SEMA4A gene predispose to

familial colorectal cancer type X. Nature communications 5: 5191. 10.1038/ncomms6191.

Sergey Chupreta, Ming Du, Andrea Todisco, and Juanita L. Merchant. EGF stimulates gastrin promoter through activation of Sp1 kinase activity.

Seto, M., Ohta, M., Ikenoue, T., Sugimoto, T., Asaoka, Y., Tada, M., Mohri, D., Kudo, Y., Ijichi, H., Tateishi, K., Otsuka, M., Hirata, Y., Maeda, S., Koike, K., Omata, M., 2011. Reduced expression of RAS protein activator like-1 in gastric cancer. International journal of cancer 128 (6): 1293–1302. 10.1002/ijc.25459.

Siebold, C., Jones, E. Y., 2013. Structural insights into semaphorins and their receptors. Seminars in cell & developmental biology 24 (3): 139–145. 10.1016/j.semcdb.2012.11.003.

Simonetti, M., Paldy, E., Njoo, C., Bali, K. K., Worzfeld, T., Pitzer, C., Kuner, T., Offermanns, S., Mauceri, D., Kuner, R., 2019. The impact of Semaphorin 4C/Plexin-B2 signaling on fear memory via remodeling of neuronal and synaptic morphology. Molecular psychiatry. 10.1038/s41380-019-0491-4.

Sot, B., Behrmann, E., Raunser, S., Wittinghofer, A., 2013. Ras GTPase activating (RasGAP) activity of the dual specificity GAP protein Rasal requires colocalization and C2 domain binding to lipid membranes. Proceedings of the National Academy of Sciences of the United States of America 110 (1): 111–116. 10.1073/pnas.1201658110.

Sot, B., Kötting, C., Deaconescu, D., Suveyzdis, Y., Gerwert, K., Wittinghofer, A., 2010. Unravelling the mechanism of dual-specificity GAPs. The EMBO journal 29 (7): 1205–1214. 10.1038/emboj.2010.20.

Sun, T., Yang, L., Kaur, H., Pestel, J., Looso, M., Nolte, H., Krasel, C., Heil, D., Krishnan, R. K., Santoni, M.-J., Borg, J.-P., Bünemann, M., Offermanns, S., Swiercz, J. M., Worzfeld, T., 2017. A reverse signaling pathway downstream of Sema4A controls cell migration via Scrib. The Journal of cell biology 216 (1): 199–215. 10.1083/jcb.201602002.

Suzuki, K., Kumanogoh, A., Kikutani, H., 2008. Semaphorins and their receptors in immune cell interactions. Nature immunology 9 (1): 17–23. 10.1038/ni1553.

Swiercz, J. M., Kuner, R., Behrens, J., Offermanns, S., 2002. Plexin-B1 directly interacts with PDZ-RhoGEF/LARG to regulate RhoA and growth cone morphology. Neuron 35 (1): 51–63. 10.1016/s0896-6273(02)00750-x.

Swiercz, J. M., Kuner, R., Offermanns, S., 2004. Plexin-B1/RhoGEF–mediated RhoA activation involves the receptor tyrosine kinase ErbB-2. The Journal of cell biology 165 (6): 869–880. 10.1083/jcb.200312094.

Swiercz, J. M., Worzfeld, T., Offermanns, S., 2008. ErbB-2 and met reciprocally regulate cellular signaling via plexin-B1. The Journal of biological chemistry 283 (4): 1893–1901. 10.1074/jbc.M706822200.

Swiercz, J. M., Worzfeld, T., Offermanns, S., 2009. Semaphorin 4D signaling requires the recruitment of phospholipase C gamma into the plexin-B1 receptor complex. Molecular and cellular biology 29 (23): 6321–6334. 10.1128/MCB.00103-09.

Takahashi, T., Fournier, A., Nakamura, F., Wang, L.-H., Murakami, Y., Kalb, R. G., Fujisawa, H., Strittmatter, S. M., 1999. Plexin-Neuropilin-1 Complexes Form Functional Semaphorin-3A Receptors. Cell 99 (1): 59–69. 10.1016/s0092-8674(00)80062-8.

Takahashi, T., Strittmatter, S. M., 2001. Plexina1 autoinhibition by the plexin sema domain. Neuron 29 (2): 429–439. 10.1016/s0896-6273(01)00216-1.

Takamatsu, H., Kumanogoh, A., 2012. Diverse roles for semaphorin-plexin signaling in the immune system. Trends in immunology 33 (3): 127–135. 10.1016/j.it.2012.01.008.

Tamagnone, L., 2012. Emerging role of semaphorins as major regulatory signals and potential therapeutic targets in cancer. Cancer cell 22 (2): 145–152. 10.1016/j.ccr.2012.06.031.

Tamagnone, L., Artigiani, S., Chen, H., He, Z., Ming, G. I., Song, H., Chedotal, A., Winberg, M. L., Goodman, C. S., Poo, M., Tessier-Lavigne, M., Comoglio, P. M., 1999. Plexins are a large family of receptors for transmembrane, secreted, and GPI-anchored semaphorins in vertebrates. Cell 99 (1): 71–80. 10.1016/s0092-8674(00)80063-x.

Tamagnone, L., Giordano, S., 2006. Semaphorin pathways orchestrate osteogenesis. Nature cell biology 8 (6): 545–547. 10.1038/ncb0606-545.

Tamagnone, L., Mazzone, M., 2011. Semaphorin signals on the road of endothelial tip cells. Developmental cell 21 (2): 189–190. 10.1016/j.devcel.2011.07.017.

Ta-Shma, A., Khan, T. N., Vivante, A., Willer, J. R., Matak, P., Jalas, C., Pode-Shakked, B., Salem, Y., Anikster, Y., Hildebrandt, F., Katsanis, N., Elpeleg, O., Davis, E. E., 2017. Mutations in TMEM260 Cause a Pediatric Neurodevelopmental, Cardiac, and Renal Syndrome. American journal of human genetics 100 (4): 666–675. 10.1016/j.ajhg.2017.02.007.

Ta-Shma, A., Pierri, C. L., Stepensky, P., Shaag, A., Zenvirt, S., Elpeleg, O., Rein, A. J. J. T., 2013. Isolated truncus arteriosus associated with a mutation

in the plexin-D1 gene. American journal of medical genetics. Part A 161A (12): 3115–3120. 10.1002/ajmg.a.36194.

Taylor, I. L., Byrne, W. J., Christie, D. L., Ament, M. E., Walsh, J. H., 1982. Effect of individual l-amino acids on gastric acid secretion and serum gastrin and pancreatic polypeptide release in humans. Gastroenterology 83 (1 Pt 2): 273–278.

Thaker, Y. R., Raab, M., Strebhardt, K., Rudd, C. E., 2019. GTPase-activating protein Rasal1 associates with ZAP-70 of the TCR and negatively regulates T-cell tumor immunity. Nature communications 10 (1): 4804. 10.1038/s41467-019-12544-4.

Tian, X., Gan, H., Zeng, Y., Zhao, H., Tang, R., Xia, Y., 2018. Inhibition of semaphorin-3a suppresses lipopolysaccharide-induced acute kidney injury. Journal of molecular medicine (Berlin, Germany) 96 (7): 713–724. 10.1007/s00109-018-1653-6.

Tong, Y., Hota, P. K., Hamaneh, M. B., Buck, M., 2008. Insights into Oncogenic Mutations of Plexin-B1 Based on the Solution Structure of the Rho GTPase Binding Domain. Structure (London, England 1993) 16 (2): 246–258. 10.1016/j.str.2007.12.012.

Tong, Y., Hota, P. K., Penachioni, J. Y., Hamaneh, M. B., Kim, S., Alviani, R. S., Shen, L., He, H., Tempel, W., Tamagnone, L., Park, H.-W., Buck, M., 2009. Structure and function of the intracellular region of the plexin-b1 transmembrane receptor. The Journal of biological chemistry 284 (51): 35962–35972. 10.1074/jbc.M109.056275.

Treps, L., Le Guelte, A., Gavard, J., 2013. Emerging roles of Semaphorins in the regulation of epithelial and endothelial junctions. Tissue barriers 1 (1): e23272. 10.4161/tisb.23272.

Turner, L. J., Hall, A., 2006. Plexin-Induced Collapse Assay in COS Cells. In: Regulators and Effectors of Small GTPases: Rho Family, 665–676: Elsevier.

Uesugi, K., Oinuma, I., Katoh, H., Negishi, M., 2009. Different requirement for Rnd GTPases of R-Ras GAP activity of Plexin-C1 and Plexin-D1. The Journal of biological chemistry 284 (11): 6743–6751. 10.1074/jbc.M805213200.

1999. Unified nomenclature for the semaphorins/collapsins. Semaphorin Nomenclature Committee. Cell 97 (5): 551–552. 10.1016/s0092-8674(00)80766-7.

van der Ven, A. T., Connaughton, D. M., Ityel, H., Mann, N., Nakayama, M., Chen, J., Vivante, A., Hwang, D.-Y., Schulz, J., Braun, D. A., Schmidt, J. M., Schapiro, D., Schneider, R., Warejko, J. K., Daga, A., Majmundar, A. J., Tan,

W., Jobst-Schwan, T., Hermle, T., Widmeier, E., Ashraf, S., Amar, A., Hoogstraaten, C. A., Hugo, H., Kitzler, T. M., Kause, F., Kolvenbach, C. M., Dai, R., Spaneas, L., Amann, K., Stein, D. R., Baum, M. A., Somers, M. J. G., Rodig, N. M., Ferguson, M. A., Traum, A. Z., Daouk, G. H., Bogdanović, R., Stajić, N., Soliman, N. A., Kari, J. A., El Desoky, S., Fathy, H. M., Milosevic, D., Al-Saffar, M., Awad, H. S., Eid, L. A., Selvin, A., Senguttuvan, P., Sanna-Cherchi, S., Rehm, H. L., MacArthur, D. G., Lek, M., Laricchia, K. M., Wilson, M. W., Mane, S. M., Lifton, R. P., Lee, R. S., Bauer, S. B., Lu, W., Reutter, H. M., Tasic, V., Shril, S., Hildebrandt, F., 2018a. Whole-Exome Sequencing Identifies Causative Mutations in Families with Congenital Anomalies of the Kidney and Urinary Tract. Journal of the American Society of Nephrology JASN 29 (9): 2348–2361. 10.1681/ASN.2017121265.

van der Ven, A. T., Vivante, A., Hildebrandt, F., 2018b. Novel Insights into the Pathogenesis of Monogenic Congenital Anomalies of the Kidney and Urinary Tract. Journal of the American Society of Nephrology JASN 29 (1): 36–50. 10.1681/ASN.2017050561.

Vetter, I. R., Wittinghofer, A., 2001. The guanine nucleotide-binding switch in three dimensions. Science (New York, N.Y.) 294 (5545): 1299–1304. 10.1126/science.1062023.

Walker, S. A., Kupzig, S., Bouyoucef, D., Davies, L. C., Tsuboi, T., Bivona, T. G., Cozier, G. E., Lockyer, P. J., Buckler, A., Rutter, G. A., Allen, M. J., Philips, M. R., Cullen, P. J., 2004. Identification of a Ras GTPase-activating protein regulated by receptor-mediated Ca2+ oscillations. The EMBO journal 23 (8): 1749–1760. 10.1038/sj.emboj.7600197.

Wang, M., He, J., Zhou, Y., Lv, N., Zhao, M., Wei, H., Li, R., 2020. Integrated analysis of miRNA and mRNA expression profiles in the brains of BTBR mice. International journal of developmental neuroscience the official journal of the International Society for Developmental Neuroscience. 10.1002/jdn.10019.

Wang, X., Kumanogoh, A., Watanabe, C., Shi, W., Yoshida, K., Kikutani, H., 2001. Functional soluble CD100/Sema4D released from activated lymphocytes: possible role in normal and pathologic immune responses. Blood 97 (11): 3498–3504. 10.1182/blood.v97.11.3498.

Wang, Y., He, H., Srivastava, N., Vikarunnessa, S., Chen, Y.-b., Jiang, J., Cowan, C. W., Zhang, X., 2012. Plexins are GTPase-activating proteins for Rap and are activated by induced dimerization. Science signaling 5 (207): ra6. 10.1126/scisignal.2002636.

Wennerberg, K., Rossman, K. L., Der, C. J., 2005. The Ras superfamily at a glance. Journal of cell science 118 (Pt 5): 843–846. 10.1242/jcs.01660.

Westbrook, T. F., Martin, E. S., Schlabach, M. R., Leng, Y., Liang, A. C., Feng, B., Zhao, J. J., Roberts, T. M., Mandel, G., Hannon, G. J., Depinho, R. A., Chin, L., Elledge, S. J., 2005. A genetic screen for candidate tumor suppressors identifies REST. Cell 121 (6): 837–848. 10.1016/j.cell.2005.03.033.

White, C. D., Erdemir, H. H., Sacks, D. B., 2012. IQGAP1 and its binding proteins control diverse biological functions. Cellular signalling 24 (4): 826–834. 10.1016/j.cellsig.2011.12.005.

Wong, O. G.-W., Nitkunan, T., Oinuma, I., Zhou, C., Blanc, V., Brown, R. S. D., Bott, S. R. J., Nariculam, J., Box, G., Munson, P., Constantinou, J., Feneley, M. R., Klocker, H., Eccles, S. A., Negishi, M., Freeman, A., Masters, J. R., Williamson, M., 2007. Plexin-B1 mutations in prostate cancer. Proceedings of the National Academy of Sciences of the United States of America 104 (48): 19040–19045. 10.1073/pnas.0702544104.

Wormald, M. R., Petrescu, A. J., Pao, Y.-L., Glithero, A., Elliott, T., Dwek, R. A., 2002. Conformational studies of oligosaccharides and glycopeptides: complementarity of NMR, X-ray crystallography, and molecular modelling. Chemical reviews 102 (2): 371–386. 10.1021/cr990368i.

Worzfeld, T., Offermanns, S., 2014. Semaphorins and plexins as therapeutic targets. Nature reviews. Drug discovery 13 (8): 603–621. 10.1038/nrd4337.

Worzfeld, T., Swiercz, J. M., 2017. Characterizing ErbB-2-Mediated Tyrosine Phosphorylation and Activation of Plexins. Methods in molecular biology (Clifton, N.J.) 1493: 129–146. 10.1007/978-1-4939-6448-2_9.

Worzfeld, T., Swiercz, J. M., Looso, M., Straub, B. K., Sivaraj, K. K., Offermanns, S., 2012. ErbB-2 signals through Plexin-B1 to promote breast cancer metastasis. The Journal of clinical investigation 122 (4): 1296–1305. 10.1172/JCI60568.

Worzfeld, T., Swiercz, J. M., Sentürk, A., Genz, B., Korostylev, A., Deng, S., Xia, J., Hoshino, M., Epstein, J. A., Chan, A. M., Vollmar, B., Acker-Palmer, A., Kuner, R., Offermanns, S., 2014. Genetic dissection of plexin signaling in vivo. Proceedings of the National Academy of Sciences of the United States of America 111 (6): 2194–2199. 10.1073/pnas.1308418111.

Xia, J., Swiercz, J. M., Bañón-Rodríguez, I., Matković, I., Federico, G., Sun, T., Franz, T., Brakebusch, C. H., Kumanogoh, A., Friedel, R. H., Martín-Belmonte, F., Gröne, H.-J., Offermanns, S., Worzfeld, T., 2015. Semaphorin-

Plexin Signaling Controls Mitotic Spindle Orientation during Epithelial Morphogenesis and Repair. Developmental cell 33 (3): 299–313. 10.1016/j.devcel.2015.02.001.

Xia, J., Worzfeld, T., 2016. Semaphorins and Plexins in Kidney Disease. Nephron 132 (2): 93–100. 10.1159/000443645.

Yao, X., Forte, J. G., 2003. Cell biology of acid secretion by the parietal cell. Annual review of physiology 65: 103–131. 10.1146/annurev.physiol.65.072302.114200.

Yukawa, K., Tanaka, T., Kishino, M., Yoshida, K., Takeuchi, N., Ito, T., Takamatsu, H., Kikutani, H., Kumanogoh, A., 2010a. Deletion of Sema4D gene reduces intimal neovascularization and plaque growth in apolipoprotein E-deficient mice. International Journal of Molecular Medicine 26 (1): 39–44. 10.3892/ijmm_00000432.

Yukawa, K., Tanaka, T., Yoshida, K., Takeuchi, N., Ito, T., Takamatsu, H., Kikutani, H., Kumanogoh, A., 2010b. Sema4A induces cell morphological changes through B-type plexin-mediated signaling. International Journal of Molecular Medicine 25 (2): 225–230.

Zhao, X.-Y., Chen, L., Xu, Q., Li, Y.-H., 2006. Expression of semaphorin 6D in gastric carcinoma and its significance. World journal of gastroenterology 12 (45): 7388–7390. 10.3748/wjg.v12.i45.7388.

Zhu, J., Jiang, Z., Gao, F., Hu, X., Zhou, L., Chen, J., Luo, H., Sun, J., Wu, S., Han, Y., Yin, G., Chen, M., Han, Z., Li, X., Huang, Y., Zhang, W., Zhou, F., Chen, T., Fa, P., Wang, Y., Sun, L., Leng, H., Sun, F., Liu, Y., Ye, M., Yang, H., Cai, Z., Gui, Y., Zhang, X., 2011. A systematic analysis on DNA methylation and the expression of both mRNA and microRNA in bladder cancer. PloS one 6 (11): e28223. 10.1371/journal.pone.0028223.

Verzeichnis der akademischen Lehrenden

Meine akademisch Lehrenden waren in Marburg:

Koert; Roling; Seubert; von Hänisch

Meine akademisch Lehrenden waren in Frankfurt am Main:

Böning; Boon; Brandes; Brüne; Büchel; Buchholz; Christen; Dimmeler; Dötsch; Eberhardt; Ebersberger; Farin; Fißlthaler; Fleming; Glaubitz; Göbel; Gottschalk; Greten; Grösch; Grünewald; Güntert; Herrmann; Hildt; Klein; Kössl; Krueger; Lausen; Liebner; Lötsch; Ludwig; Meyer zu Heringdorf; Modlich; Mühl; Niederberger; Offermanns; Osiewacz; Plate; Pos; Radeke; Randriamboavonjy; Schäfer; Schmidt; Scholich; Schröder; Schulte; Schwalbe; Stainier; Steinle; Stellos; Strebhardt; Tampe; Tegeder; van Zandbergen; Wels; Wettschureck

Danksagung

Eine Promotion ist ein langer Weg, den man ohne die Hilfe anderer Personen nicht beschreiten könnte. In diesem Sinne möchte ich mich bei denjenigen bedanken, die zur Gesamtheit dieser Arbeit in ihrer jetzigen Form beigetragen haben. Mein besonderer Dank gilt:

Herrn Prof. Dr. Thomas Worzfeld, der mir die Möglichkeit gab, an seinem Institut zu promovieren, mich als Doktorvater stets unterstützt und motiviert hat und dabei immer ein offenes Ohr hatte.

Den Mitarbeitern des Pharmakologischen Institut der Philipps-Universität Marburg, deren Unterstützung und fachliche Kompetenz mir eine große Hilfe waren. An dieser Stelle möchte ich besonders Luisa Schäfer danken, die mich während ihrer Ausbildung zur Chemielaborantin nicht nur begleitet hat, sondern mir auch im Labor tatkräftig zur Seite stand.

Großer Dank gebührt meinen Doktorandenkollegen Florian, Javier, Ivana und Chen, mit denen ich während unserer gemeinsamen Zeit zum Einen zahlreiche fachliche und anregende Diskussionen hatte, und die mir zum Anderen auch abseits der täglichen Arbeit zu Freunden geworden sind und mich in schwierigen Zeiten unterstützt haben.

Zum Schluss möchte ich mich noch bei meiner Familie, insbesondere meinen Eltern und Schwestern, bedanken, ohne die ich nie so weit gekommen wäre. Ebenso danke ich Luisa, die mir während der gesamten Zeit eine moralische Stütze war, und niemals an mir gezweifelt hat.